Sparse Arrays and Sparse Waveforms: Design, Processing, and Applications, Part II

Yimin D. Zhang
Temple University, USA

Shunqiao Sun
The University of Alabama, USA

EUSIPCO Tutorial
Palermo, Italy
September 8, 2025

Acknowledgement: Ruxin Zheng, Lifan Xu, Yunqiao Hu

NSF, Alabama Transportation Institute
NXP Semiconductors, Spartan Radar and Mathworks

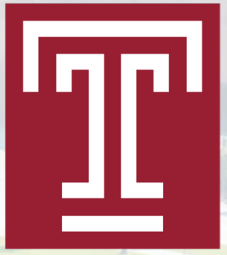

Agenda

- **Background and Motivation of DL for DOA Estimation**
  - ✓ Overview of deep learning (DL) for DOA estimation
  - ✓ Comparison: data-driven vs. model-based approaches
  - ✓ Why hybrid model-based deep learning matters
- **DL for High-Resolution Radar Imaging**
  - ✓ Unrolling IAA
  - ✓ Physics-guided 1D neural networks for radar imaging
  - ✓ DOA estimation considering antenna failure
  - ✓ Off-grid DOA estimation with 1-bit single-snapshot sparse array
  - ✓ Siamese neural networks for DOA estimation
- **DL for Integrated Sensing and Communications (ISAC)**
- **DL Enabled Sparse Array Interpolation**
  - ✓ Unrolling IHT for matrix completion
  - ✓ Transformer based array interpolation

DOA Estimation & Signal Model

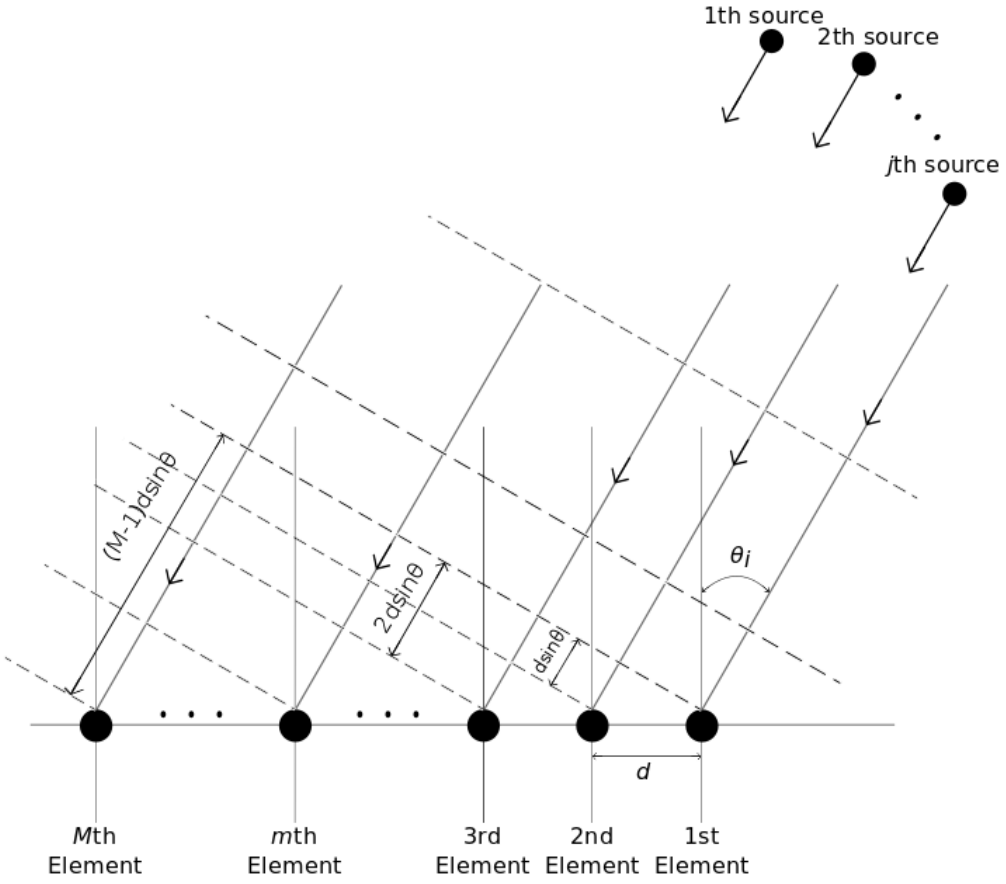

The signal model:

$$\boldsymbol{y}(t) = \sum_{k=1}^{K} \boldsymbol{a}(\theta_k) s_k(t) + \boldsymbol{n}(t) \quad \rightarrow \text{noise}$$
$$= \boldsymbol{A}(\boldsymbol{\theta})\boldsymbol{s}(t) + \boldsymbol{n}(t)$$

The array manifold matrix:

$$\boldsymbol{A}(\boldsymbol{\theta}) = [a(\theta_1), a(\theta_2) \cdots a(\theta_k)]$$

$$\boldsymbol{a}(\theta) = \left[1, e^{2\pi d_2/\lambda}, \cdots, e^{2\pi d_N/\lambda}\right]^{\mathsf{T}}$$

The source vector:

$$\boldsymbol{s}(t) = [s_1(t), s_2(t), \cdots, s_k(t)]^{\mathsf{T}}$$

The **single snapshot** model:

$$\boldsymbol{y} = \boldsymbol{A}(\boldsymbol{\theta})\boldsymbol{s} + \boldsymbol{n}$$

S. Sun, A. P. Petropulu and H. V. Poor, "MIMO radar for advanced driver-assistance systems and autonomous driving: Advantages and challenges," IEEE Signal Processing Magazine, vol. 37, no. 4, pp. 98-117, 2020.

S. Rao, R. Narasimha and S. Sun, "Signal processing challenges in automotive radar," in Proc. IEEE 50th International Conference on Acoustics, Speech, and Signal Processing (ICASSP), Hyderabad, India, April 6-11, 2025.

DL-Based DOA Estimation

- **Deep Learning**

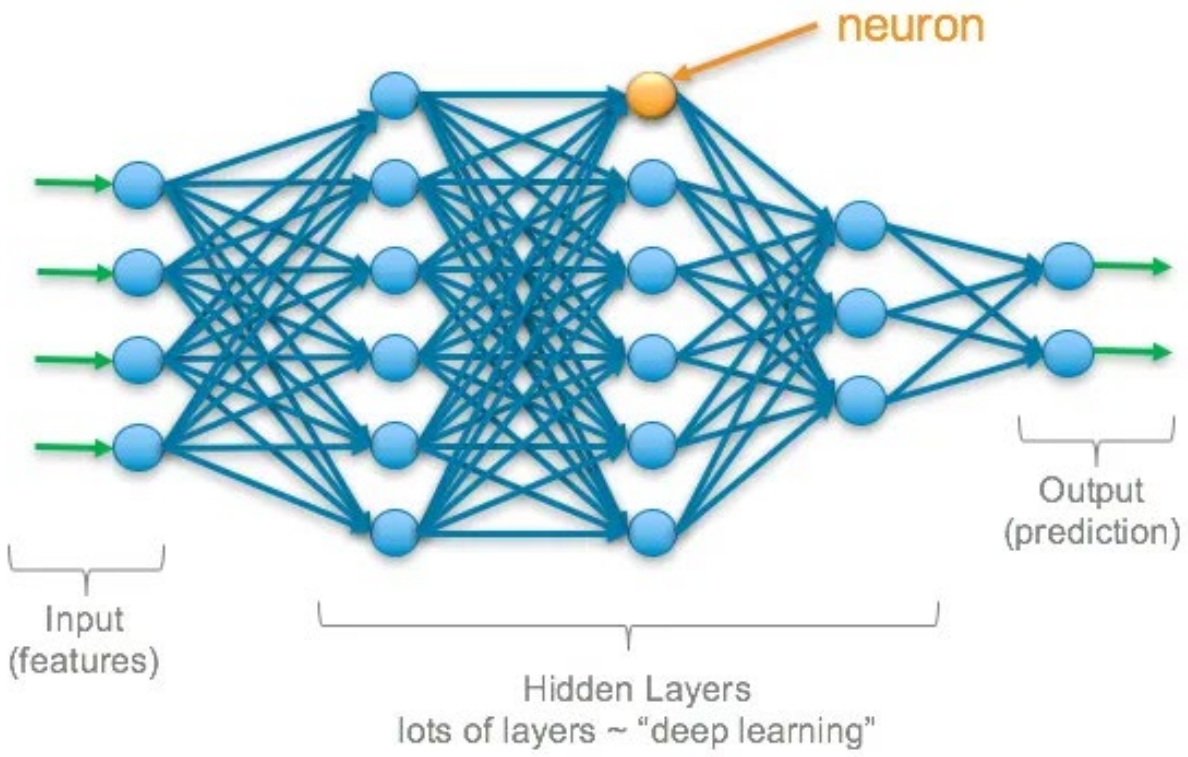

Yann LeCun, Yoshua Bengio & Geoffrey Hinton, "Deep learning", Nature, Vol. 521, pp. 436-444, 2015.

K. He, X. Zhang, S. Ren, J. Sun, "Deep residual learning for image recognition," CVPR, 2016.

DL-Based DOA Estimation

- **Deep Learning**
- **Key Input Representations:**

✓Raw time-series data

✓Covariance matrices

✓Spectrum

- **Key Output Representations:**

✓Sudo-spectrum/spectrum

✓DOAs

DL-Based DOA Estimation

- **Multilabel classification (Sudo spectrum)**

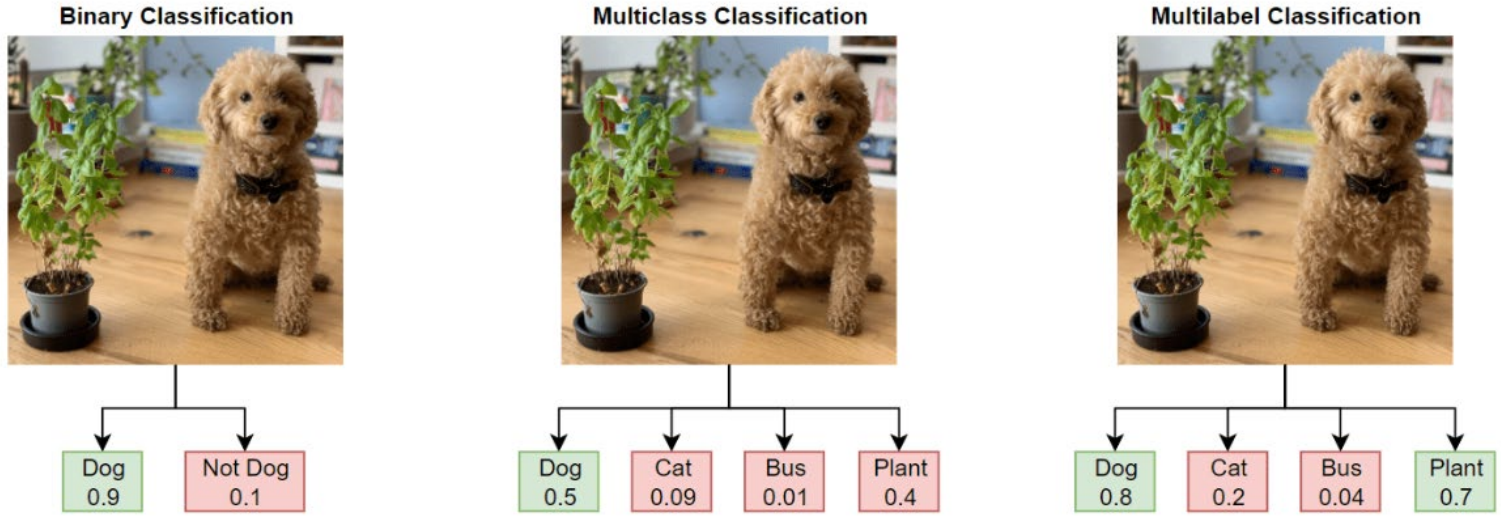

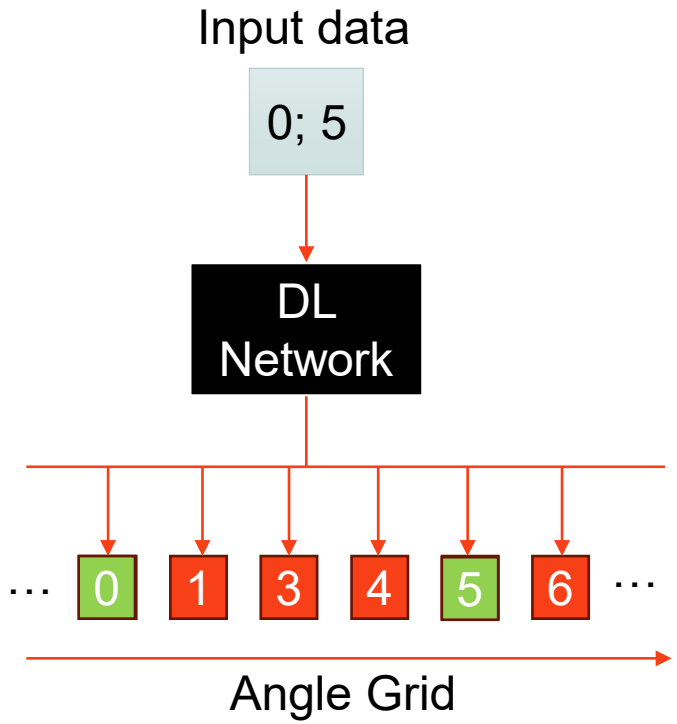

https://www.mathworks.com/help/deeplearning/ug/multilabel-image-classification-using-deep-learning.html

DL-Based DOA Estimation: Data-Driven Approach

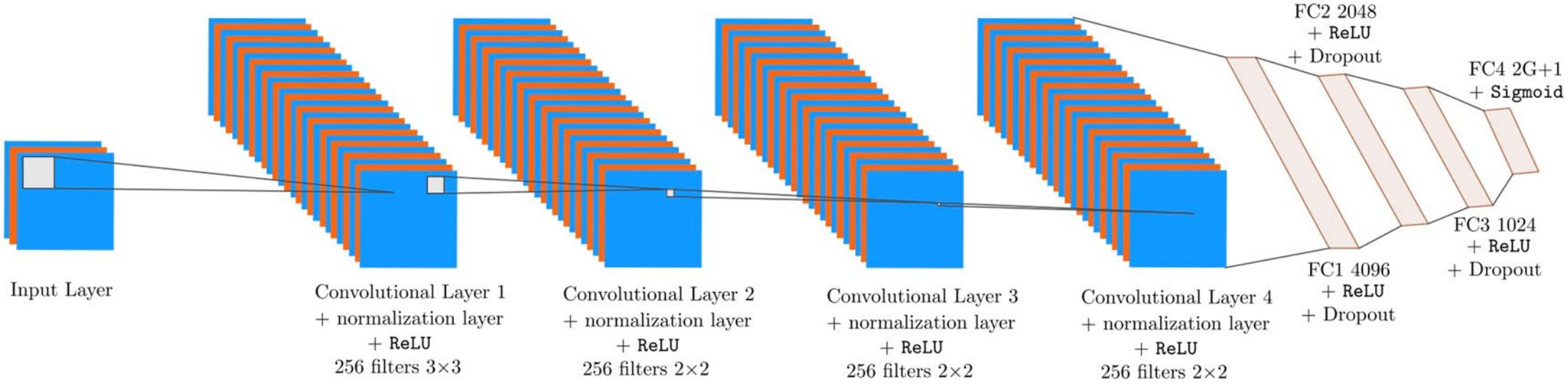

G. K. Papageorgiou, M. Sellathurai and Y. C. Eldar, "Deep networks for direction-of-arrival estimation in low SNR," in *IEEE Transactions on Signal Processing*, vol. 69, pp. 3714-3729, 2021.

DL-Based DOA Estimation

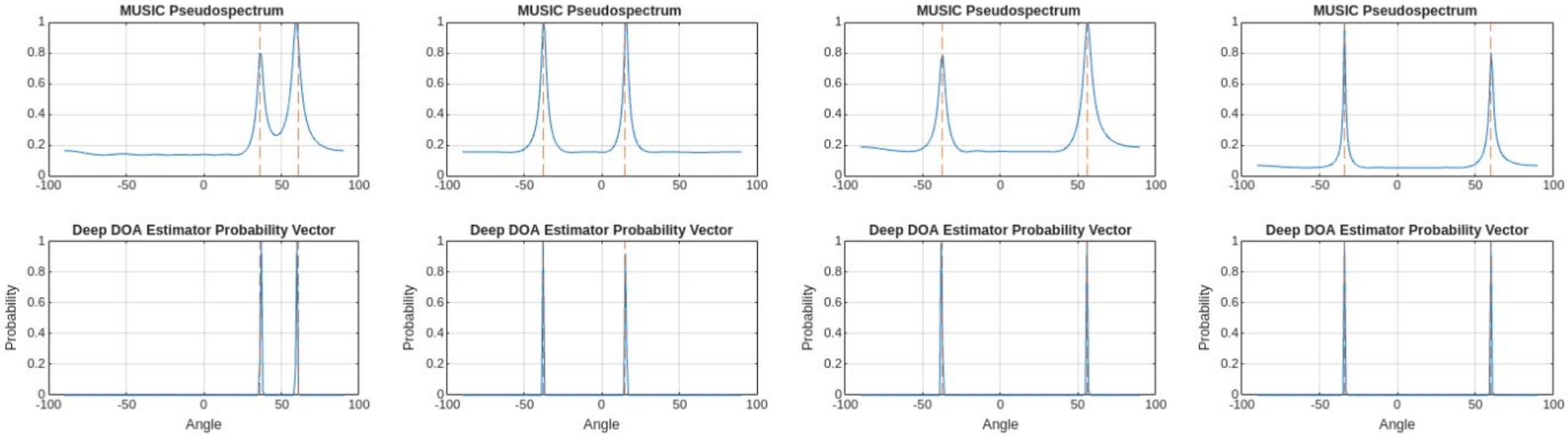

https://www.mathworks.com/help/phased/ug/direction-of-arrival-estimation-using-deep-learning.html

DL-Based DOA Estimation

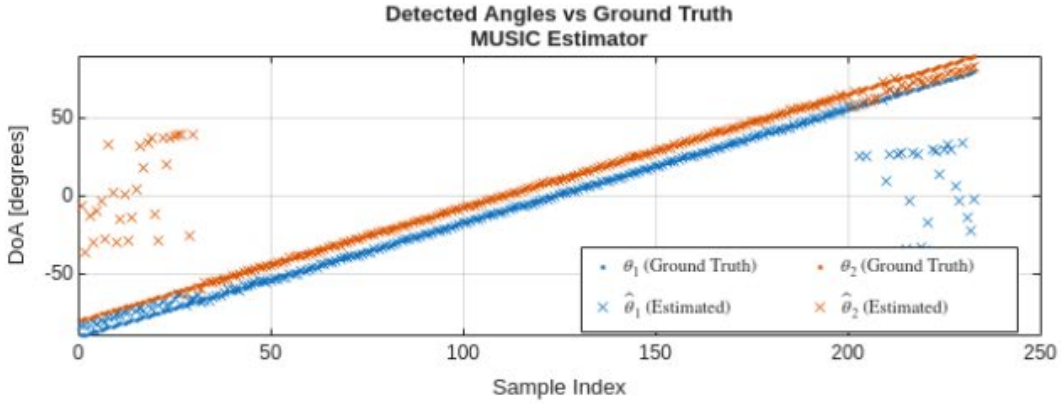

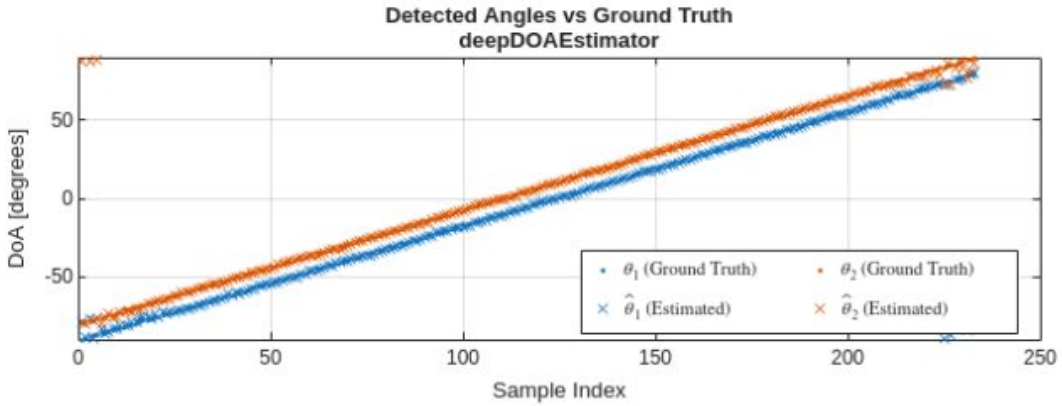

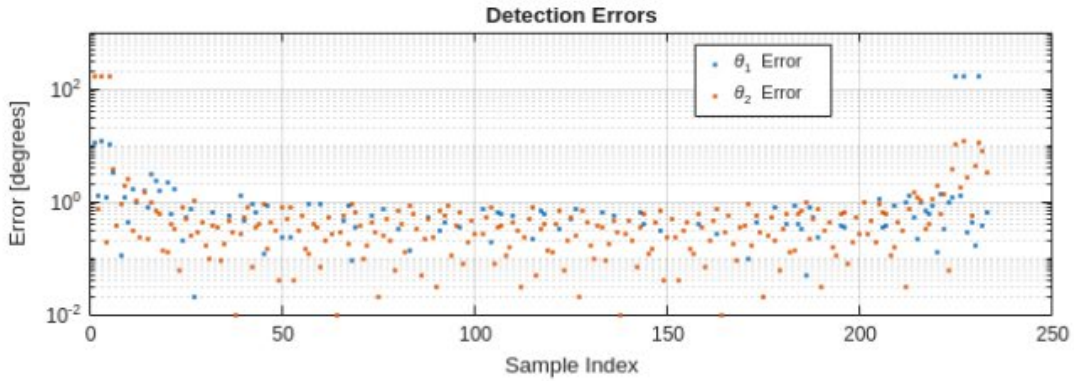

https://www.mathworks.com/help/phased/ug/direction-of-arrival-estimation-using-deep-learning.html

DL DOA Estimation: Multilabel Classification

- **Key Disadvantages:**
  - ✓ Fixed Grid Resolution
- Combinatorial Explosion:
  - ✓ With **N** possible target directions and **G** grid bins, the number of possible label combinations is: $\sum_{k}^{N}\binom{G}{k}$.
  - ✓ Grows **exponentially** with grid size and number of sources.
  - ✓ For example: A DOA grid from −60° to 60° with up to 3 targets results in 300,201 possible label combinations

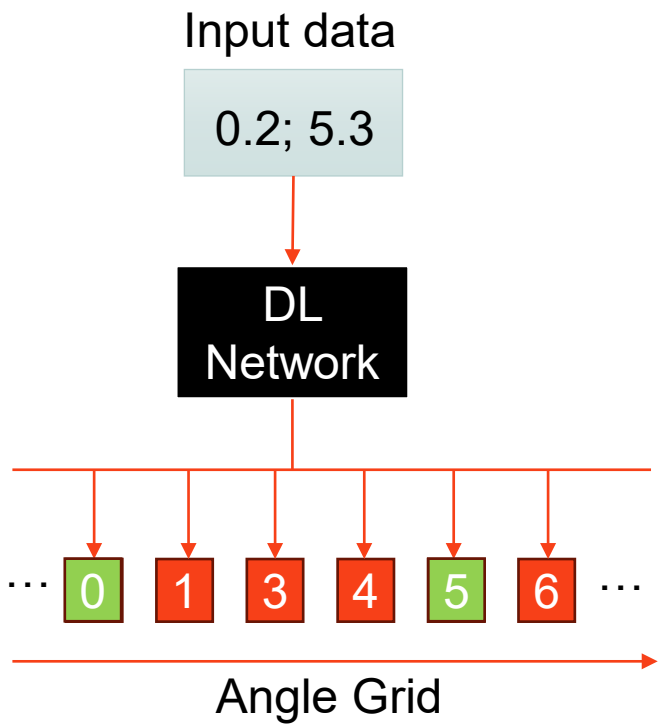

DL-Based DOA Estimation: Regression

- **Benefit**:

✓ Regression directly predicts the continuous angle values from the received radar/array signals.

✓ This allows estimation with finer resolution and avoids grid mismatch problems

- **Disadvantages**:

✓ Fixed Output Dimensionality

Network outputs a fixed number of DOAs. This means the architecture cannot easily adapt when the number of sources changes at runtime.

✓ Target Permutation Ambiguity

Ordering of output targets is arbitrary (e.g., source at 10° vs. 30° could be swapped in labels). This creates a permutation ambiguity problem — the loss function must be permutation-invariant (e.g., using Hungarian matching or set-based loss) to avoid penalizing correct but reordered predictions.

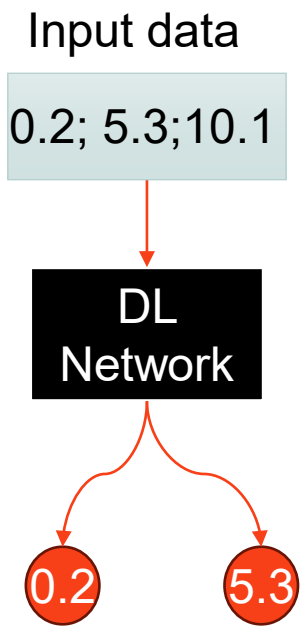

Model-Based vs. DL-Based DOA Estimation

Aspect	Model-Based	Deep Learning-Based
Accuracy	High under ideal assumptions	High with proper training
Interpretability	Transparent and explainable	Black-box; less interpretable
Data Requirement	Minimal	Large datasets needed
Robustness	Sensitive to mismatch/noise	Robust to noise and imperfections
Computation	Expensive at inference	Expensive to train, fast inference
Adaptability	Hard to adapt to new settings	Flexible; supports retraining
Prior Knowledge Use	Strong use of physics/model	May ignore priors unless guided
Scalability	Limited by matrix ops and grid size	Scales well with architecture

Model-Based Deep Learning

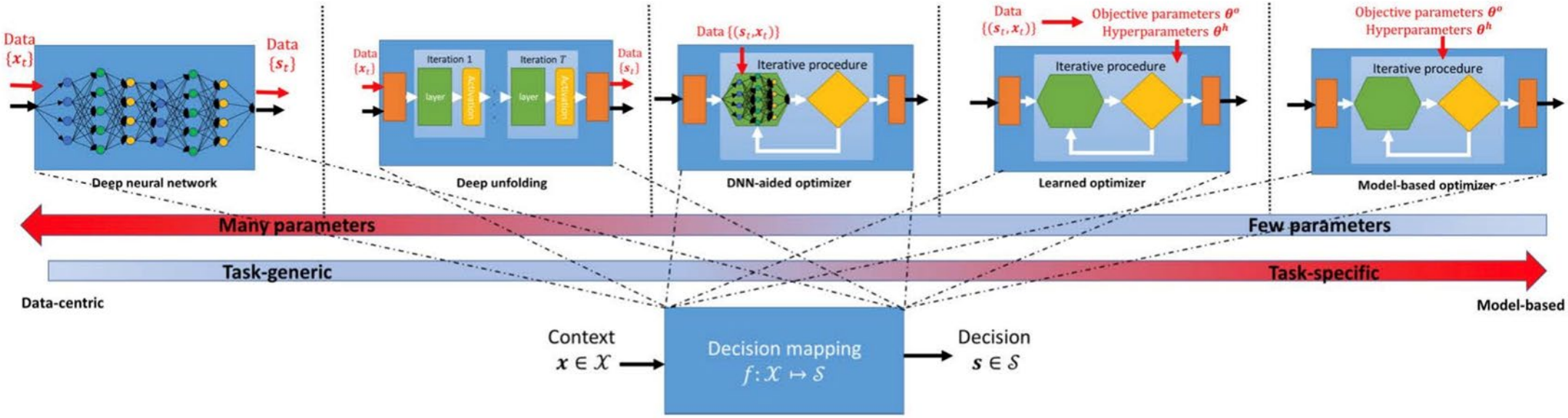

- Combining traditional mathematical models with data-driven systems.
- Utilizing domain knowledge and tailored mathematical structures.
- Creating principled and interpretable frameworks.
- Enhancing performance even with limited data availability.

N. Shlezinger, J. Whang, Y. C. Eldar and A. G. Dimakis, "Model-Based Deep Learning," in *Proceedings of the IEEE*, vol. 111, no. 5, pp. 465-499, May 2023.

Model-Based Deep Learning

- **Subspace based approaches:**

✓Model based: MUSIC, ESPRIT

✓Model based DL: SubspaceNet

- **Compressive Sensing based approaches:**

✓Model based: L1 norm optimization- ISTA, OMP

✓Model based DL: LISTA/T-LISTA/CC-LISTA

SubspaceNet

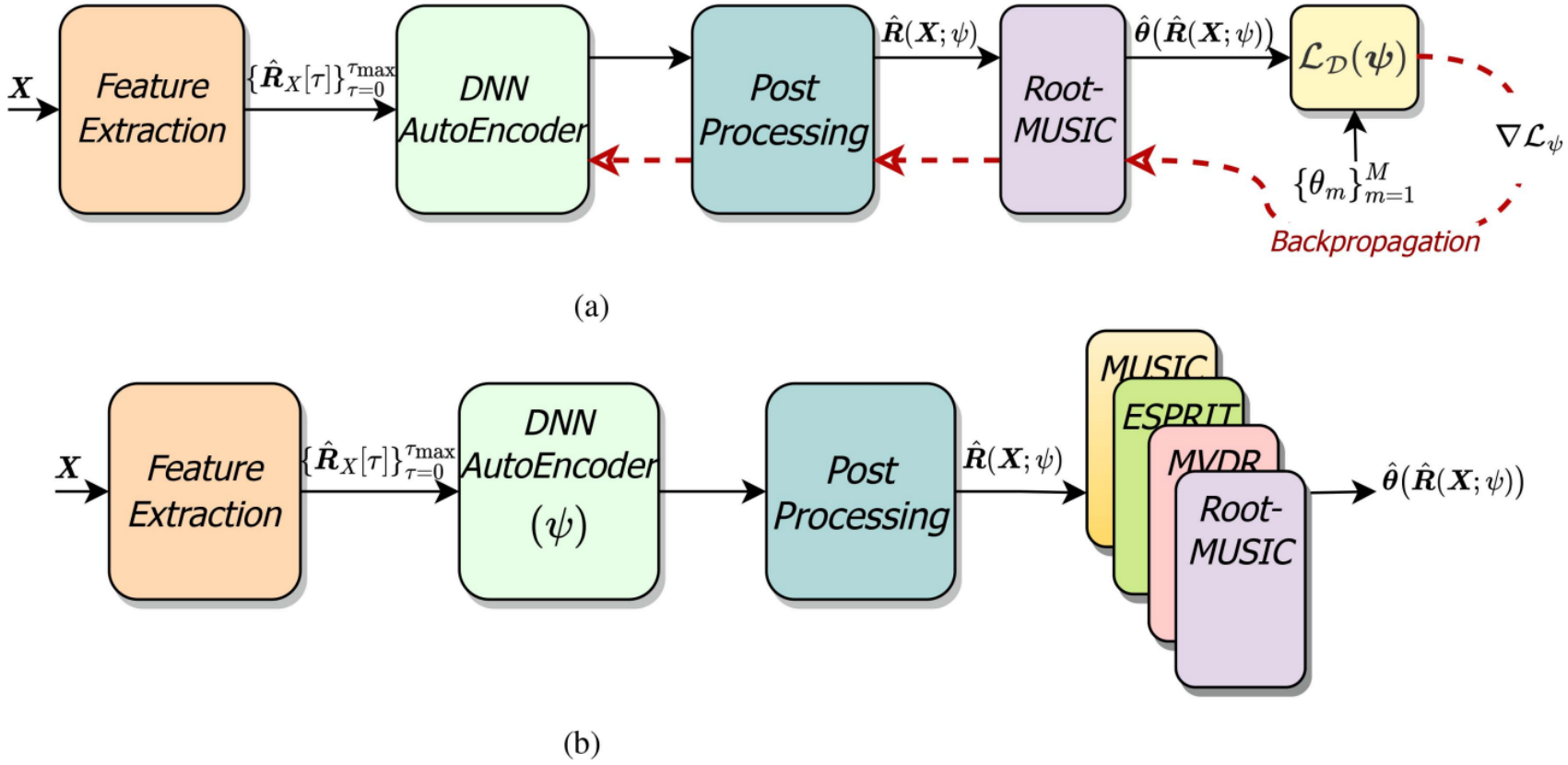

D. H. Shmuel, J. P. Merkofer, G. Revach, R. J. G. van Sloun and N. Shlezinger, “SubspaceNet: Deep Learning-Aided Subspace Methods for DoA Estimation,” in IEEE Transactions on Vehicular Technology, vol. 74, no. 3, pp. 4962-4976, March 2025.

SubspaceNet

Signals:
Low Rank
Low Snapshot
Low SNR
Coherent Sources

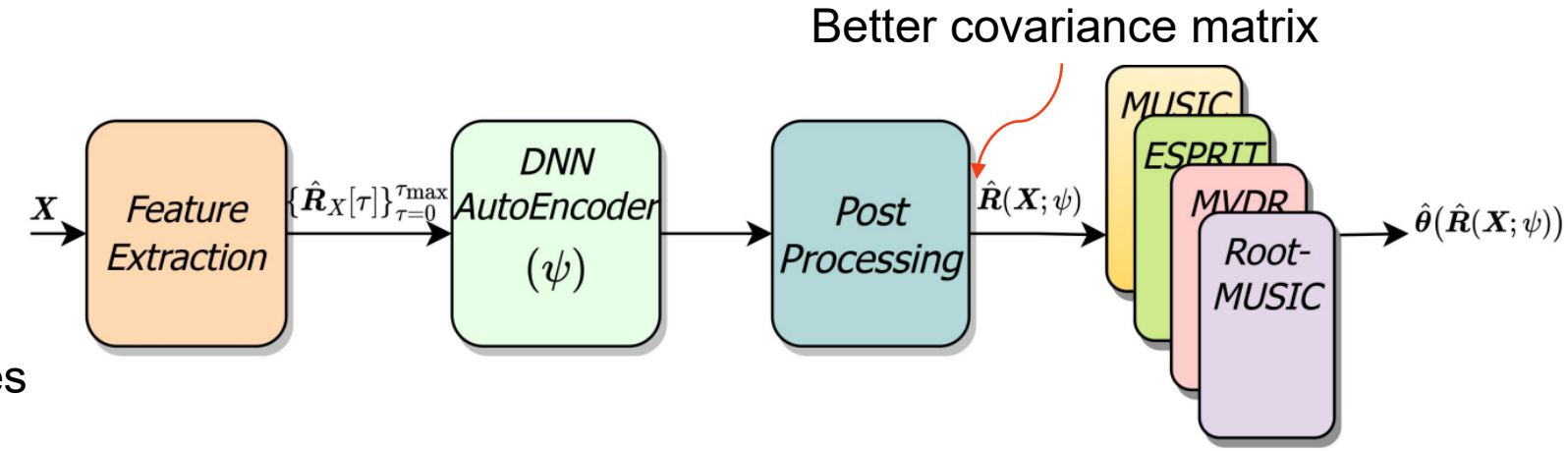

Target	Predicted (°)	Ground Truth (°)	Difference (°)
1	-49.37	-49.14	0.23
2	-22.24	-22.16	0.08

D. H. Shmuel, J. P. Merkofer, G. Revach, R. J. G. van Sloun and N. Shlezinger, “SubspaceNet: Deep Learning-Aided Subspace Methods for DoA Estimation,” in IEEE Transactions on Vehicular Technology, vol. 74, no. 3, pp. 4962-4976, March 2025.

Compressive Sensing

Array response can be written as: $\mathbf{y} = \mathbf{A}\mathbf{x} + \mathbf{n},$

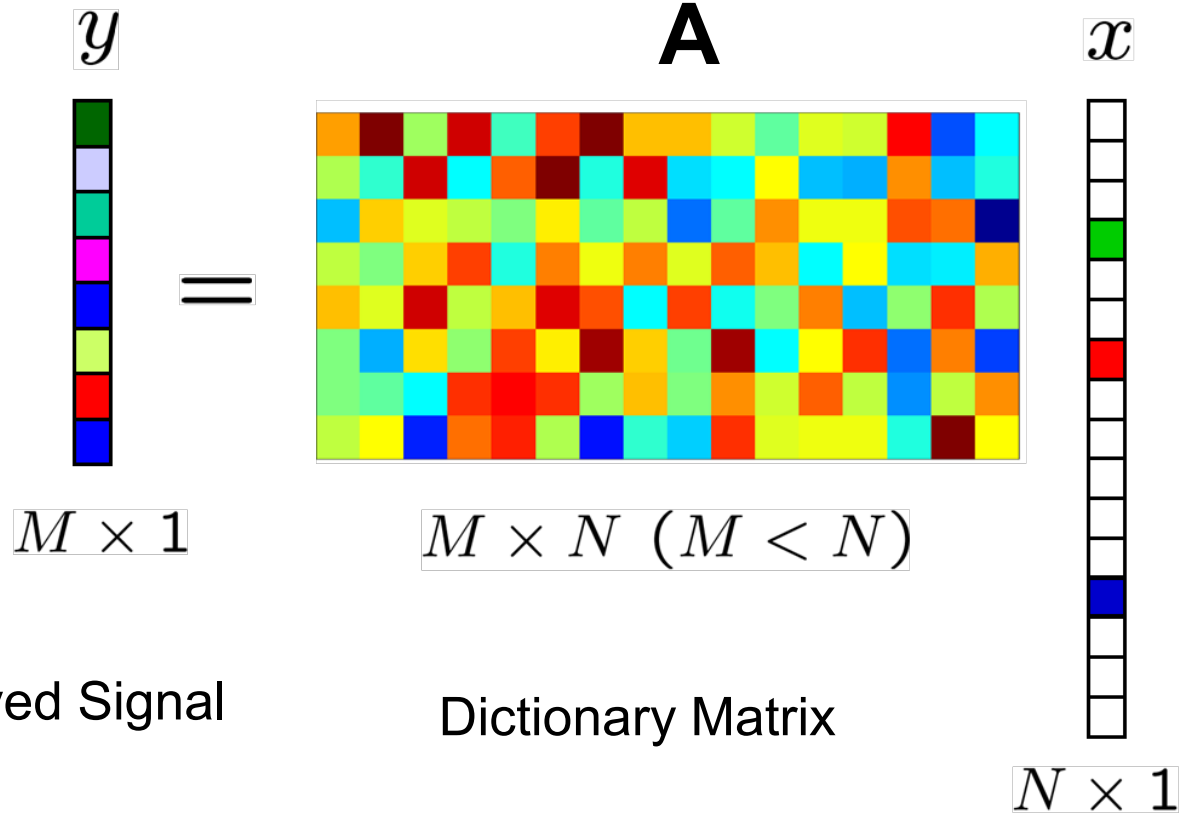

Received Signal

Dictionary Matrix

DOA estimation Spectrum

Compressive Sensing

- **L1-norm optimization problem**

$$\min_{x} \frac{1}{2} \|Ax - Y\|_2^2 + \lambda \|x\|_1$$

✓Iterative soft threshold algorithm (ISTA)

- **Greedy algorithms**

✓Orthogonal matching pursuit (OMP)

Iterative Soft Threshold Algorithm (ISTA)

- L1-norm optimization problem

$$\min_x \frac{1}{2}\|Ax - Y\|_2^2 + \lambda\|x\|_1$$

- Iteratively update x

$$x^{(t+1)} = S_\theta\left(\frac{1}{L}\boldsymbol{A}^H y + \left(\boldsymbol{I} - \frac{1}{\mathrm{L}}\boldsymbol{A}^H\mathbf{A}\right)x^{(t)}\right)$$

- FISTA/LISTA

ISTA vs FISTA Example

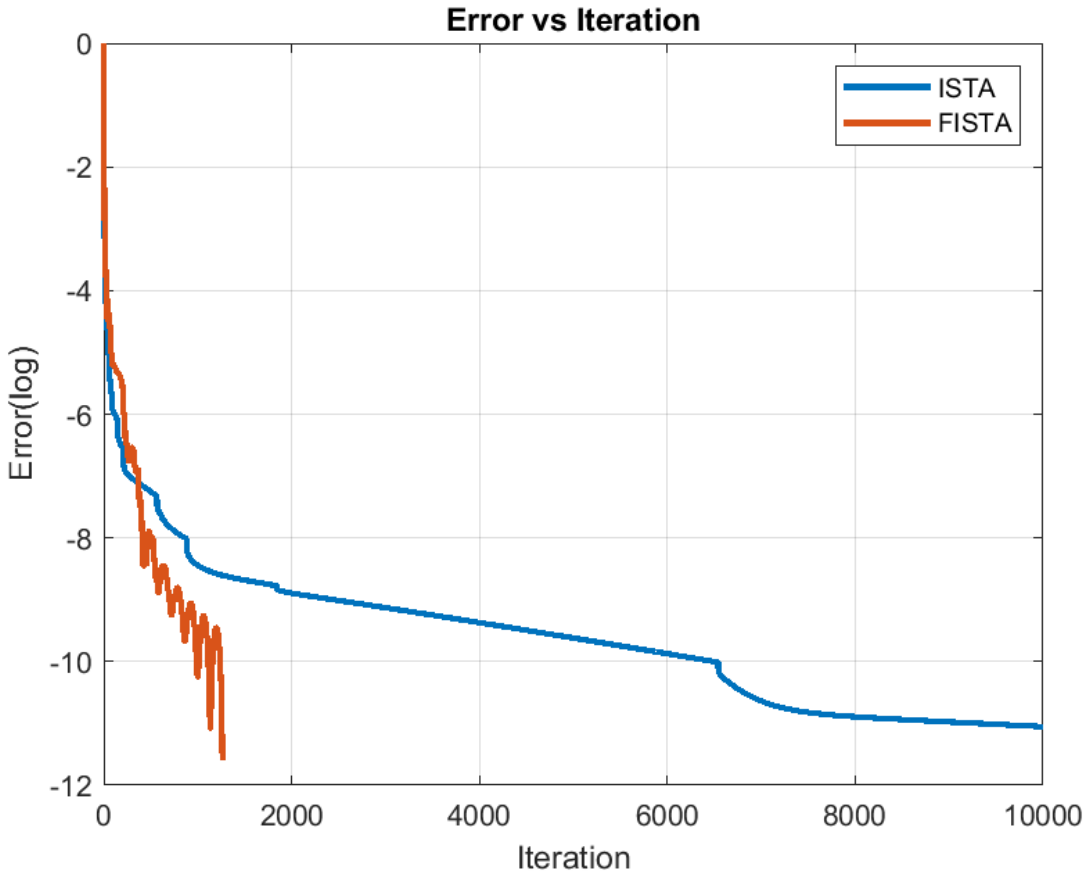

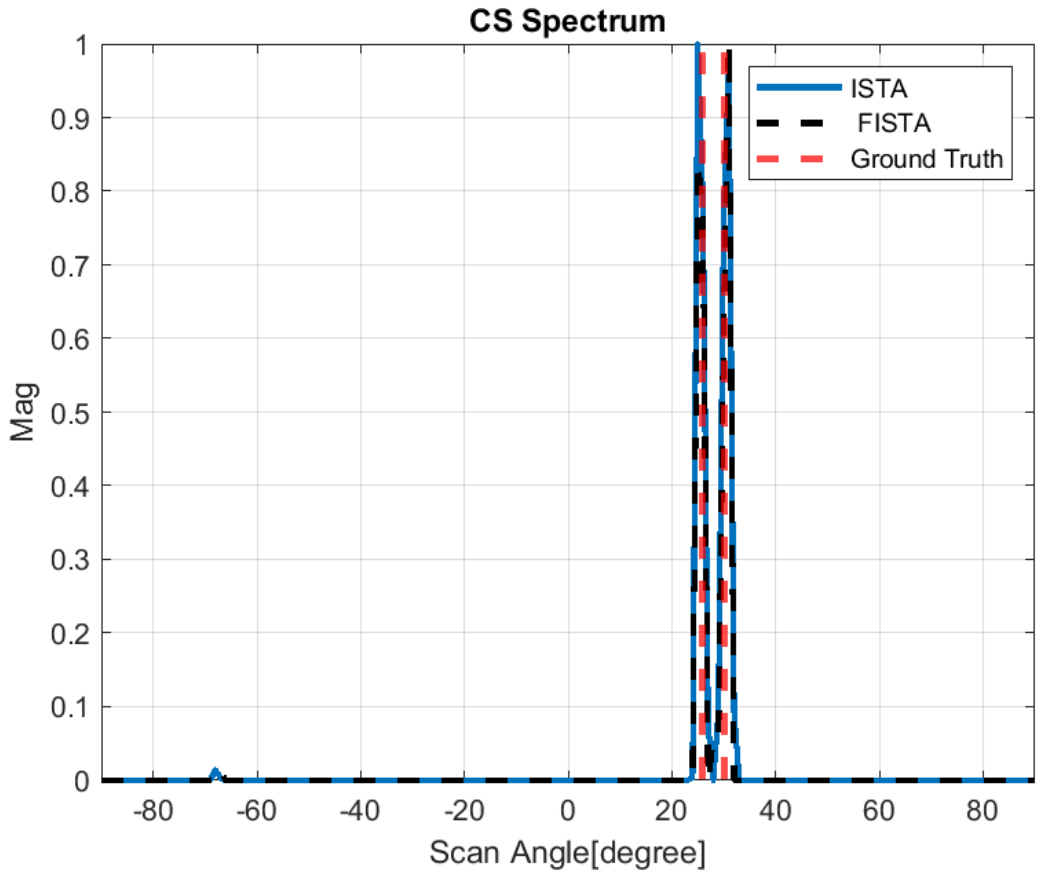

Deep Unrolling: LISTA

- **ISTA**

$$x^{(t+1)} = S_\theta\left(\frac{1}{L}A^H y + \left(I - \frac{1}{L}A^H A\right)x^{(t)}\right)$$

- **LISTA**

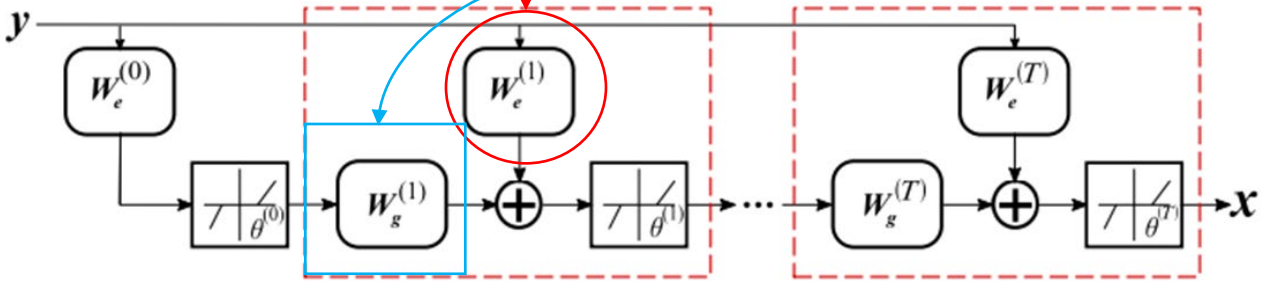

- **T-LISTA/CC-LISTA**
- Lower trainable parameters

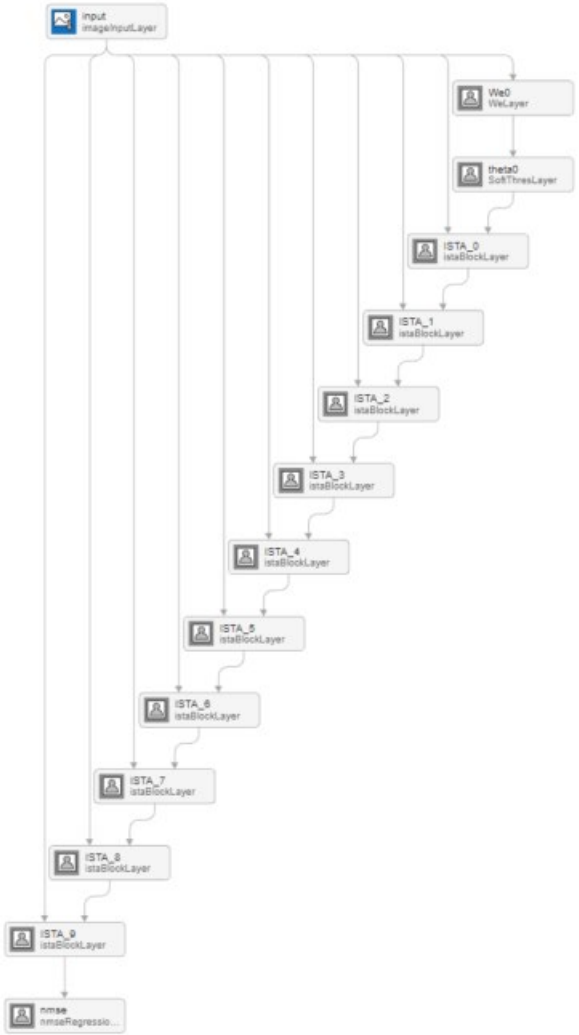

Karol Gregor and Yann LeCun, “Learning Fast Approximations of Sparse Coding,” ICML, 2010.

LISTA vs FISTA

```
tic
out0 = forward(net,tmpdl);
toc
```

LISTA

```
Elapsed time is 0.096694 seconds.
```

```
tic
[x_ista,error_ista] = ista(X.',Adict,'FISTA',true);
toc
```

```
Elapsed time is 0.212798 seconds.
```

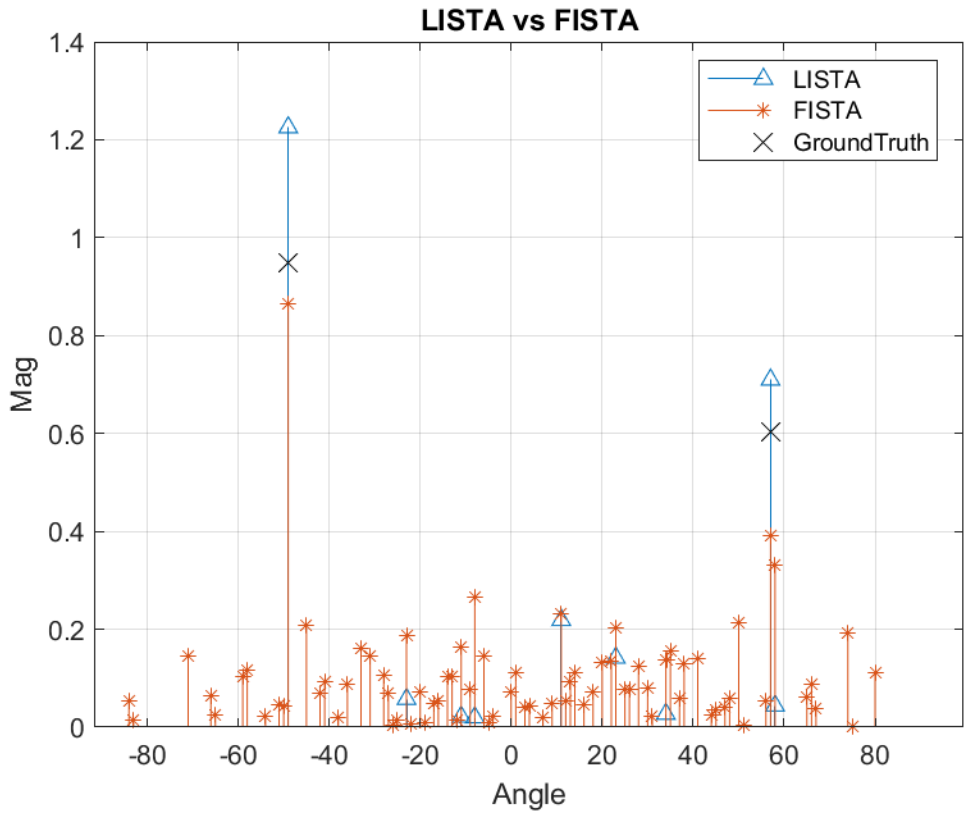

Iterative Adaptive Approach (IAA)

- Iterative adaptive approach (IAA) tries to solve a weighted least square problem.
- The cost function is $\|\boldsymbol{y} - s_l \boldsymbol{a}(\theta_l)\|^2_{\boldsymbol{Q}^{-1}(\theta_l)}$, where $\|\boldsymbol{X}\|^2_{\boldsymbol{Q}^{-1}(\theta_l)} = \boldsymbol{X}^H \boldsymbol{Q}^{-1}(\theta_l)\, \boldsymbol{X}$ and interference and noise covariance matrix is denoted by $\boldsymbol{Q}(\theta_l) = \boldsymbol{R}_f - P_l \boldsymbol{a}(\theta_l)\boldsymbol{a}^H(\theta_l)$.
- Here, $\boldsymbol{R}$ is the constructed array covariance matrix $\mathbf{R}_f = \mathbf{A}(\boldsymbol{\theta})\mathbf{P}\mathbf{A}^H(\boldsymbol{\theta})$ with P being a diagonal matrix and the

$$P_l = \frac{1}{T}\sum_{t=1}^{T} |\hat{s}(t)|^2$$

- The weighted least square solution is

$$\hat{s}_l = \frac{\mathbf{a}^H(\theta_l)\mathbf{R}_f^{-1}}{\mathbf{a}^H(\theta_l)\mathbf{R}_f^{-1}\mathbf{a}(\theta_l)}\mathbf{y}.$$

Yardibi, Tarik, et al. "Source localization and sensing: A nonparametric iterative adaptive approach based on weighted least squares." *IEEE Transactions on Aerospace and Electronic Systems* 46.1 (2010): 425-443.

Iterative Adaptive Approach (IAA)

TABLE II
The IAA-APES Algorithm

$$\hat{P}_k = \frac{1}{(\mathbf{a}^H(\theta_k)\mathbf{a}(\theta_k))^2 N} \sum_{n=1}^{N} |\mathbf{a}^H(\theta_k)\mathbf{y}(n)|^2, \qquad k = 1,\ldots,K$$

Beam Scan

repeat

$$\mathbf{R} = \mathbf{A}(\theta)\hat{\mathbf{P}}\mathbf{A}^H(\theta)$$

for $k = 1,\ldots,K$

$$\hat{s}_k(n) = \frac{\mathbf{a}^H(\theta_k)\mathbf{R}^{-1}\mathbf{y}(n)}{\mathbf{a}^H(\theta_k)\mathbf{R}^{-1}\mathbf{a}(\theta_k)}, \qquad n = 1,\ldots,N$$

MPDR

$$\hat{P}_k = \frac{1}{N}\sum_{n=1}^{N} |\hat{s}_k(n)|^2$$

end for

until (convergence)

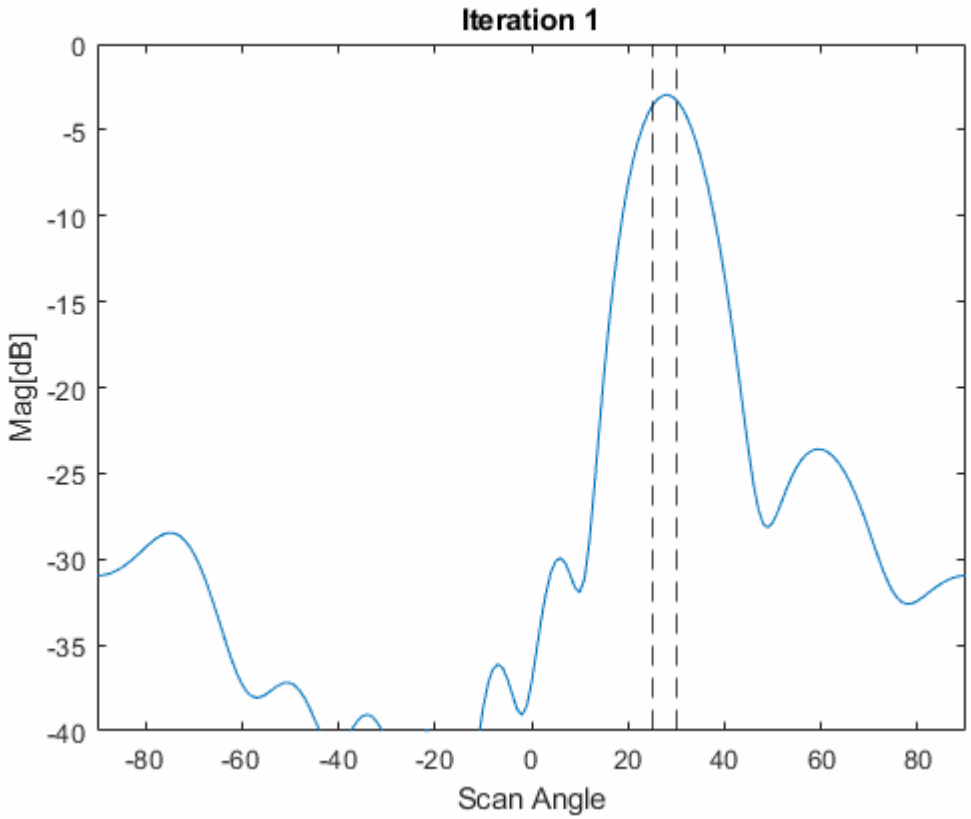

Yardibi, Tarik, et al. "Source localization and sensing: A nonparametric iterative adaptive approach based on weighted least squares." *IEEE Transactions on Aerospace and Electronic Systems* 46.1 (2010): 425-443.

Agenda

- **Background and Motivation of DL for DOA Estimation**
  - ✓ Overview of deep learning (DL) for DOA estimation
  - ✓ Comparison: data-driven vs. model-based approaches
  - ✓ Why hybrid model-based deep learning matters
- **DL for High-Resolution Radar Imaging**
  - ✓ Unrolling IAA
  - ✓ Physics-guided 1D neural networks for radar imaging
  - ✓ DOA estimation considering antenna failure
  - ✓ Off-grid DOA estimation with 1-bit single-snapshot sparse array
  - ✓ Siamese neural networks for DOA estimation
- **DL for Integrated Sensing and Communications (ISAC)**
- **DL Enabled Sparse Array Interpolation**
  - ✓ Unrolling IHT for matrix completion
  - ✓ Transformer based array interpolation

Unrolling IAA

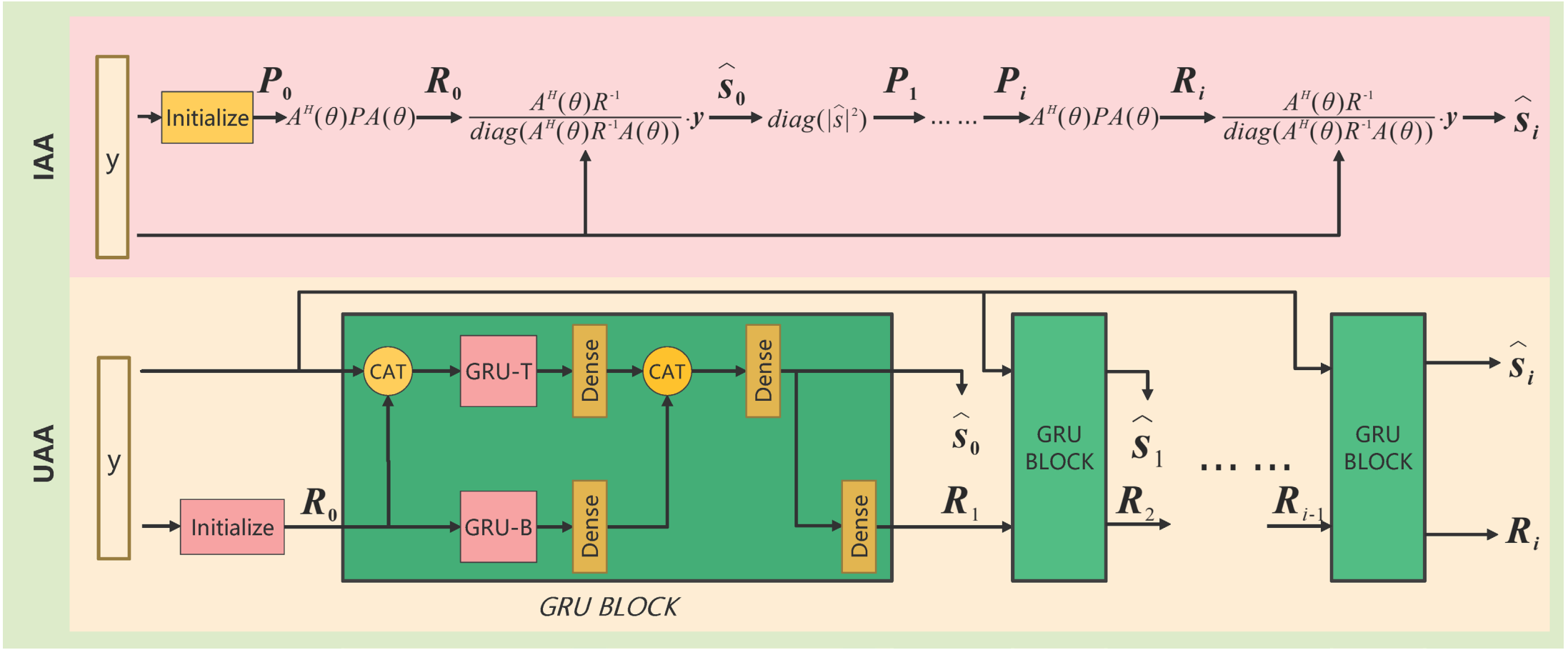

R. Zheng, H. Liu, S. Sun, and J. Li, “Deep learning based computationally efficient unrolling IAA for direction-of-arrival estimation,” in Proc. European Signal Processing Conference (EUSIPCO), Helsinki, Finland, Sept. 4-8, 2023.

Unrolling IAA

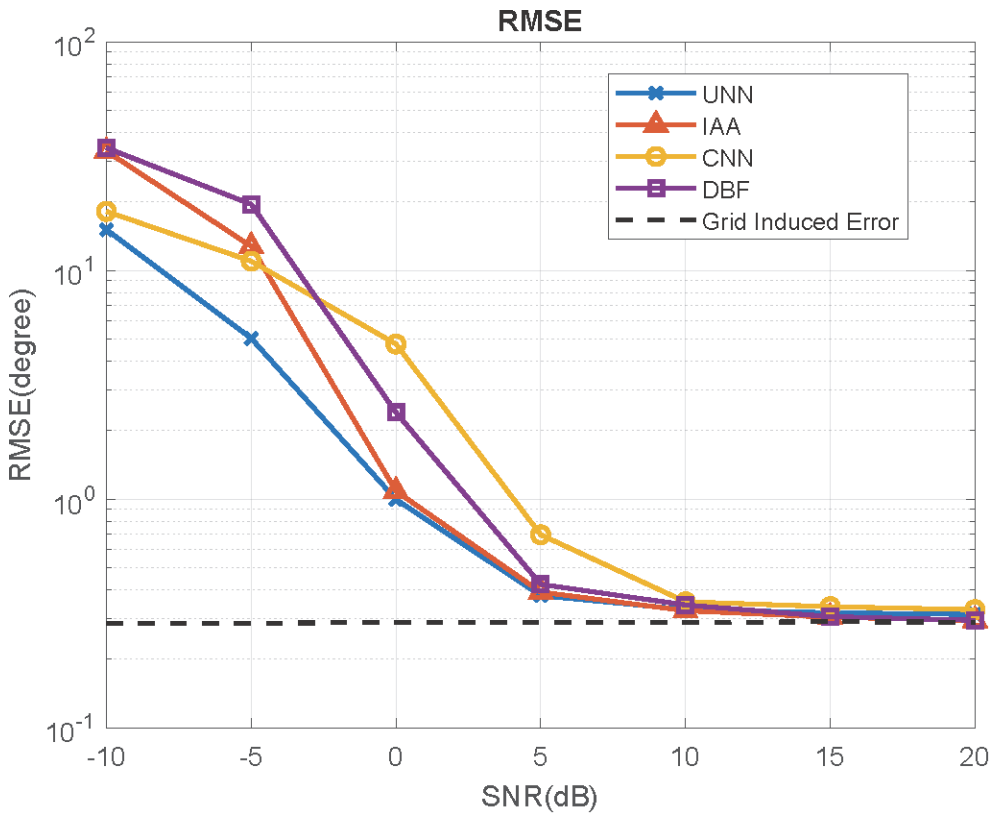

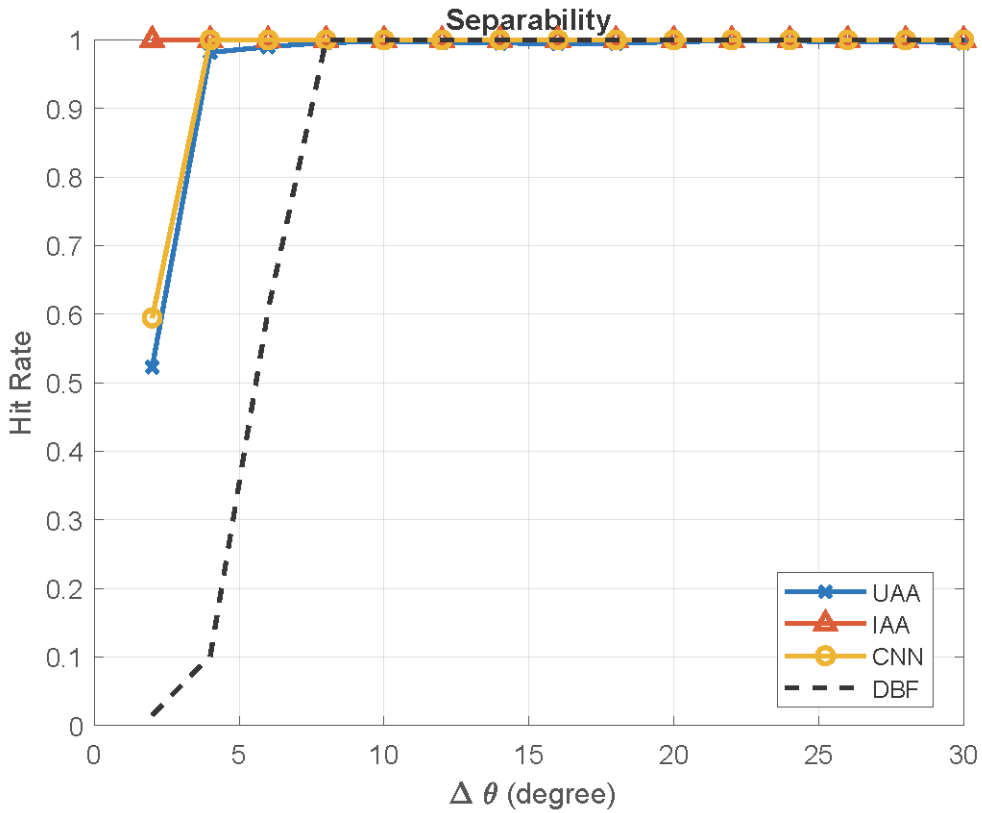

Unrolling IAA

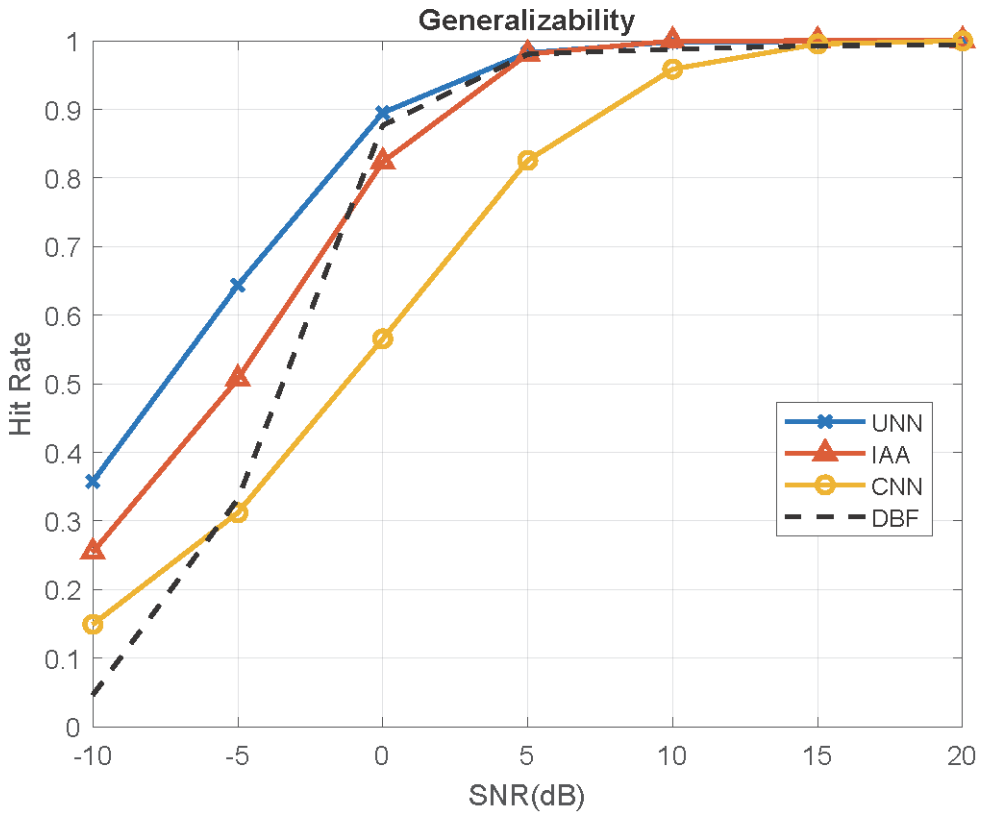

Methods	Inference Time (ms)	# Trainable Parameters
DBF	0.12	–
IAA	49.9	–
CNN	1.0	49, 216, 317
UAA	5.7	127, 4096

Agenda

- **Background and Motivation of DL for DOA Estimation**
  - ✓ Overview of deep learning (DL) for DOA estimation
  - ✓ Comparison: data-driven vs. model-based approaches
  - ✓ Why hybrid model-based deep learning matters
- **DL for High-Resolution Radar Imaging**
  - ✓ Unrolling IAA
  - ✓ Physics-guided 1D neural networks for radar imaging
  - ✓ DOA estimation considering antenna failure
  - ✓ Off-grid DOA estimation with 1-bit single-snapshot sparse array
  - ✓ Siamese neural networks for DOA estimation
- **DL for Integrated Sensing and Communications (ISAC)**
- **DL Enabled Sparse Array Interpolation**
  - ✓ Unrolling IHT for matrix completion
  - ✓ Transformer based array interpolation

Model-Based Knowledge-Driven Learning Approach for Enhanced High-Resolution Automotive Radar Imaging

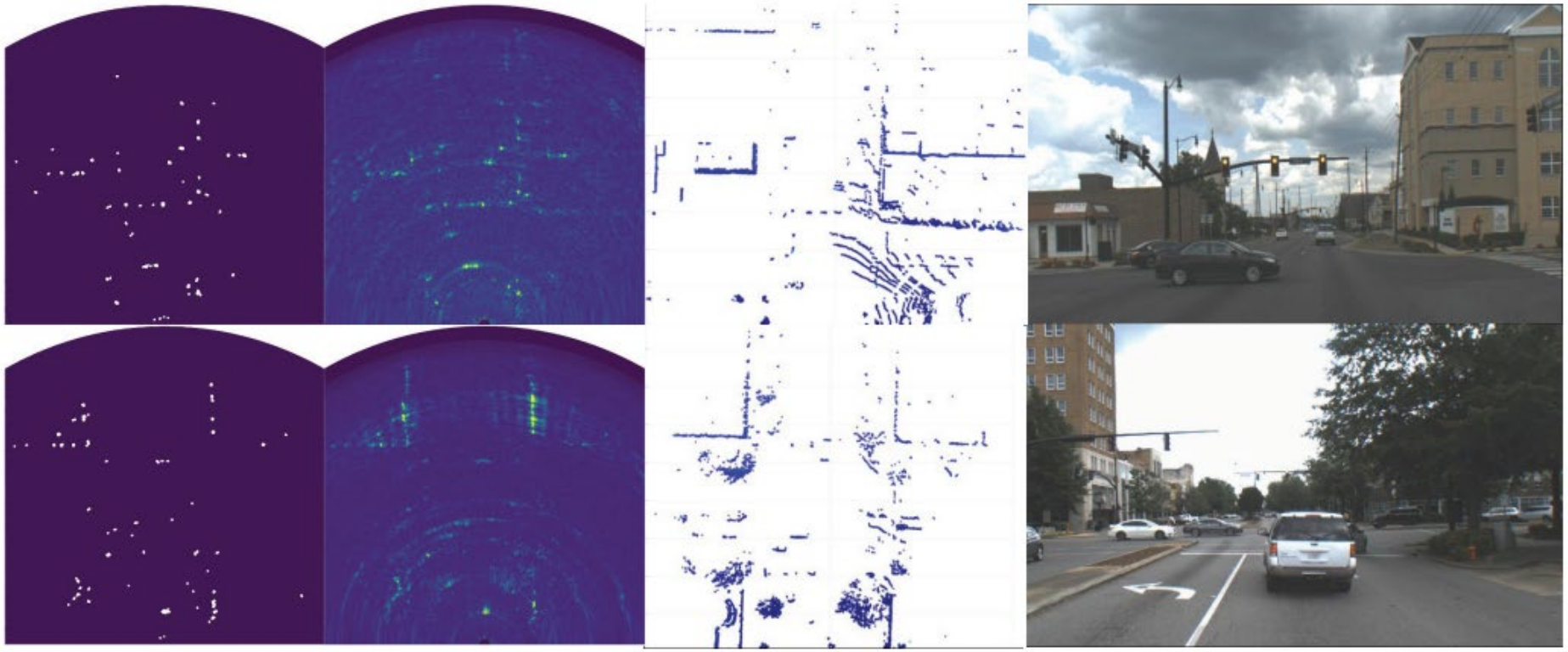

Fig. 2. Radar point clouds, RA maps in Cartesian coordinates, LiDAR point clouds in bird's eye view, and camera image (left-to-right).

R. Zheng, S. Sun, H. Liu, H. Chen and J. Li, "Model-Based Knowledge-Driven Learning Approach for Enhanced High-Resolution Automotive Radar Imaging," in IEEE Transactions on Radar Systems, vol. 3, pp. 709-723, 2025.

Current Radar Image Super-Resolution

- **Image super resolution**

✓ Increase the pixel density

- **Radar image**

✓ Fixed pixel density

Current Radar Image Super-Resolution

- **Image super resolution**

✓ Increase the pixel density

- **Radar image**

✓ Fixed pixel density

- **Current solution**

✓ Image-to-image → UNet 2d

✓ Range-Azimuth heatmap

✓ Volume-to-volume→ UNet 3d

✓ Range-Doppler-Azimuth heatmap

✓ Lack of domain knowledge

- **Small aperture → large aperture**

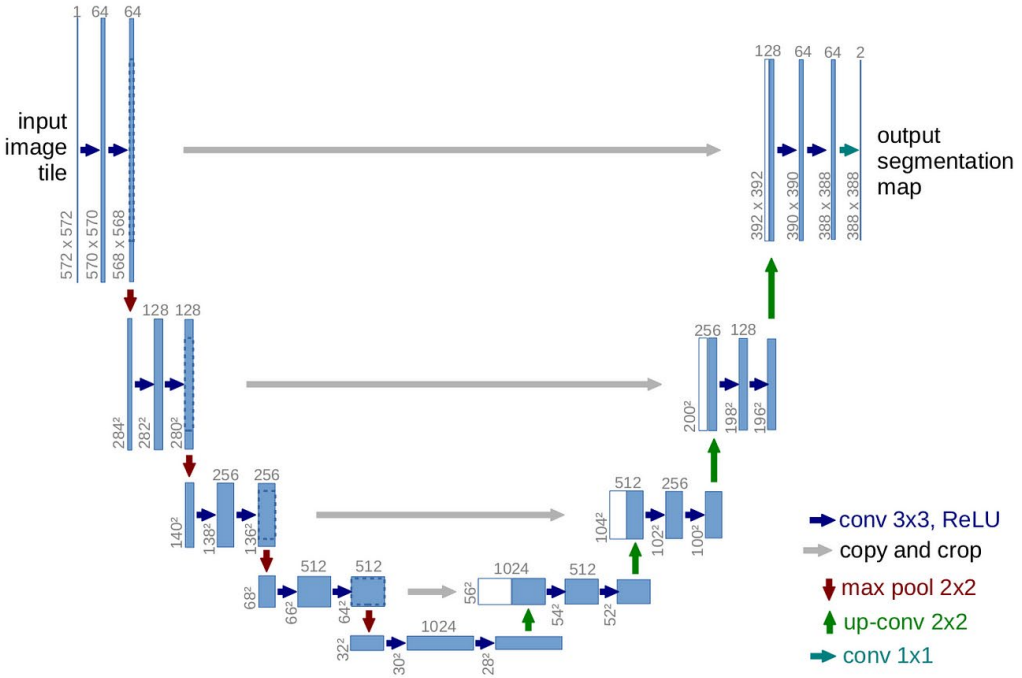

Proposed Method

- **Ground Truth Processing: Use a super-resolution algorithm (IAA) on a larger antenna array to create high-resolution images as ground truth.**
- **Signal-to-Spectrum Approach: Frame radar image super-resolution as a one-dimensional signal to super-resolution spectrum problem.**
- **Incorporate Radar Expertise:**

✓ Normalize data for consistency.

✓ Tailor loss function to radar imaging specifics.

✓ Signal level augmentation

- **Advantages:**

✓ Enhanced performance in image resolution.

✓ Reduced need for extensive training datasets.

✓ Lightweight model architecture.

✓ Scalable across different radar imaging applications.

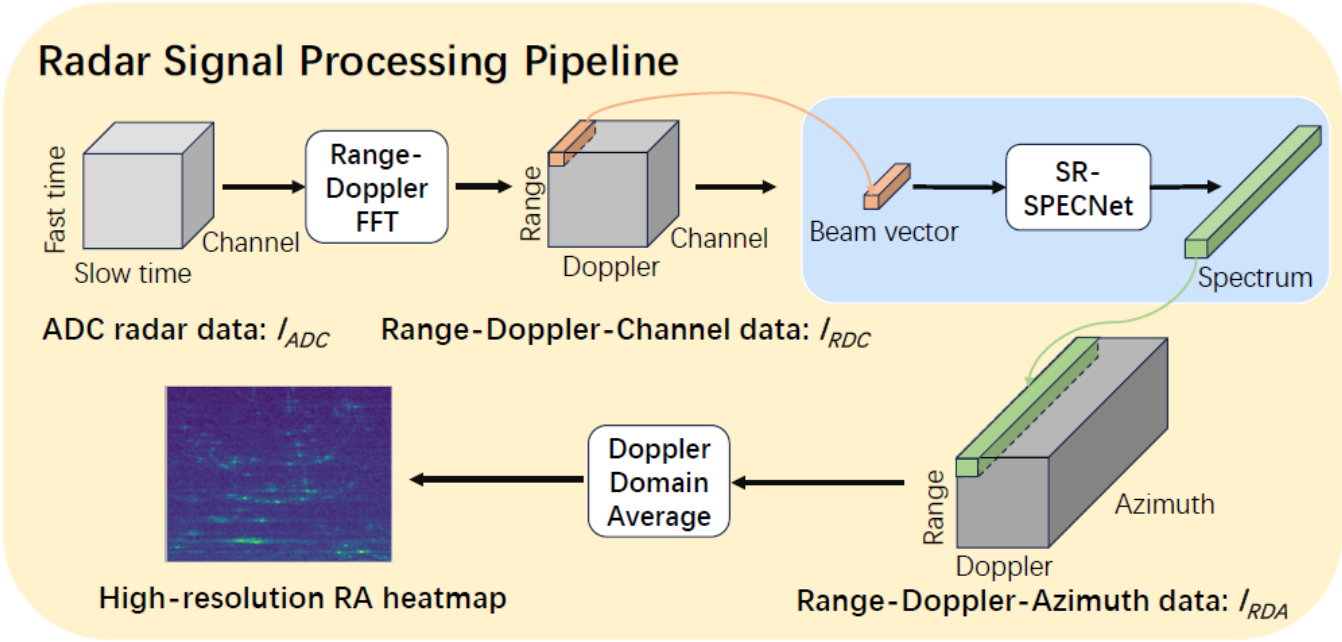

Iterative Adaptive Approach (IAA)

TABLE II
The IAA-APES Algorithm

$$\hat{P}_k = \frac{1}{(\mathbf{a}^H(\theta_k)\mathbf{a}(\theta_k))^2 N} \sum_{n=1}^{N} |\mathbf{a}^H(\theta_k)\mathbf{y}(n)|^2, \qquad k = 1,\ldots,K$$

Beam Scan

repeat

$$\mathbf{R} = \mathbf{A}(\boldsymbol{\theta})\hat{\mathbf{P}}\mathbf{A}^H(\boldsymbol{\theta})$$

for $k = 1,\ldots,K$

$$\hat{s}_k(n) = \frac{\mathbf{a}^H(\theta_k)\mathbf{R}^{-1}\mathbf{y}(n)}{\mathbf{a}^H(\theta_k)\mathbf{R}^{-1}\mathbf{a}(\theta_k)}, \qquad n = 1,\ldots,N$$

MPDR

$$\hat{P}_k = \frac{1}{N}\sum_{n=1}^{N} |\hat{s}_k(n)|^2$$

end for

until (convergence)

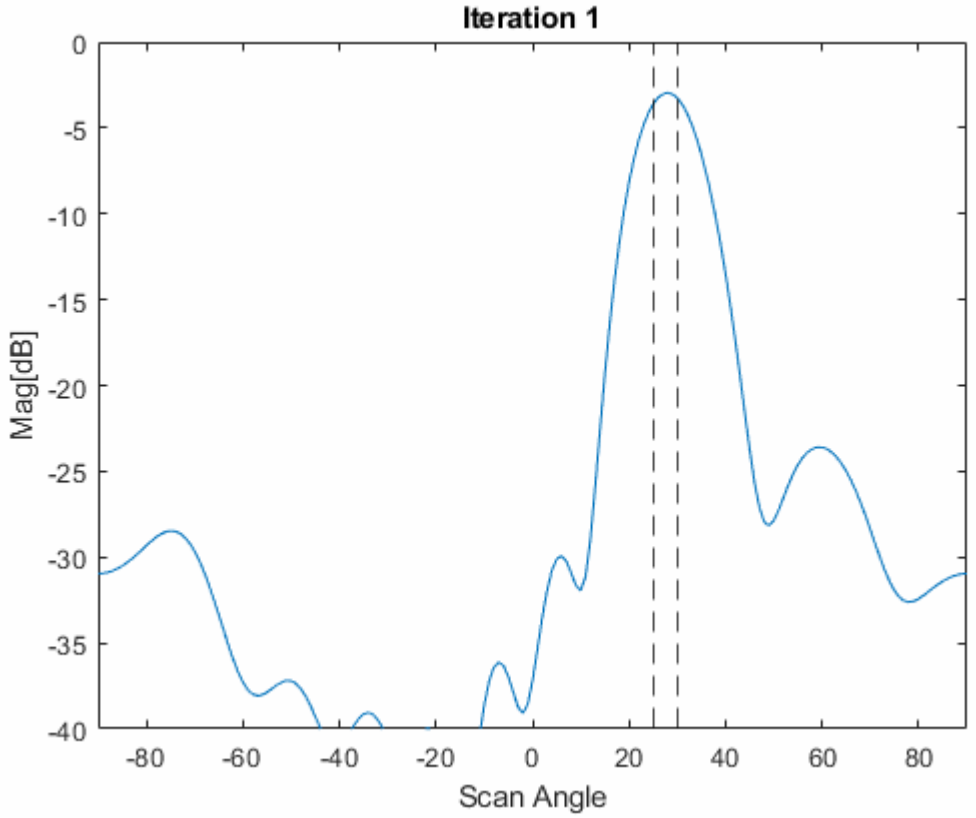

Yardibi, Tarik, et al. "Source localization and sensing: A nonparametric iterative adaptive approach based on weighted least squares." *IEEE Transactions on Aerospace and Electronic Systems* 46.1 (2010): 425-443.

SR-SPECNet

IAA

$$\hat{s}_{l(n)} = \frac{\mathbf{a}^H(\theta_l)\,\mathbf{R}_{(n-1)}^{-1}\mathbf{y}}{\mathbf{a}^H(\theta_l)\,\mathbf{R}_{(n-1)}^{-1}\mathbf{a}(\theta_l)}.$$

$$\hat{\mathbf{s}}_{(n)} = T\left(\hat{\mathbf{s}}_{(n-1)}, \mathbf{y}\right) \oslash B\left(\hat{\mathbf{s}}_{(n-1)}\right)$$

$$\hat{s}_{l(0)} = \left|\frac{\mathbf{a}^H(\theta_l)\,\mathbf{y}}{N_{\text{ch}}}\right|$$

$$T\left(\hat{\mathbf{s}}_{(n-1)}, \mathbf{y}\right) = \mathbf{A}^H(\boldsymbol{\theta})\,\mathbf{R}_{(n-1)}^{-1}\mathbf{y}$$

$$B\left(\hat{\mathbf{s}}_{(n-1)}\right) = \text{Diag}\left(\mathbf{A}^H(\boldsymbol{\theta})\,\mathbf{R}_{(n-1)}^{-1}\mathbf{A}(\boldsymbol{\theta})\right)$$

$$\mathbf{R}_{(n-1)} = \mathbf{A}(\boldsymbol{\theta})\,\text{diag}\left(\hat{\mathbf{s}}_{(n-1)}^2\right)\mathbf{A}^H(\boldsymbol{\theta})$$

SR-SPECNet

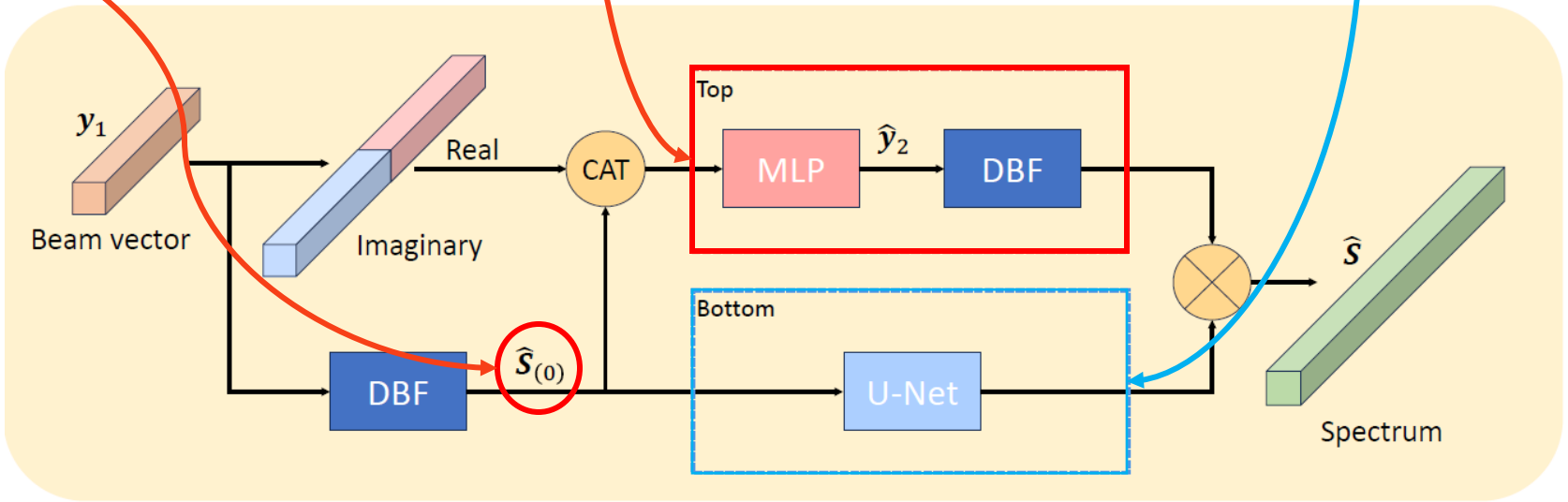

SR-SPECNet

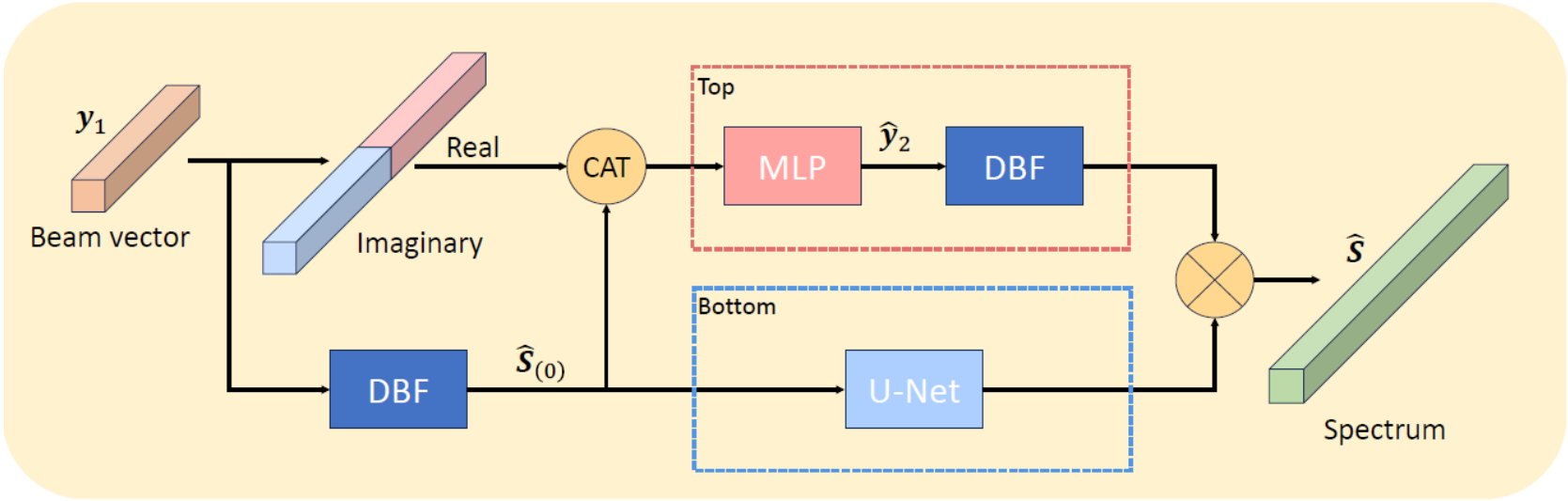

Data Preprocessing

Frequency domain normalization,

$y_{norm} = \frac{y}{\alpha}$,

where $\alpha = \max(\frac{A_H(\theta)y}{N_{ch}})$

SR-SPECNet

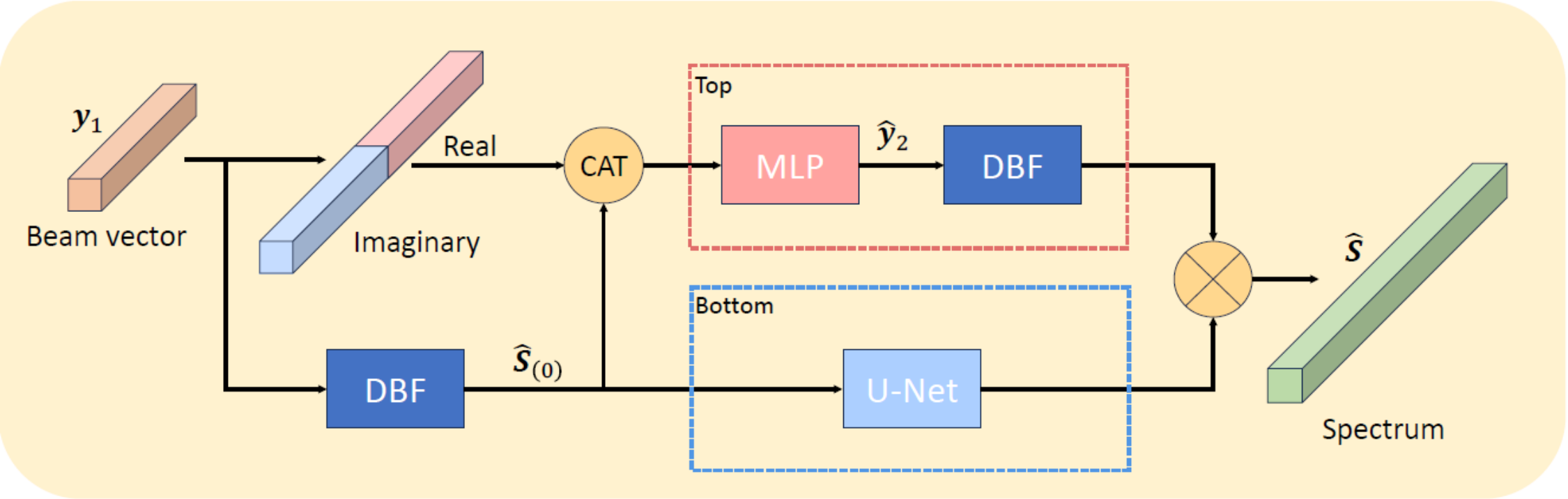

Data Preprocessing

Frequency domain normalization,

$y_{norm} = \frac{y}{\alpha}$,

where $\alpha = \max(\frac{A_H(\theta)y}{N_{ch}})$

Signal level Augmentation

Flip: Conjugate of the signal

Shift: $y_{shift} = a(\Delta\theta) \otimes y$

SR-SPECNet

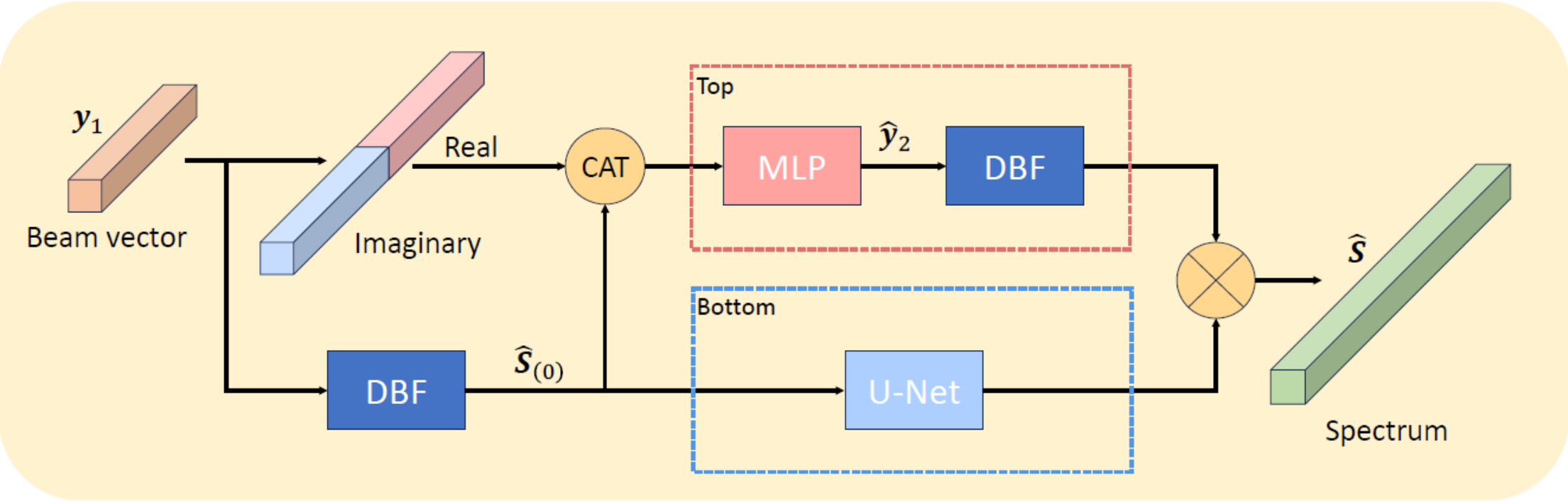

Data Preprocessing

Frequency domain normalization,

$y_{norm} = \frac{y}{\alpha}$,

where $\alpha = \max(\frac{A_H(\theta)y}{N_{ch}})$

Signal level Augmentation

Flip: Conjugate of the signal

Shift: $y_{shift} = a(\Delta\theta) \otimes y$

SNR-Guided Loss Function

$$L_{SNR} = \alpha \frac{1}{L} \sum_{i=1}^{L} (S_i - \hat{S}_i)^2$$

Data Collection Platform

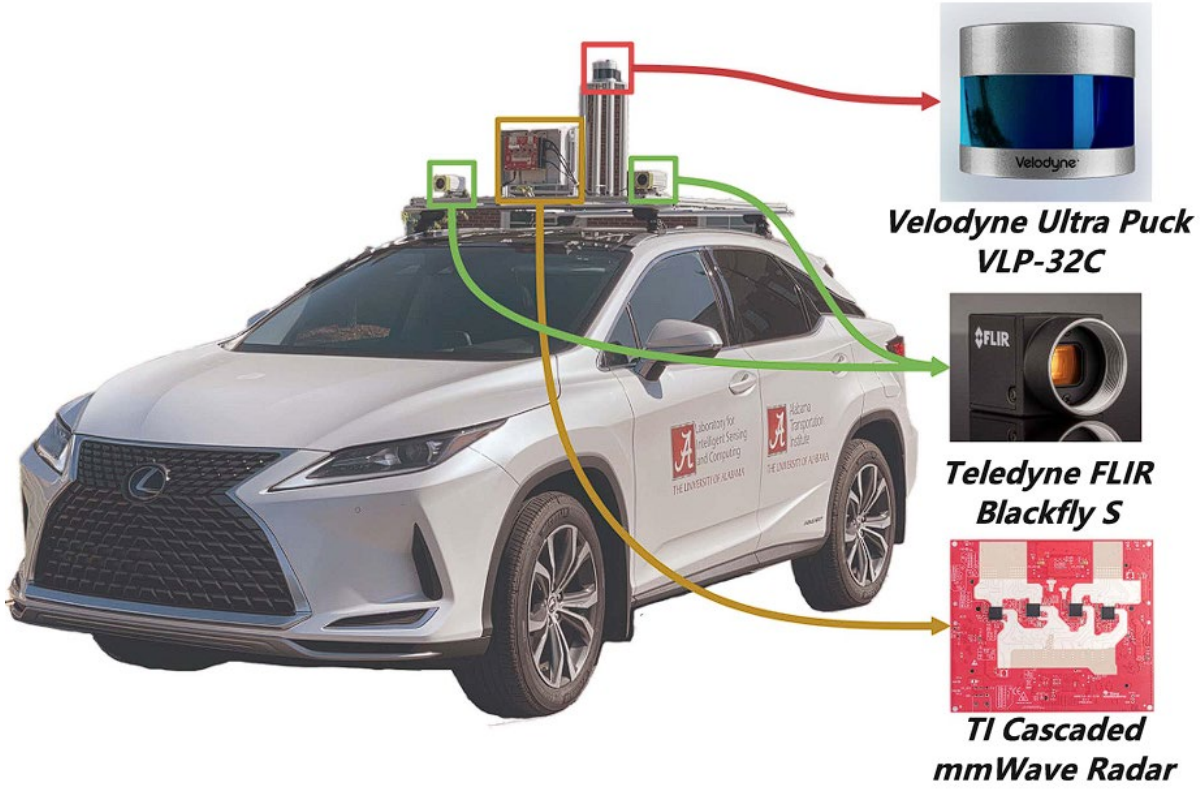

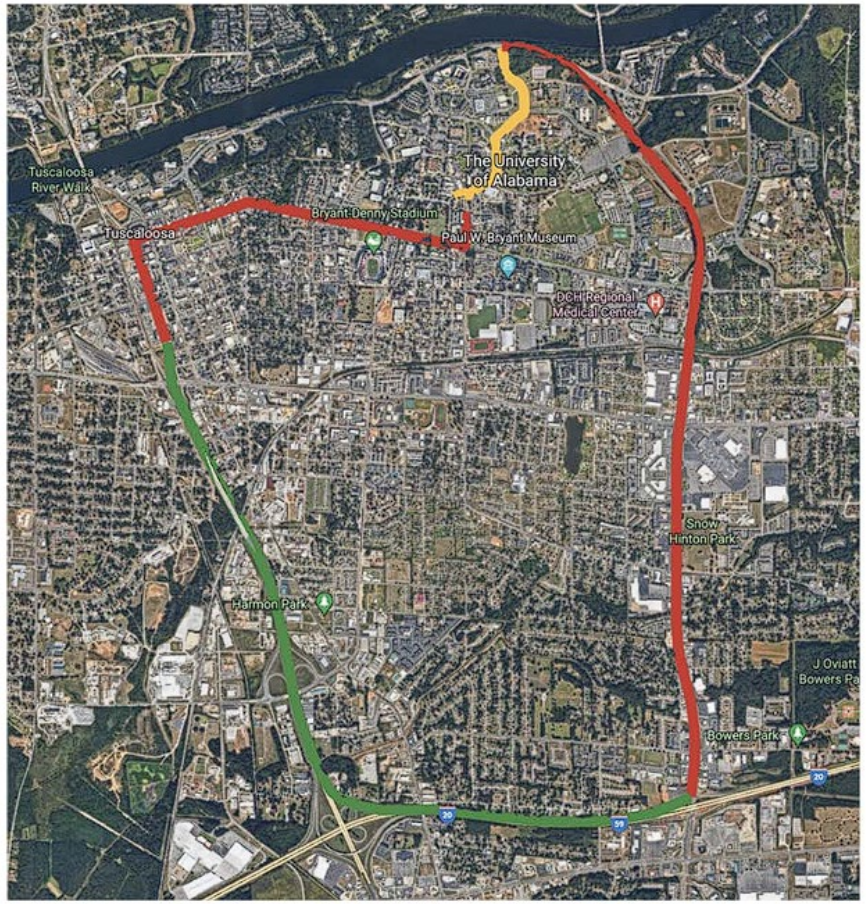

R. Zheng, S. Sun, H. Liu and T. Wu, “Deep-Neural-Network-Enabled Vehicle Detection Using High-Resolution Automotive Radar Imaging,” in IEEE Transactions on Aerospace and Electronic Systems, vol. 59, no. 5, pp. 4815-4830, Oct. 2023.

RA Examples

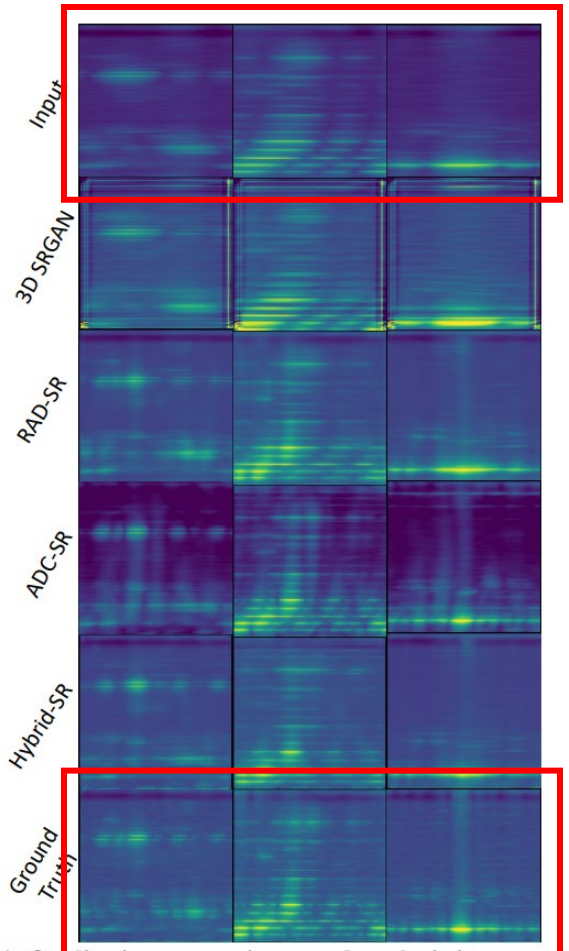

Figure 6. **Qualitative comparisons and analysis in reconstruction of Range-Azimuth (RA) maps.**

10-element ULA

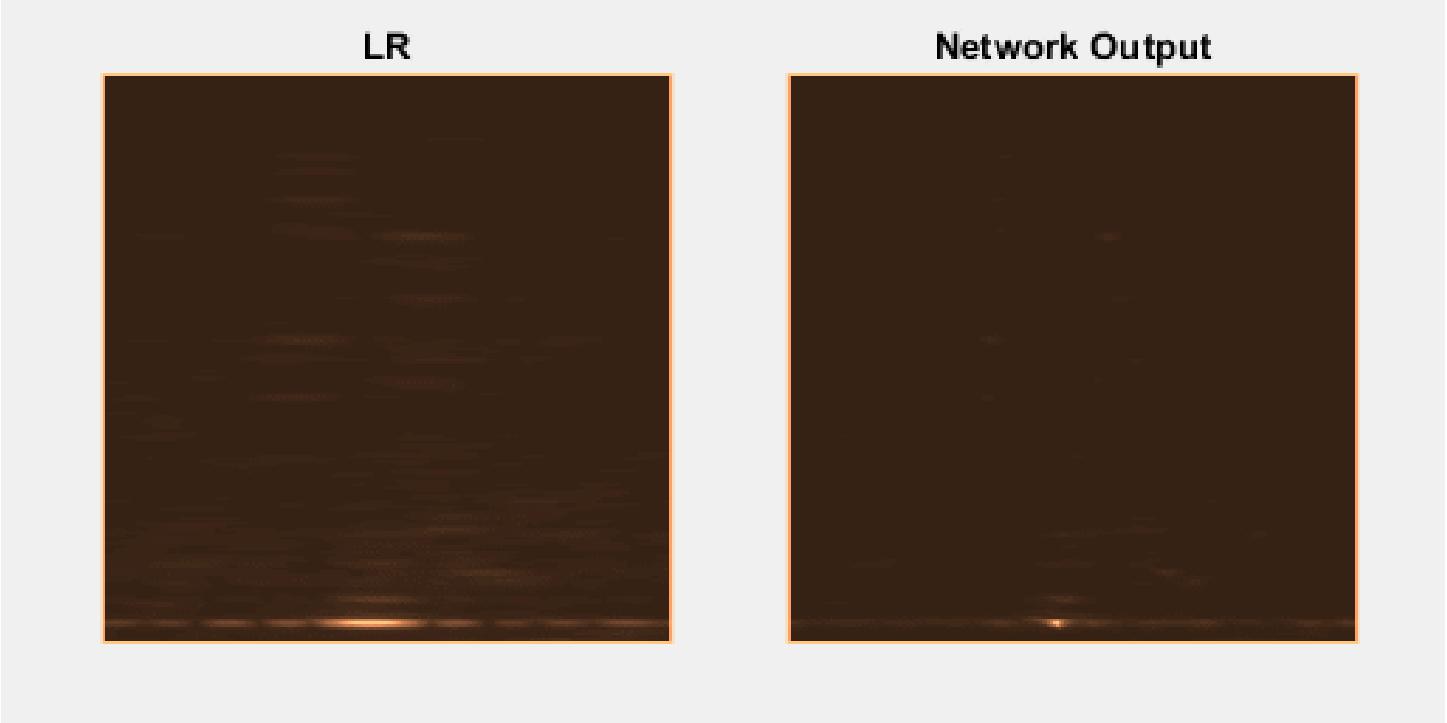

Y.-J. Li, S. Hunt, J. Park, M. O'Toole, and K. Kitani, "Azimuth super-resolution for FMCW radar in autonomous driving," in Proc. IEEE/CVF Conf. Comput. Vis. Pattern Recognit. (CVPR), Jun. 2023.

Agenda

- **Background and Motivation of DL for DOA Estimation**
  - ✓ Overview of deep learning (DL) for DOA estimation
  - ✓ Comparison: data-driven vs. model-based approaches
  - ✓ Why hybrid model-based deep learning matters
- **DL for High-Resolution Radar Imaging**
  - ✓ Unrolling IAA
  - ✓ Physics-guided 1D neural networks for radar imaging
  - ✓ DOA estimation considering antenna failure
  - ✓ Off-grid DOA estimation with 1-bit single-snapshot sparse array
  - ✓ Siamese neural networks for DOA estimation
- **DL for Integrated Sensing and Communications (ISAC)**
- **DL Enabled Sparse Array Interpolation**
  - ✓ Unrolling IHT for matrix completion
  - ✓ Transformer based array interpolation

DOA Estimation Considering Antenna Failure

Sparse Augmentation Layer

Purpose:
- ▶ Introduce controlled sparsity into the dataset.
- ▶ Enhance model robustness and prevent overfitting.

Mechanism:
- ▶ Generates a random binary mask.
- ▶ Applies mask to input signal to create sparsity.
- ▶ Configurable maximum sparsity level

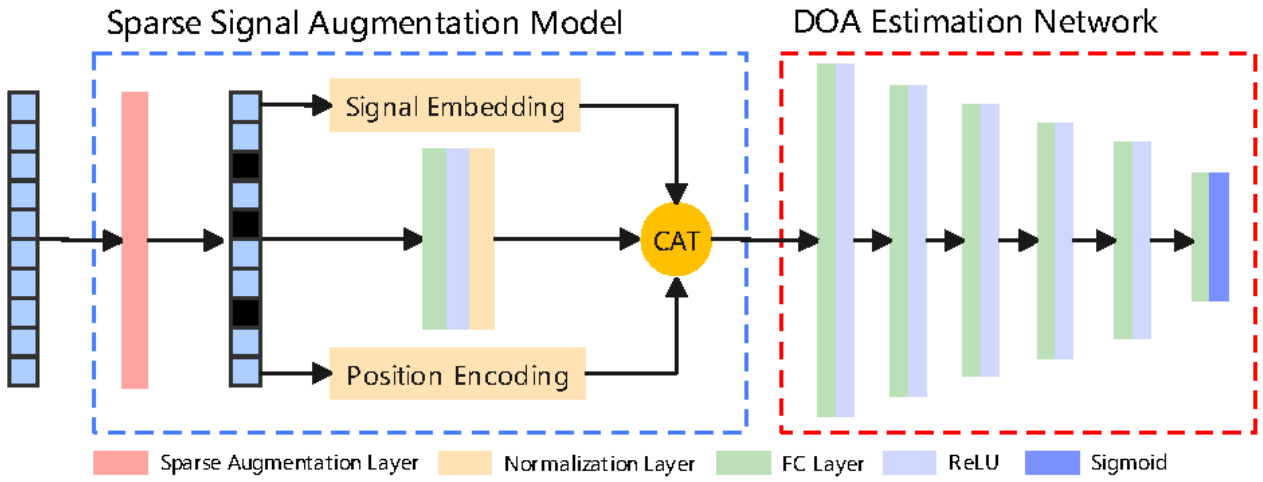

R. Zheng, S. Sun, H. Liu, H. Chen, M. Soltanalian and J. Li, “Antenna failure resilience: Deep learning-enabled robust DOA estimation with single snapshot sparse arrays,” in Proc. 58th Annual Asilomar Conference on Signals, Systems, and Computers (Asilomar), Pacific Grove, CA, Oct. 27 – Oct. 30, 2024

Domain Crafted Features

- **Importance**:
  - Enhances model performance by incorporating expert insights.
- **Features Used**:
  - Sparse Signal Frequency Embedding
  - Active Antenna Position Encoding
- **Embedding Process**:

$$\text{output} = \frac{\mathbf{A}^H \times \text{input}}{N_{\text{SLA}}} \tag{6}$$

  - $\mathbf{A}^H$: Hermitian transpose of array manifold matrix.
  - Transforms sparse signal and active antenna positions into frequency domain.

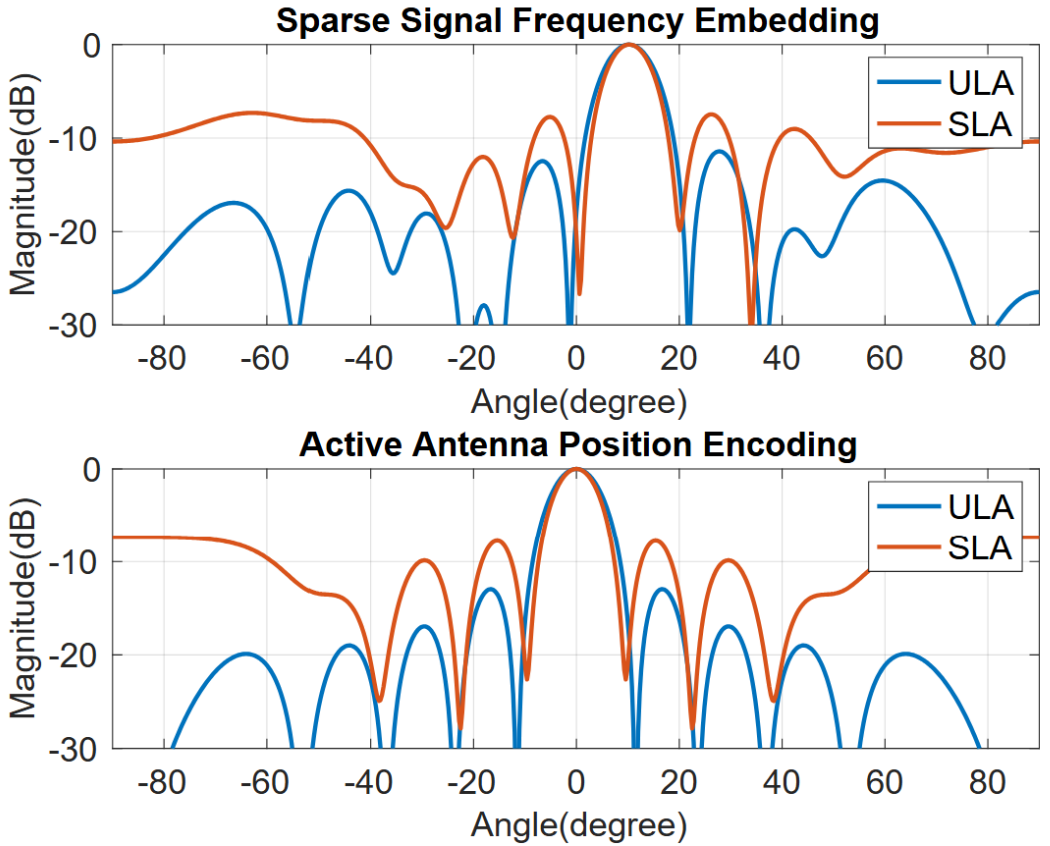

Numerical Results

- **Dataset Gap:**
  - No public real-world DOA datasets; existing models use simulated data
- **Our Solution:**
  - Custom dataset created in parking lot setup
  - TI radar data from a corner reflector, 15m away
- **Collection Details:**
  - 195 high-SNR signals from multiple angles
  - Simulated multi-target scenarios via superposition
- **Purpose:**
  - Used exclusively for testing, not training
- More detail in `https://github.com/ruxinzh/Deep_RSA_DOA/tree/main/real_World_DOA_dataset`

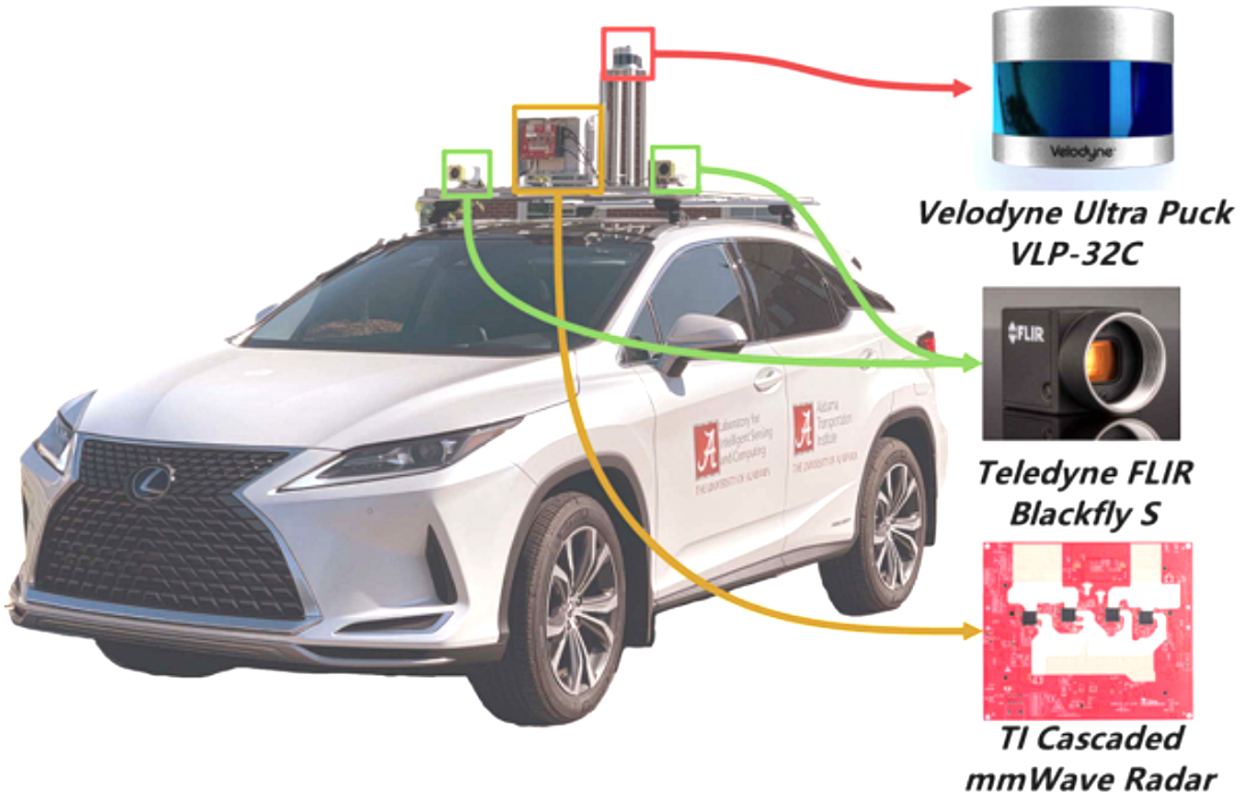

Source Code: https://github.com/ruxinzh/Deep_RSA_DOA/
Real Measurement Data: https://github.com/ruxinzh/Deep_RSA_DOA/tree/main/real_World_DOA_dataset

Numerical Results

Single Target

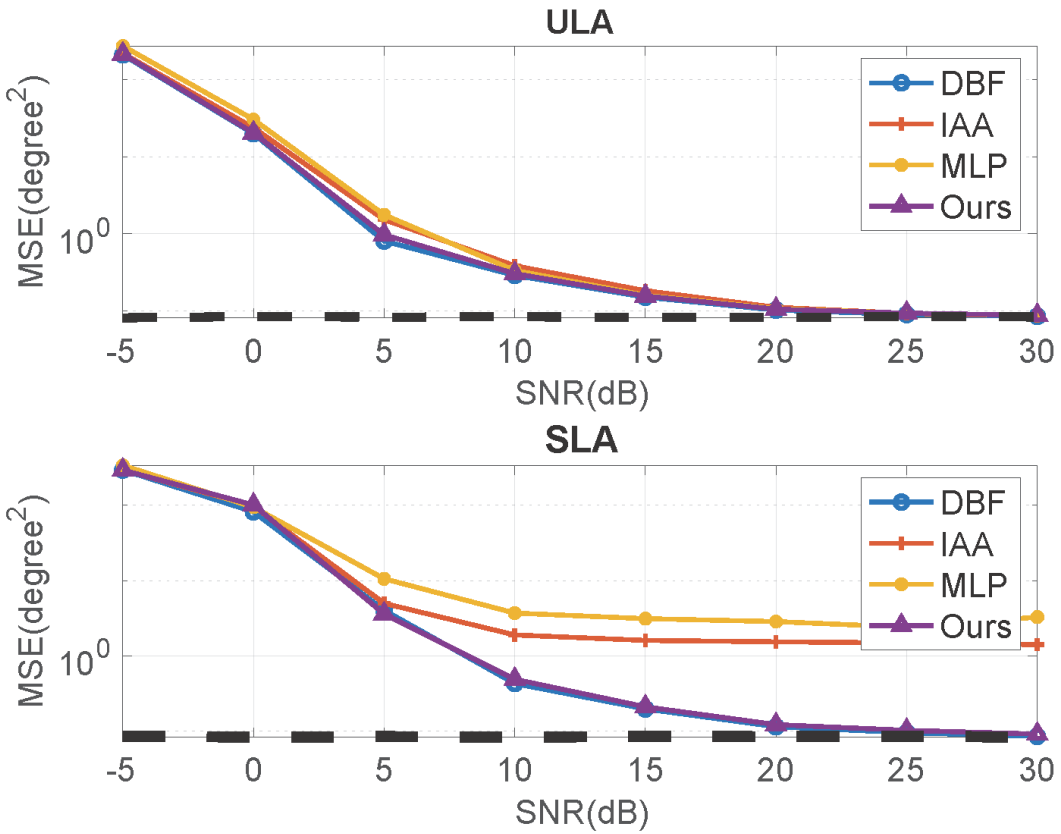

Two Targets

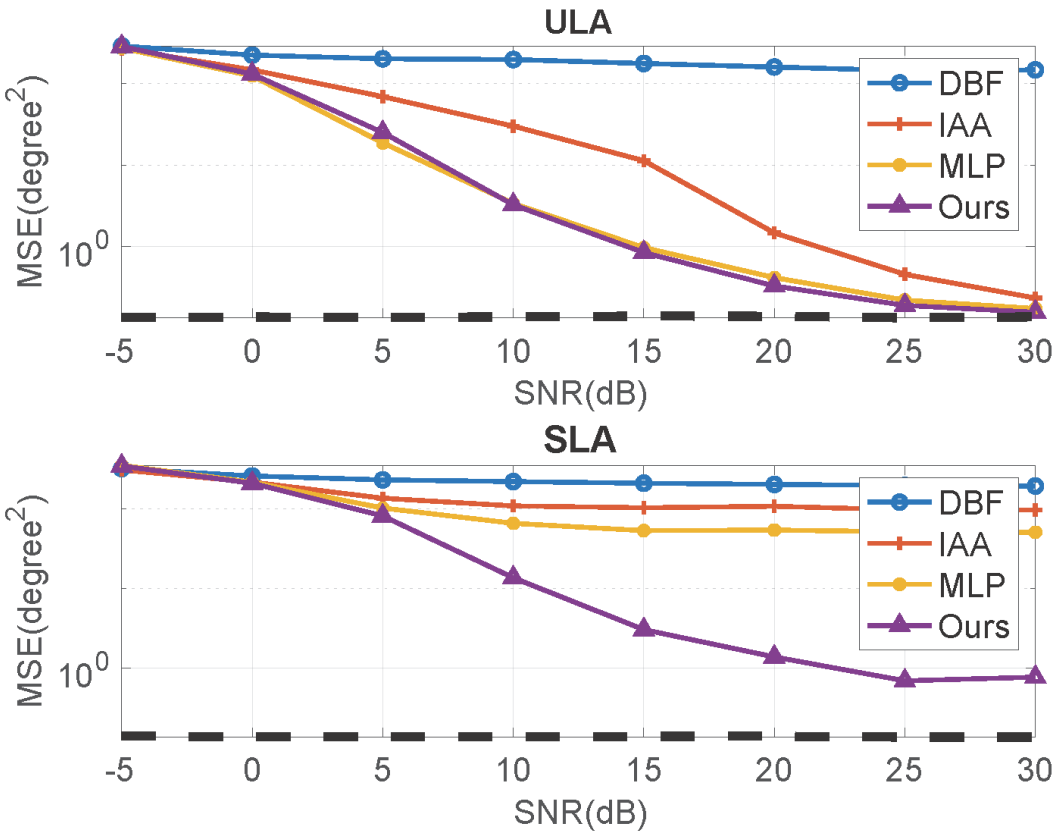

Numerical Results

Separation

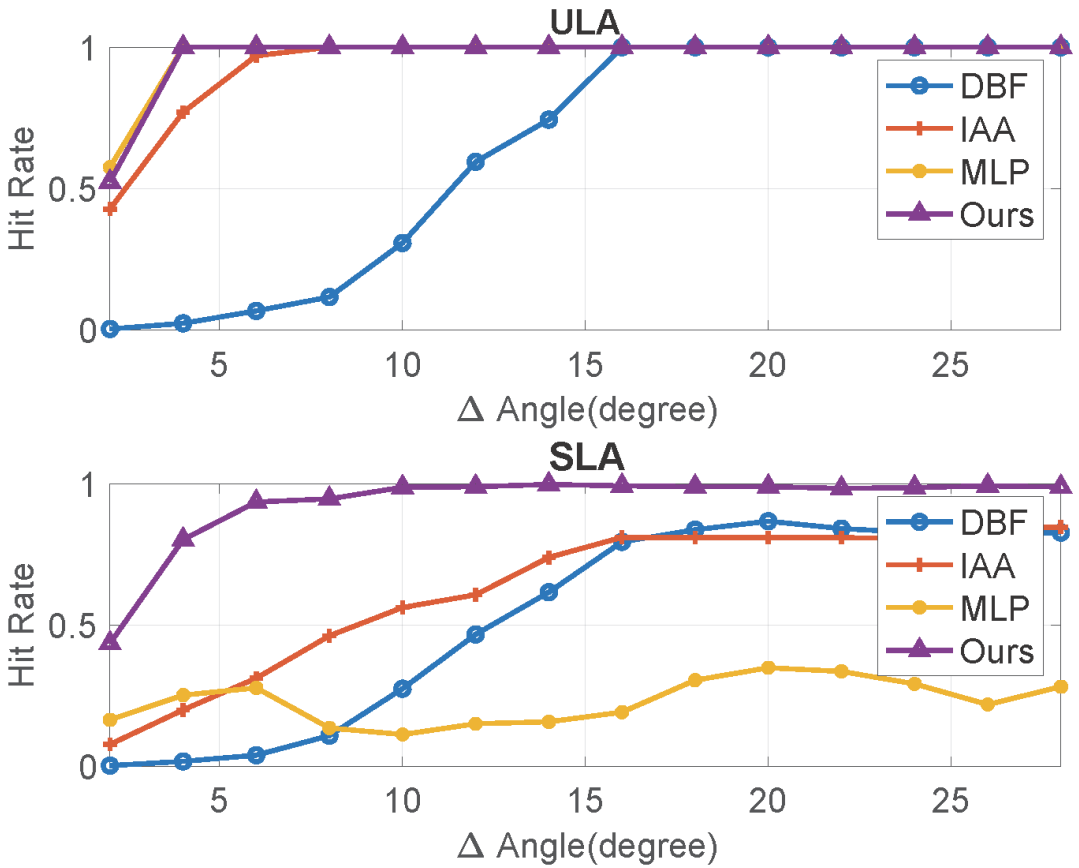

Complexity

Method	Inference Time (ms)	Trainable Parameters
DBF	0.3	N/A
IAA	32.8	N/A
MLP	2.3	2,848,829
Our Method	3.1	4,106,301

Numerical Results

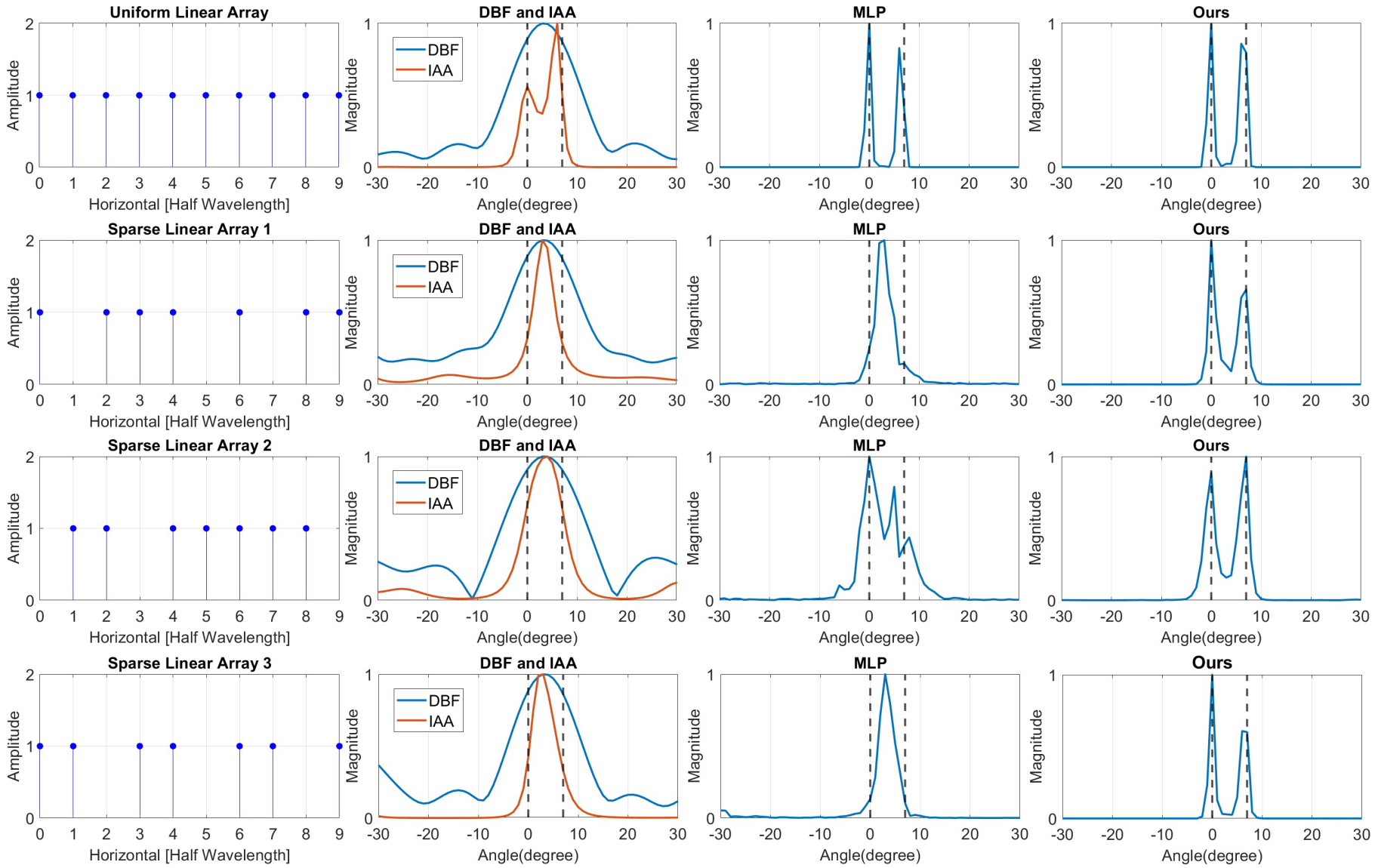

Agenda

- **Background and Motivation of DL for DOA Estimation**
  - ✓ Overview of deep learning (DL) for DOA estimation
  - ✓ Comparison: data-driven vs. model-based approaches
  - ✓ Why hybrid model-based deep learning matters
- **DL for High-Resolution Radar Imaging**
  - ✓ Unrolling IAA
  - ✓ Physics-guided 1D neural networks for radar imaging
  - ✓ DOA estimation considering antenna failure
  - ✓ Off-grid DOA estimation with 1-bit single-snapshot sparse array
  - ✓ Siamese neural networks for DOA estimation
- **DL for Integrated Sensing and Communications (ISAC)**
- **DL Enabled Sparse Array Interpolation**
  - ✓ Unrolling IHT for matrix completion
  - ✓ Transformer based array interpolation

Off-Grid DOA Estimation with 1-Bit Sparse Array

Benefits of One-bit ADC Quantization

- Reduced hardware cost and power consumption of ADCs.
- Enhanced data compression for storage and transmission, etc.

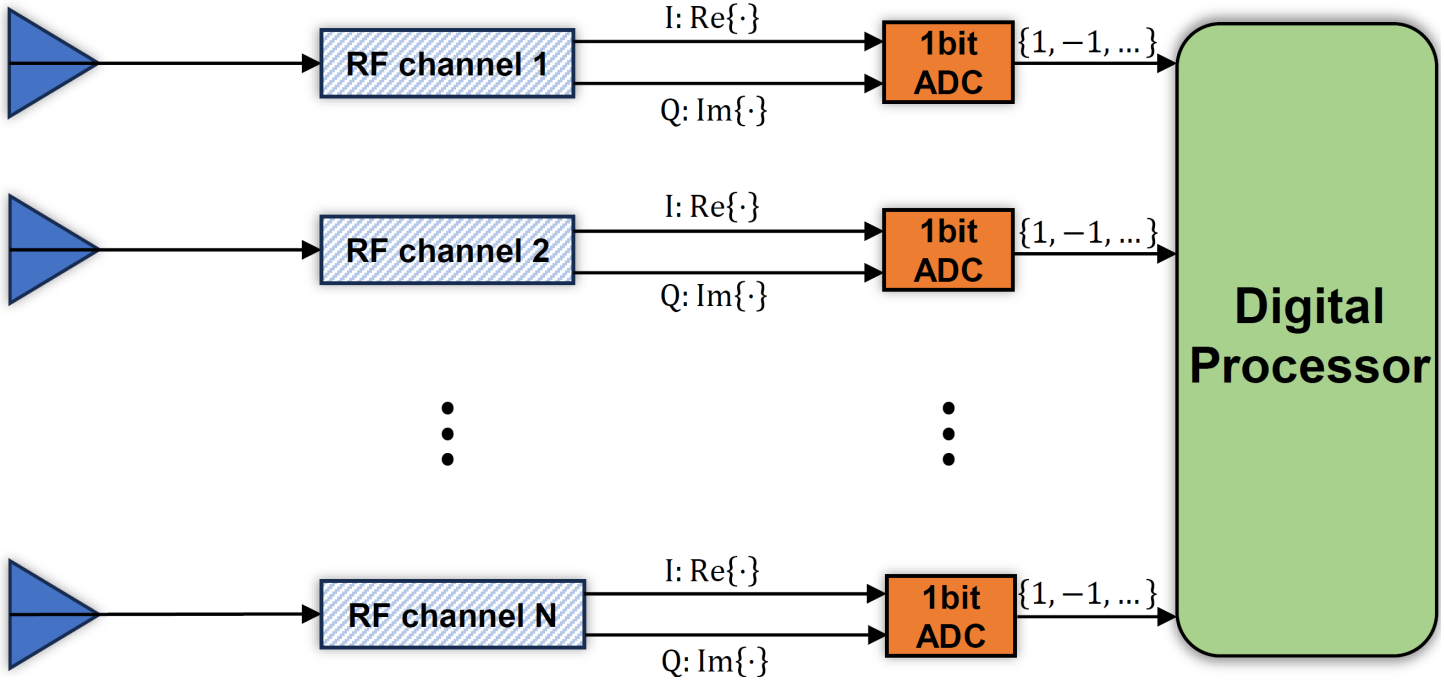

Y. Hu, S. Sun and Y. D. Zhang, "Enhancing off-grid one-bit DOA estimation with learning-based sparse Bayesian approach for non-uniform sparse array," in Proc. 58th Annual Asilomar Conference on Signals, Systems, and Computers (Asilomar), Pacific Grove, CA, Oct. 27 – Oct. 30, 2024.

Algorithms for One-Bit DOA Estimation

- Grid dependency
- On-grid methods (e.g., one-bit MUSIC) require dense grids for off-grid signals → high complexity.
- High computational burden
- Sparse recovery algorithms demand many iterations for accurate estimation.
- Handcrafted parameter tuning
- Parametric methods rely on prior knowledge (e.g., sparsity levels).
- Not robust across varying conditions such as different SNRs.

X. Huang and B. Liao, ”One-Bit MUSIC,” in IEEE Signal Processing Letters, vol. 26, no. 7, pp. 961-965, July 2019.

Pengyu Wang, Huichao Yang, Zhongfu Ye, “1-Bit direction of arrival estimation via improved complex-valued binary iterative hard thresholding,” Digital Signal Processing, vol. 120, 2022.

Algorithms for One-Bit Off-Grid DOA Estimation

Algorithms for One-Bit Off-Grid DOA Estimation

- Require many iterations for accurate estimation.
- Grid search needed for updates → high complexity.
- Typically designed for multiple snapshots → struggle in single snapshot scenarios.

From Deep Learning to Deep Unrolling

- Deep Learning Approaches:
- Strong model fitting capability.
- Purely data-driven → limited by insufficient training data.
- Lack interpretability.

Deep Unrolling Approaches

- Embed model priors into networks to reduce data dependency.
- Inspired by interpretable algorithms; often outperform originals by learning parameters automatically.

Monga, Vishal, Yuelong Li, and Yonina C. Eldar. ”Algorithm unrolling: Interpretable, efficient deep learning for signal and image processing.” IEEE Signal Processing Magazine 38.2(2021): 18-44.

Signal Model for One-Bit Off-Grid DOA Estimation

- **Scenario Assumptions**:
  - K narrowband, far-field source signals $\mathbf{s} = [s_k]$, $k = 1, \ldots, K$.
  - Signals arrive at a linear, omnidirectional antenna array with N elements.
  - Arrival directions are $\boldsymbol{\theta} = [\theta_k]$, $k = 1, \ldots, K$.
- **Objective**:
  - Estimate the directions of arrival (DOAs) $\boldsymbol{\theta}$ using one bit quantized received data.
- **Data Model for One-bit DoA Estimation**:

$$\mathbf{y}(t) = \operatorname{csgn}\left(\mathbf{A}(\boldsymbol{\theta})\mathbf{s}(t) + \mathbf{n}(t)\right), \quad t = 1, \ldots, T \tag{1}$$

where $\mathbf{y}(t)$ is received signal vector, $\mathbf{A}(\boldsymbol{\theta}) = [\mathbf{a}(\theta_1), \mathbf{a}(\theta_2), \ldots, \mathbf{a}(\theta_K)]$ is array manifold matrix, $\mathbf{s}(t)$ is source signal vector, $\mathbf{n}(t)$ is complex Gaussian noise, $\operatorname{csgn}(\cdot) = \operatorname{sign}(\Re(\cdot)) + j\operatorname{sign}(\Im(\cdot))$ is complex sign function, and $\mathbf{a}(\theta_i) = \left[1, e^{j\frac{2\pi d_2}{\lambda}\sin\theta_i}, \ldots, e^{j\frac{2\pi d_N}{\lambda}\sin\theta_i}\right]^T$ is steering vector.

ULA and SLA:

- For uniform linear array (ULA), $d_i = \frac{(i-1)\lambda}{2}$, $i = 1, \ldots, N$.
- For sparse linear array (SLA), $d_i = \frac{s_i\lambda}{2}$, $s_i \in \{0, 1, \ldots, N-1\}$, $i = 1, \ldots, M$, and $M \ll N$.

Single-Snapshot Model:

- In high dynamic automotive scenarios, only one snapshot ($T = 1$) data is available. The model is simplified to:

$$\mathbf{y} = \operatorname{csgn}\left(\mathbf{A}(\boldsymbol{\theta})\mathbf{s} + \mathbf{n}\right) \tag{2}$$

On-Grid Model vs. Off-Grid Model

- **On-grid Model**:
  - The grid size is fixed: $\Delta\tilde{\boldsymbol{\theta}} = \left|\tilde{\theta}_i - \tilde{\theta}_{i-1}\right| = const.$
  - When DoAs are on the grid, there is no grid gap.
  - When DoAs are off the grid, the grid gaps always exist.

- **Off-grid Model**:
  - Consider the estimation of the off-grid gap.
  - When DoAs are off the grid, the gaps will be reduced.

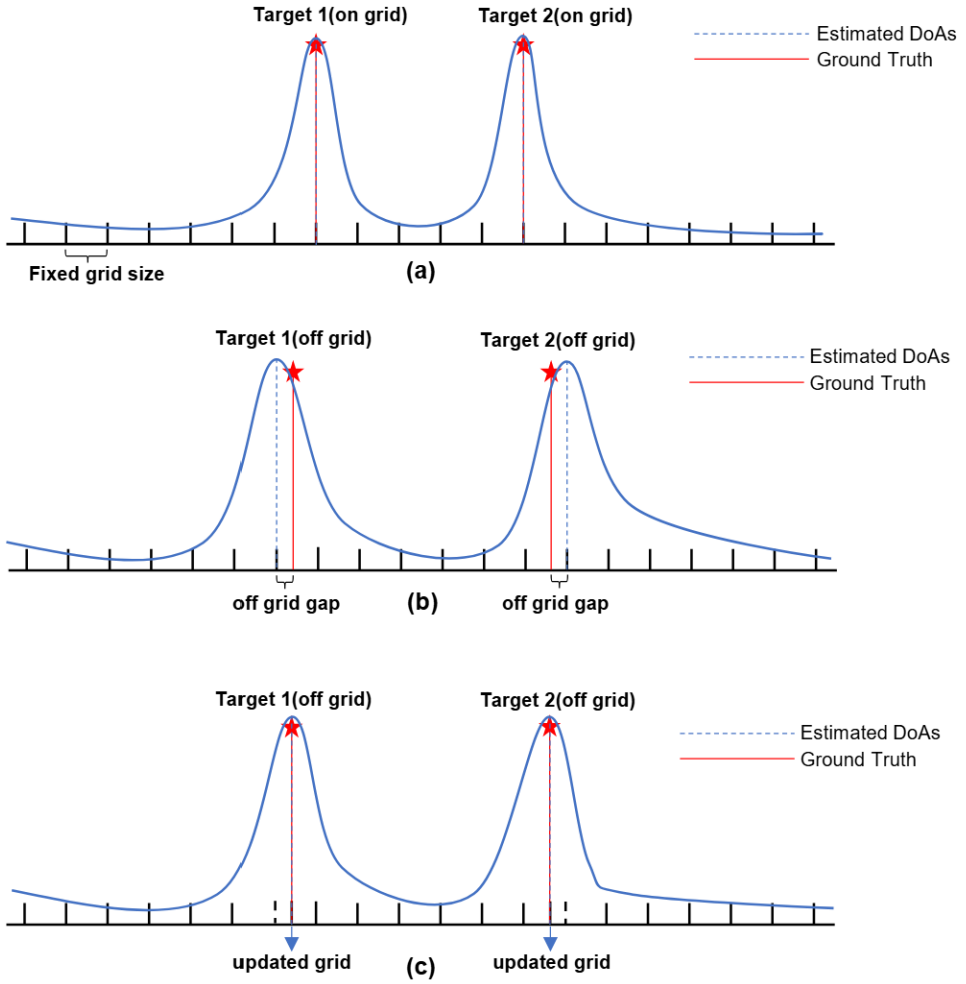

The diagram illustrating on-grid and off grid DOA estimation.

Problem Formulation for One-Bit Off-Grid DOA

- **Off-grid Model based on First-order Grid Approximation**
  - Suppose the grid dividing is sufficiently dense, and the K signals fall into different grid regions.
  - Assume that the fixed grid nearest to ith DoA θ_i is θ_{ni}, the first-order approximation for off-grid steering vector is:

$$\mathbf{a}(\theta_i) = \mathbf{a}(\tilde{\theta}_{ni}) + \mathbf{b}(\tilde{\theta}_{ni})\left(\theta_i - \tilde{\theta}_{ni}\right) \tag{3}$$

    where $\mathbf{b}(\tilde{\theta}_{ni}) = \frac{\partial \boldsymbol{a}(\tilde{\theta}_{ni})}{\partial \tilde{\theta}_{ni}}$ is the first order derivative of $\mathbf{a}(\tilde{\theta}_{ni})$, and $\left\{\tilde{\theta}_{ni}\right\}$ are the fixed divided grids.
  - The first-order approximation of the manifold matrix:

$$\mathbf{C}(\boldsymbol{\beta}) = \mathbf{A} + \mathbf{B}\mathrm{diag}(\boldsymbol{\beta}) \tag{4}$$

    where $\mathbf{A} = \left[\mathbf{a}(\tilde{\theta}_1), \mathbf{a}(\tilde{\theta}_2), \ldots, \mathbf{a}(\tilde{\theta}_N)\right]$, $\mathbf{B} = \left[\mathbf{b}(\tilde{\theta}_1), \mathbf{b}(\tilde{\theta}_2), \ldots, \mathbf{b}(\tilde{\theta}_N)\right]$, $\boldsymbol{\beta} = [\beta_1, \beta_2, \ldots, \beta_N]$ are the grid gaps. The grid gaps satisfy:

$$\beta_n = \begin{cases} \theta_k - \theta_{n_k}, \textit{if } \mathrm{n}{=}\mathrm{n}_k, k \in \{1, 2, \ldots, K\} \\ 0, \textit{othercases} \end{cases} \tag{5}$$

  - By absorbing the approximation error in the measurement noise, the model can be rewritten as:

$$\mathbf{y} = \mathrm{csgn}\left(\mathbf{C}(\boldsymbol{\beta})\mathbf{s} + \mathbf{n}\right), \tag{6}$$

Problem Formulation for One-Bit Off-Grid DOA

- **Sparse Bayesian Formulation**:
  - The likelihood function $p(\mathbf{y}|\mathbf{s};\boldsymbol{\beta})$ is given by[e]:

$$p(\mathbf{y}|\mathbf{s};\boldsymbol{\beta}) = \prod_{m=1}^{M} \Phi\left(\frac{\Re(y_m)\,\Re\left(\boldsymbol{c}_m^{\mathrm{T}}(\boldsymbol{\beta})\,\mathbf{s}\right)}{\sigma/\sqrt{2}}\right) \times \Phi\left(\frac{\Im(y_m)\,\Im\left(\boldsymbol{c}_m^{\mathrm{T}}(\boldsymbol{\beta})\,\mathbf{s}\right)}{\sigma/\sqrt{2}}\right)$$

  - An appropriate prior probability density function (pdf) of $\mathbf{s}$ should be chosen to promote sparsity, for example, the Laplacian distribution, the exponential distribution. Here we assume:

$$p(\mathbf{s}) = \prod_{i=1}^{N} \exp\left(\frac{-\lambda\,|s_i|^p}{p}\right), 0 < p \leq 1 \qquad (7)$$

  - The pdf of grid gap is given by:

$$p(\boldsymbol{\beta}) \sim U\left(-\frac{r}{2}, \frac{r}{2}\right) \qquad (8)$$

  - Taking Maximum A Posteriori (MAP) criterion, with Bayes rules, the estimator $\{\mathbf{s}^*, \boldsymbol{\beta}^*\}$ is given by:

$$\begin{aligned}\{\mathbf{s}^*, \boldsymbol{\beta}^*\} &= \arg\max_{s,\beta} \ln p(\mathbf{y}|\mathbf{s};\boldsymbol{\beta}) + \ln p(\mathbf{s}) + \ln p(\boldsymbol{\beta}) \\ &= \arg\min_{s,\beta} -\ln p(\mathbf{y}|\mathbf{s};\boldsymbol{\beta}) - \ln p(\mathbf{s}) - \ln p(\boldsymbol{\beta})\end{aligned}$$

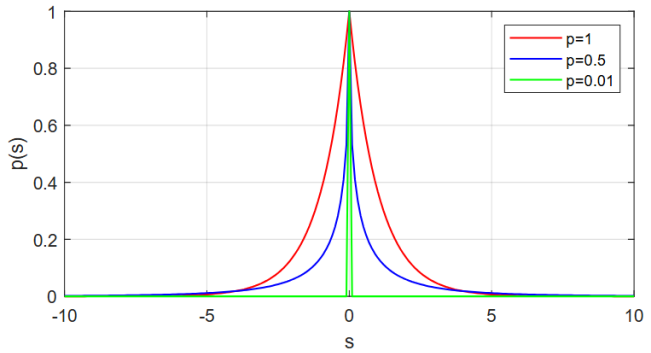

Figure 3: Example of pdf of $\mathbf{s}$ w.r.t. different parameters.

$$\begin{aligned}&= \arg\min_{s,\beta} -\prod_{m=1}^{M} \ln\Phi\left(\Re(y_m)\,\Re\left(\boldsymbol{c}_m^{\mathrm{T}}(\boldsymbol{\beta})\,\hat{\mathbf{s}}\right)\right) \\ &- \prod_{m=1}^{M} \ln\Phi\left(\Im(y_m)\,\Im\left(\boldsymbol{c}_m^{\mathrm{T}}(\boldsymbol{\beta})\,\hat{\mathbf{s}}\right)\right) + \sum_{i=1}^{N} \frac{\lambda\,|s_i|^p}{p} - \frac{1}{r},\end{aligned} \qquad (9)$$

where $\Phi(\cdot)$ is the cumulative distribution function (CDF) of the standard normal distribution.

J. Ren, T. Zhang, J. Li and P. Stoica, "Sinusoidal parameter estimation from signed measurements via majorization–minimization based RELAX," in IEEE Transactions on Signal Processing, vol. 67, no. 8, pp. 2173-2186, 2019.

Algorithm for One-Bit Off-Grid DOA Estimation

- **Majorization-Minimization**:
  - Let $f(\mathbf{s}, \boldsymbol{\beta})$ denotes the cost function (9), find a majorizing function $g\left(\mathbf{s}, \boldsymbol{\beta} | \tilde{\mathbf{s}}, \tilde{\boldsymbol{\beta}}\right)$ for $f(\mathbf{s}, \boldsymbol{\beta})$, such that:

$$f(\mathbf{s}, \boldsymbol{\beta}) \leq g\left(\mathbf{s}, \boldsymbol{\beta} | \tilde{\mathbf{s}}^t, \tilde{\boldsymbol{\beta}}^t\right) \tag{10}$$

$$f\left(\tilde{\mathbf{s}}^t, \tilde{\boldsymbol{\beta}}^t\right) = g\left(\tilde{\mathbf{s}}^t, \tilde{\boldsymbol{\beta}}^t | \tilde{\mathbf{s}}^t, \tilde{\boldsymbol{\beta}}^t\right) \tag{11}$$

  - Lemma 1: Let $\mathrm{I}(x) \triangleq -\ln\Phi(x), x \in \mathbb{R}$, and $\mathrm{I}(x)$ is upper bounded by [e]:

$$\mathrm{I}(x) \leq \mathrm{I}(x_0) + \mathrm{I}'(x_0)(x - x_0) + \frac{1}{2}(x - x_0)^2 \tag{12}$$

where $\mathrm{I}'(x) = -\exp\left(-x_0^2/2\right) / \left(\sqrt{2\pi}\Phi(x_0)\right)$.

- **Smooth approximation of l_p norm term**:
  - For the case of $0 < p \leq 1$, l_p norm can be smoothly approximated as:

$$\|\mathbf{s}\|_p \approx \sum_{i=1}^{N} \left(|s_i|^2 + \eta\right)^{\frac{p}{2}} \tag{13}$$

where η is a very small factor, usually $\eta = 10^{-6}$.

- **The Algorithm framework**:
  - Using (12) and (13), the cost function (9) satisfies:

$$\begin{aligned} f(\mathbf{s}, \boldsymbol{\beta}) \leq & \sum_{m=1}^{M} \frac{1}{2}\left(\Re(y_m)\Re\left(\boldsymbol{c}_m^{\mathrm{T}}(\boldsymbol{\beta})\mathbf{s}\right)\right)^2 \\ & + \frac{1}{2}\left(\Im(y_m)\Im\left(\boldsymbol{c}_m^{\mathrm{T}}(\boldsymbol{\beta})\mathbf{s}\right)\right)^2 \\ & - \Re\left(v_m^t\right)\left(\Re(y_m)\Re\left(\boldsymbol{c}_m^{\mathrm{T}}(\boldsymbol{\beta})\mathbf{s}\right)\right) \\ & - \Im\left(v_m^t\right)\left(\Im(y_m)\Im\left(\boldsymbol{c}_m^{\mathrm{T}}(\boldsymbol{\beta})\mathbf{s}\right)\right) \\ & + \frac{\lambda}{p}\sum_{i=1}^{N}\left(|s_i|^2 + \eta\right)^{\frac{p}{2}} + const \\ = & \frac{1}{2}\left\|\mathbf{C}(\boldsymbol{\beta})\mathbf{s} - \mathbf{v}^t\right\|_2^2 + \frac{\lambda}{p}\sum_{i=1}^{N}\left(|s_i|^2 + \eta\right)^{\frac{p}{2}} + const' \end{aligned} \tag{14}$$

where $\mathbf{v}^t = \left[\Re(\mathbf{y}) \odot \Re\left(\tilde{\mathbf{v}}^t\right)\right] + j\left[\Im(\mathbf{y}) \odot \Im\left(\tilde{\mathbf{v}}^t\right)\right]$,
$\tilde{\mathbf{v}}^t = \mathbf{D}^t - \mathrm{I}'\left(\mathbf{D}^t\right)$, and
$\mathbf{D}^t = \Re(\mathbf{y}) \odot \Re\left(\mathbf{C}\left(\boldsymbol{\beta}^t\right)\mathbf{s}^t\right) + j\Im(\mathbf{y}) \odot \Im\left(\mathbf{C}\left(\boldsymbol{\beta}^t\right)\mathbf{s}^t\right)$

J. Ren, T. Zhang, J. Li and P. Stoica, "Sinusoidal parameter estimation from signed measurements via majorization–minimization based RELAX," in IEEE Transactions on Signal Processing, vol. 67, no. 8, pp. 2173-2186, 2019.

Unrolling Algorithm for One-Bit Off-Grid DoA

- **The Algorithm framework**:
  - According to (10), The problem (9) is simplified to:

$$\arg\min_{s,\beta} \frac{1}{2}\left\|\mathbf{C}(\boldsymbol{\beta})\mathbf{s}-\mathbf{v}^t\right\|_2^2+\frac{\lambda}{p}\sum_{i=1}^{N}\left(|s_i|^2+\eta\right)^{\frac{p}{2}}$$

  - With the first order optimal condition, the update of $\mathbf{s}^{t+1}$:

$$\mathbf{s}^{t+1}=\left[\mathbf{C}^H(\boldsymbol{\beta}^t)\mathbf{C}(\boldsymbol{\beta}^t)+\lambda\sigma^2\boldsymbol{\Lambda}\left(\mathbf{s}^t\right)\right]^{-1}\mathbf{C}^H(\boldsymbol{\beta}^t)\mathbf{v}^t$$

where $\boldsymbol{\Lambda}\left(\mathbf{s}^t\right)$ is diagonal matrix:

$$\begin{bmatrix}\frac{1}{2}\left(|s_1|^2+\eta\right)^{\frac{p}{2}-1} & & \\ & \ddots & \\ & & \frac{1}{2}\left(|s_N|^2+\eta\right)^{\frac{p}{2}-1}\end{bmatrix}$$

  - The update of $\boldsymbol{\beta}^{t+1}$ ^{f}:

$$\boldsymbol{\beta}^{t+1}=\Re\left(\left(\mathbf{B}^H\mathbf{B}\right)^*\odot\mathbf{s}^{t+1}\left(\mathbf{s}^{t+1}\right)^H\right)^{-1}\Re\left(\operatorname{diag}\left(\left(\mathbf{s}^t\right)^*\right)\mathbf{B}^H\left(\mathbf{v}^t-\mathbf{A}\mathbf{s}^t\right)\right)$$

Figure 4: Overall architecture of the Unrolled Network.

- **Overview of the Network Architecture**:
  - **Initialization Block:** Gives initialized estimate.
  - **Unrolled Block1:** Contains a few unrolled layers, updates the estimate of $\mathbf{s}$, sets the grid gap parameters $\boldsymbol{\beta}$ zeros.
  - **Unrolled Block2:** Contains a few unrolled layers, updates $\mathbf{s}$, and the grid gap parameters $\boldsymbol{\beta}$ at the same time.

Z. Yang, L. Xie and C. Zhang, "Off-grid direction of arrival estimation using sparse Bayesian inference," in IEEE Transactions on Signal Processing, vol. 61, no. 1, pp. 38-43, Jan.1, 2013.

Unrolling Algorithm for One-Bit Off-Grid DoA

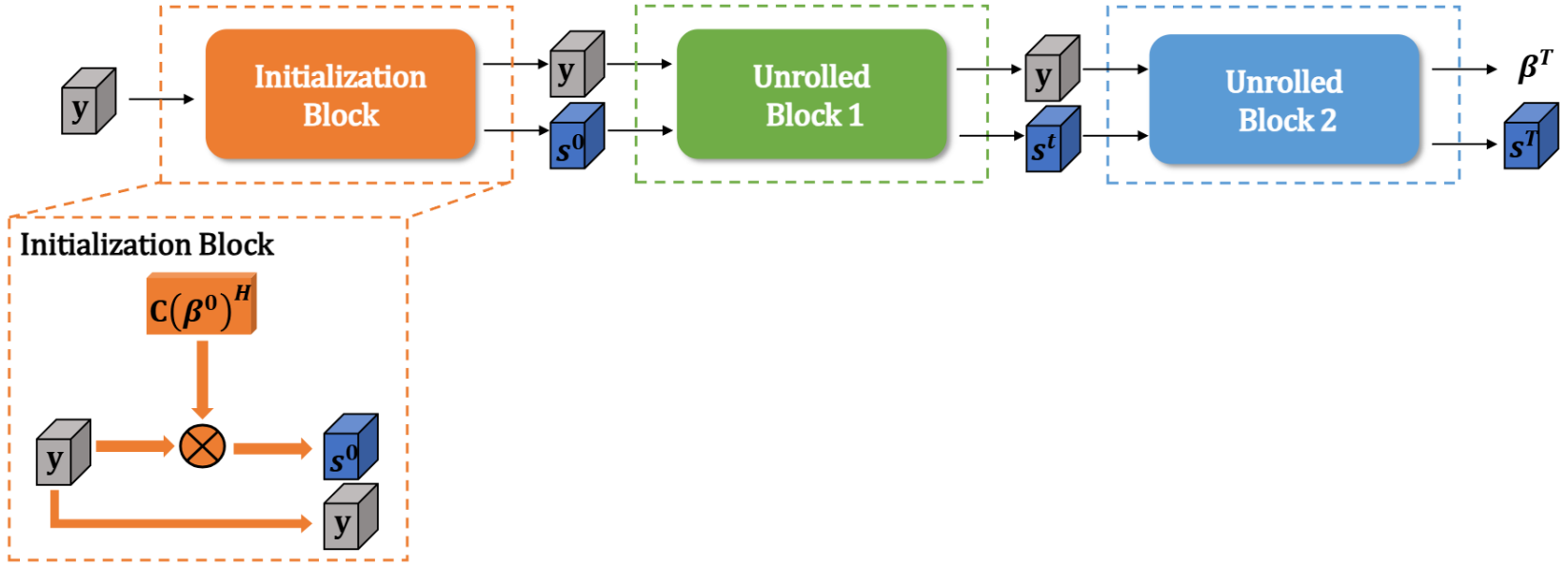

Figure 5: Architecture of the initialization block.

- Initialization operation:

$$\mathbf{x}^0 = \mathbf{C}^H\left(\boldsymbol{\beta}^0\right)\mathbf{y} \tag{15}$$

where $\boldsymbol{\beta}^0 = \mathbf{0}$

Unrolling Algorithm for One-Bit Off-Grid DoA

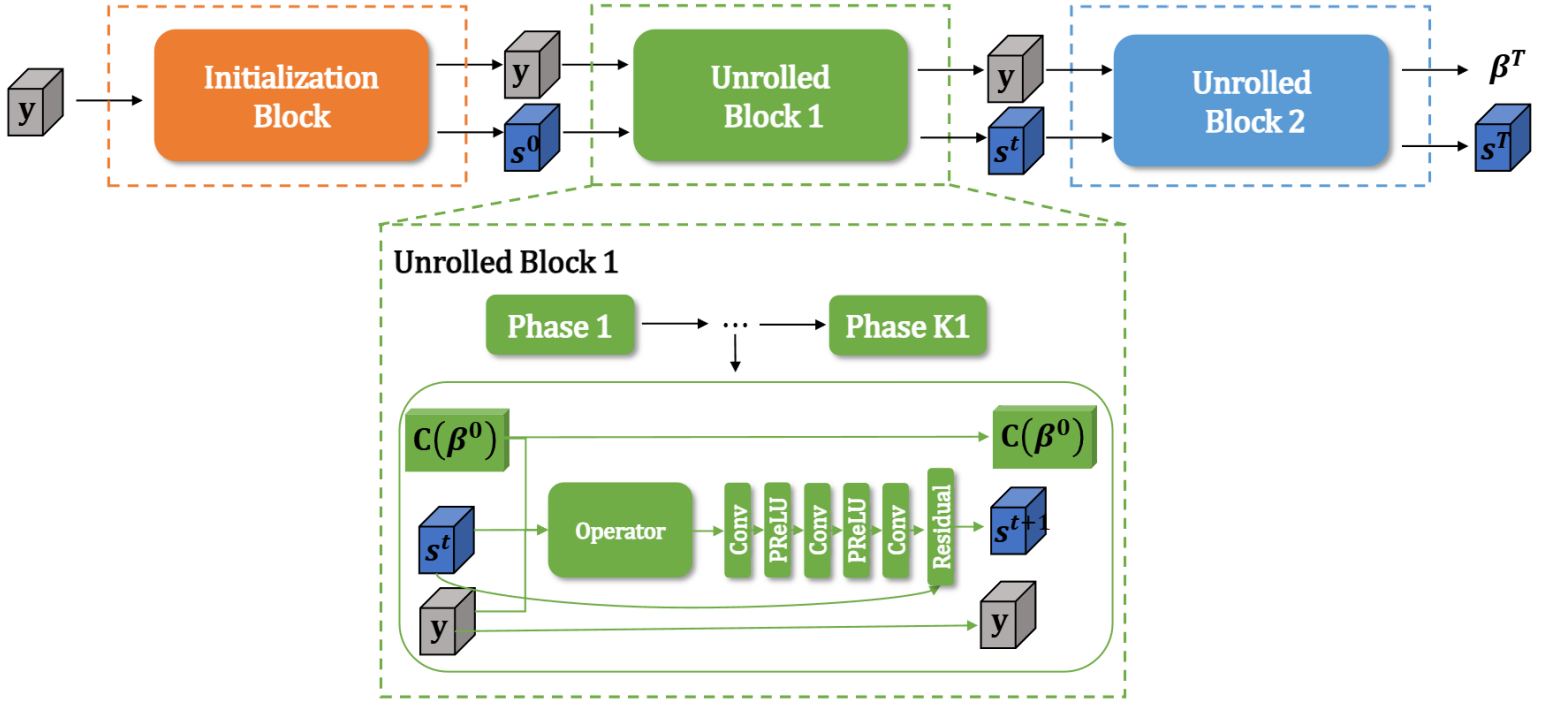

Figure 6: Architecture of Unrolled Block1.

- Operator is defined as:

$$\tilde{\mathbf{v}}^t = \mathbf{C}^H\left(\beta^0\right)\mathbf{v}^t \tag{16}$$

where $\beta^0 = \mathbf{0}$, $\mathbf{v}^t = [\Re(\mathbf{y}) \odot \Re(\tilde{\mathbf{v}}^t)] + j[\Im(\mathbf{y}) \odot \Im(\tilde{\mathbf{v}}^t)]$, $\tilde{\mathbf{v}}^t = \mathbf{D}^t - \mathrm{I}'(\mathbf{D}^t)$, and $\mathbf{D}^t = \Re(\mathbf{y}) \odot \Re\left(\mathbf{C}\left(\beta^0\right)\mathbf{s}^t\right) + j\Im(\mathbf{y}) \odot \Im\left(\mathbf{C}\left(\beta^0\right)\mathbf{s}^t\right)$

Unrolling Algorithm for One-Bit Off-Grid DoA

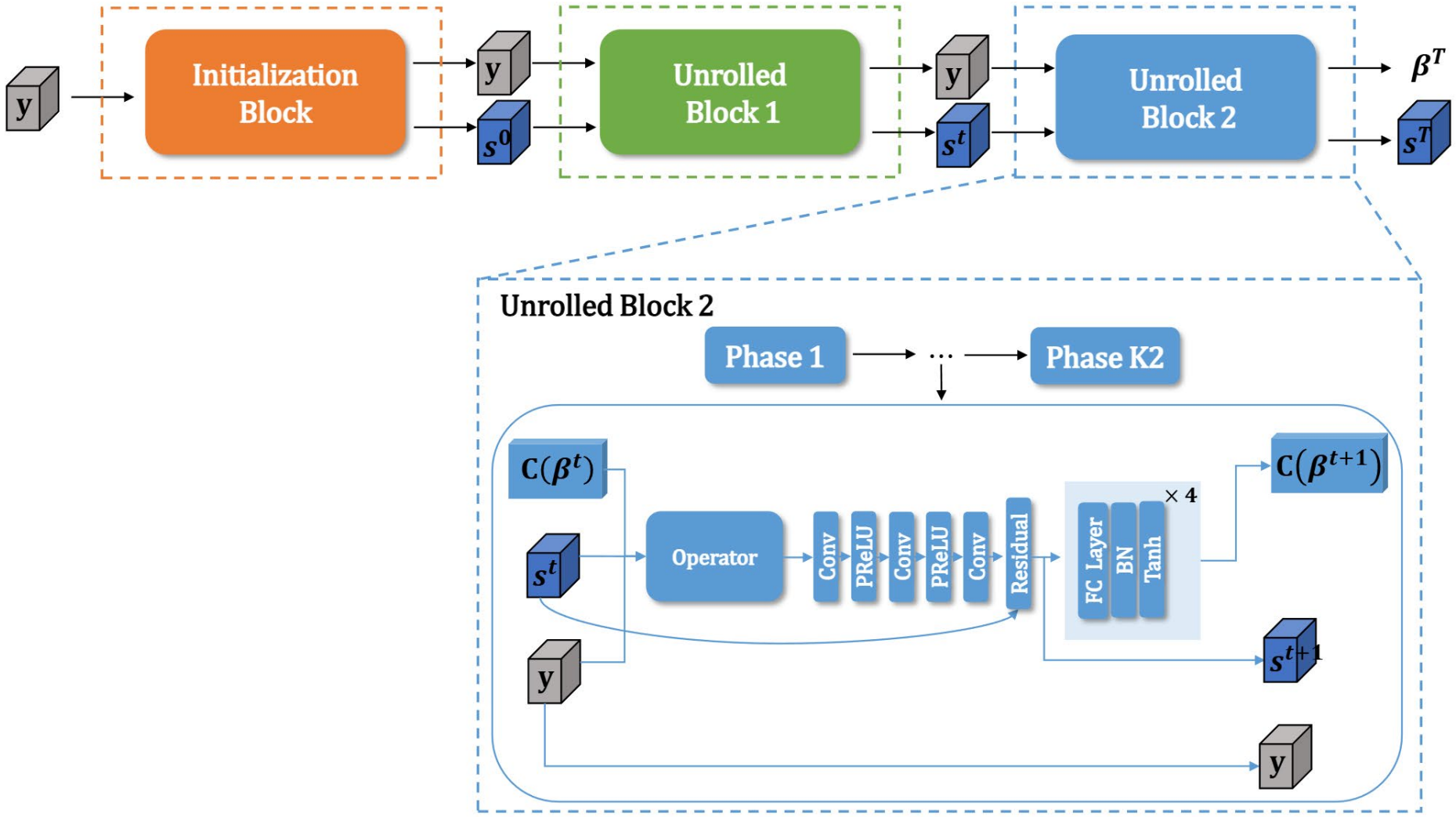

Train Unroll Network for 1-Bit Off-Grid DOA

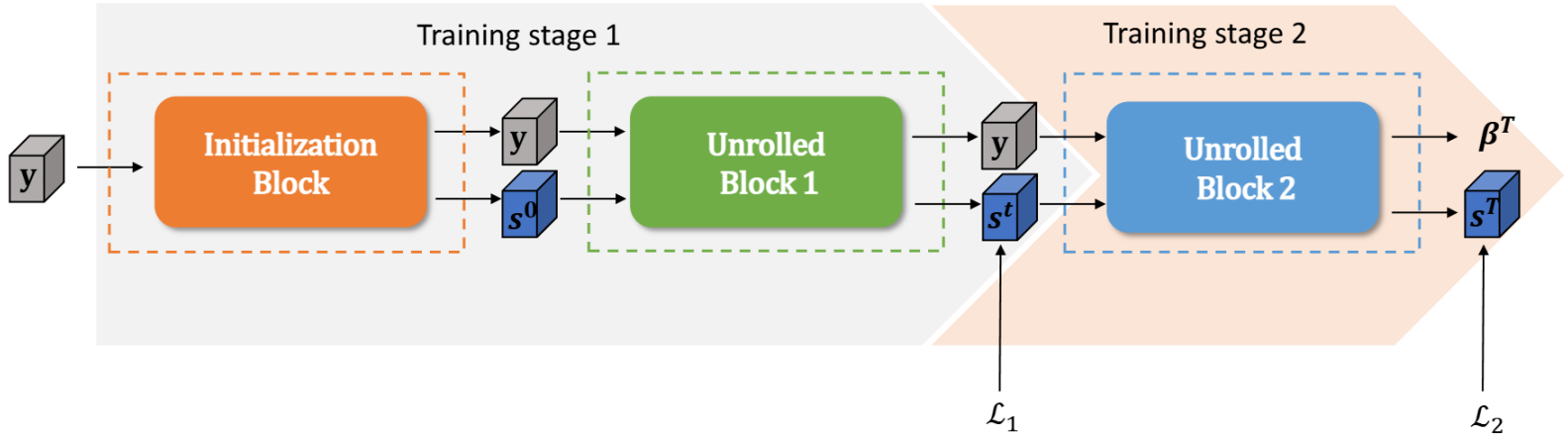

Figure 8: Training Approach for the network.

Training Approach

- **The first stage:**
  - Train the unrolled block1 of the network for 100 epochs, and freeze the parameters of unrolled block2.
  - Loss function $\mathcal{L}_1$: Binary Cross-Entropy (BCE) loss.
- **The second stage:**
  - Train the unrolled block2 of the network for 100 epochs, and freeze the parameters of unrolled block1.
  - Loss function $\mathcal{L}_2$: Mean Squared Error (MSE) Loss.

Accuracy Evaluation: Two Off-Grid Targets, Case I

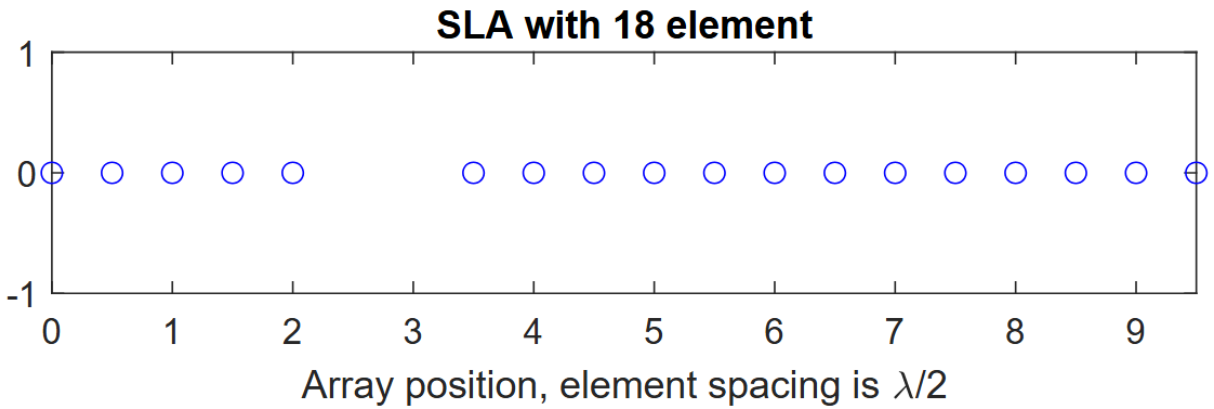

Figure 9: Antenna positions of 18-element SLA.

- **Setup**:
  - Two off-grid targets with direction in $[-10.28^\circ, 20.56^\circ]$
  - 1,024 Monte Carlo trails.
  - Varied SNR levels from 0dB to 30dB with 5dB increments.
  - The algorithm for comparison is the OGIR algorithm [g].
  - 18-element SLA:
    $[0, 1, 2, 3, 4, 7, 8, 9, 10, 11, 12, 13, 14, 15, 16, 17, 18, 19]$.
    The neural network for comparison is CNN-DNN [h].

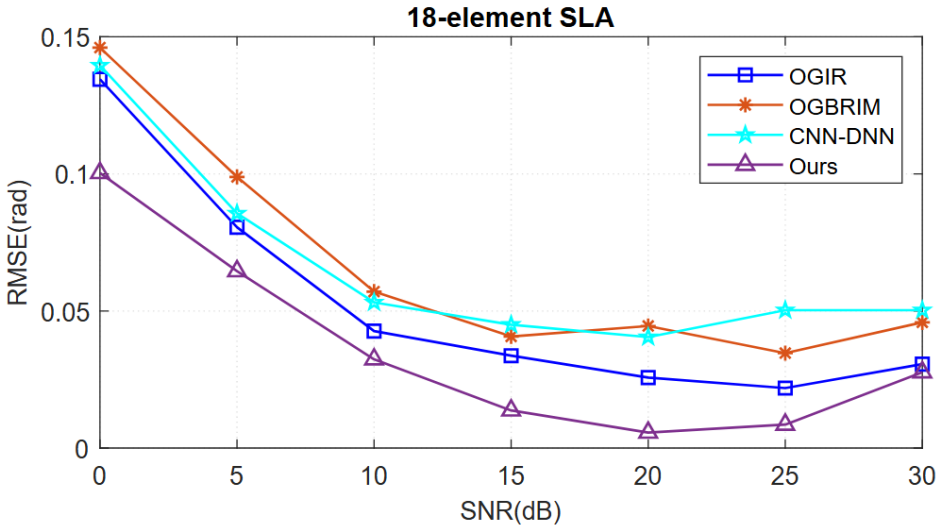

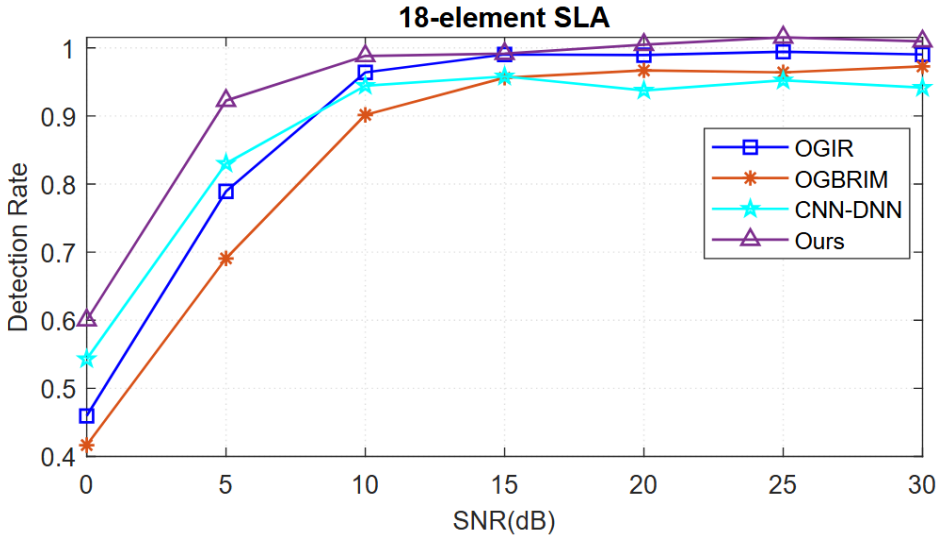

Accuracy Evaluation: Two Off-Grid Targets, Case I

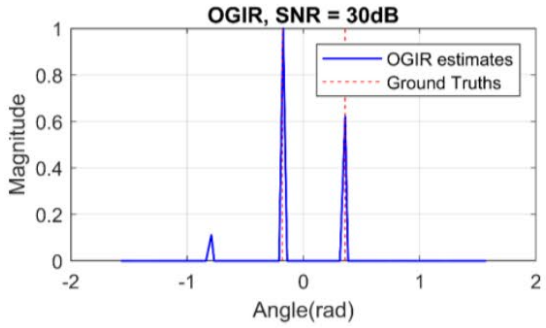

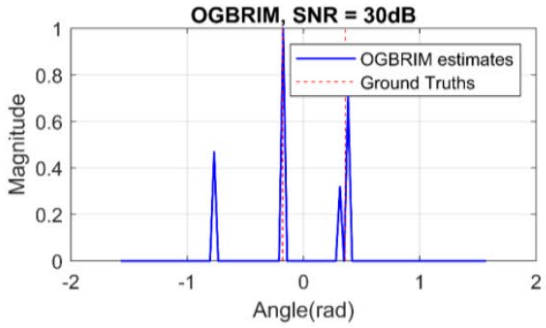

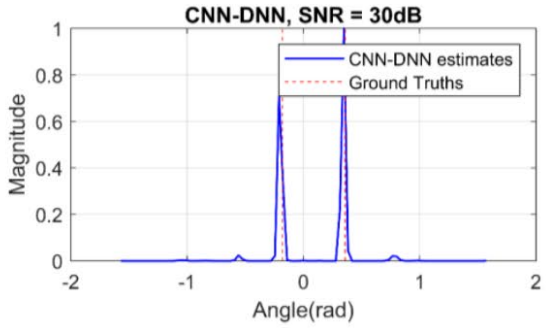

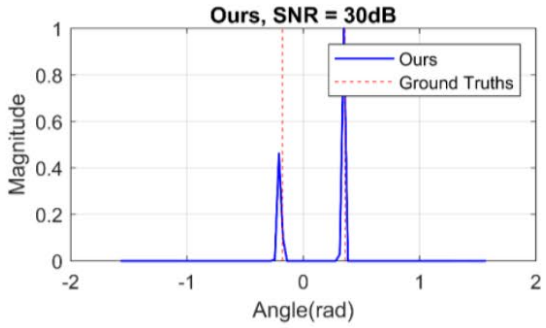

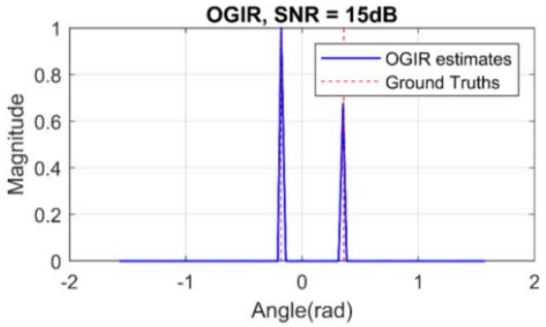

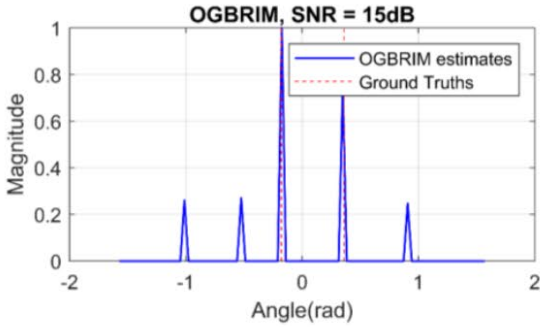

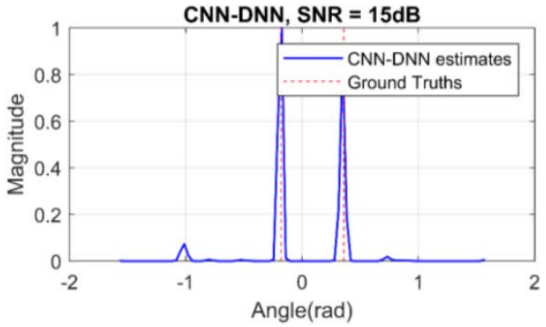

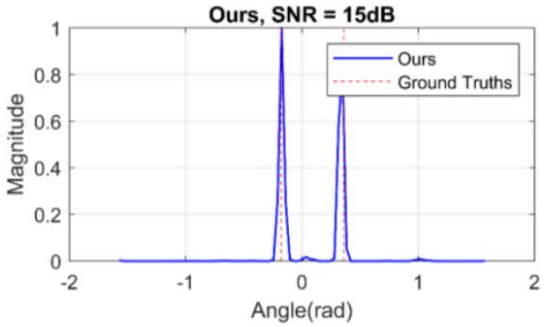

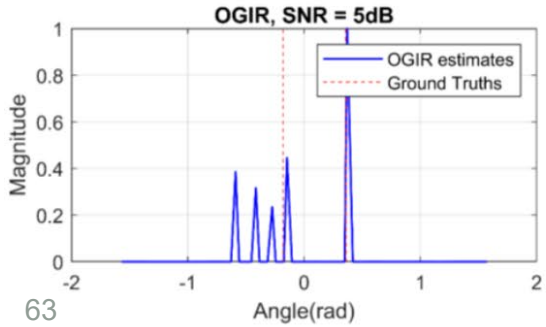

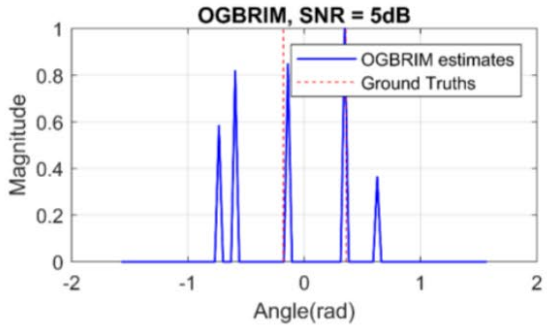

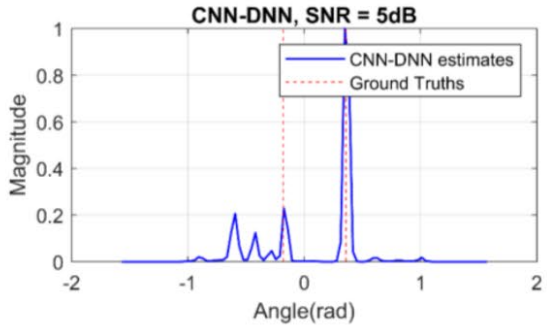

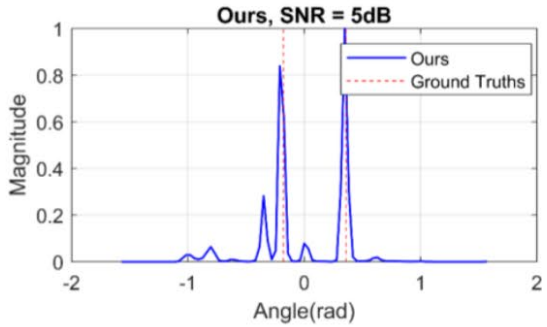

Accuracy Evaluation: Two Targets, Case II

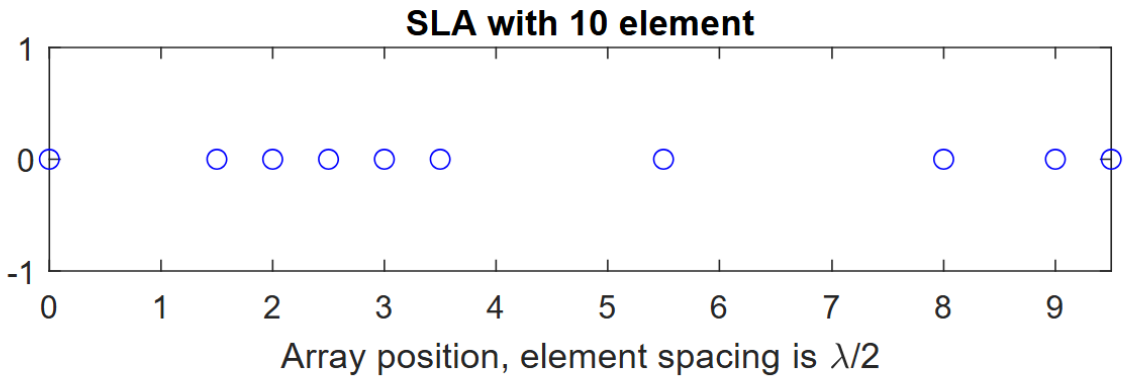

Figure 13: Antenna positions of 10-element SLA.

- **Setup**:
  - Two off-grid targets in $[-10.28°, 20.56°]$
  - 1,024 Monte Carlo trails.
  - Varied SNR levels from 0dB to 30dB with 5dB increments.
  - 10-element SLA: $[0, 3, 4, 5, 6, 7, 11, 16, 18, 19]$.

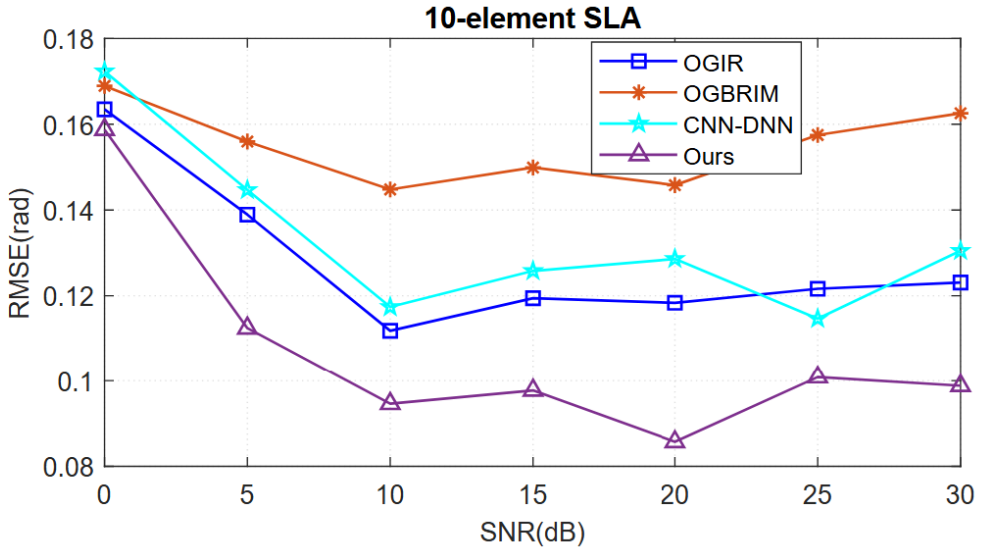

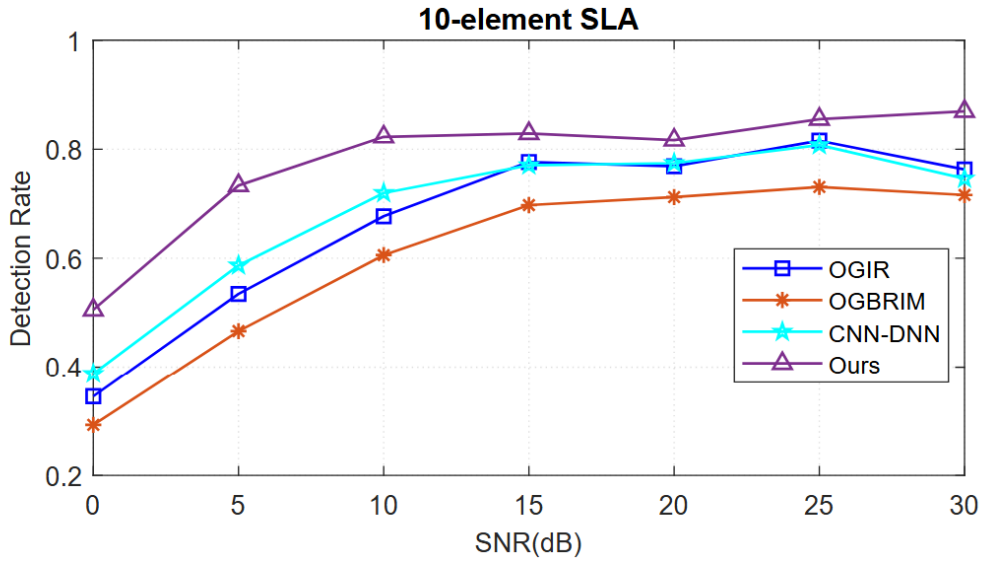

Accuracy Evaluation: Two Targets, Case II

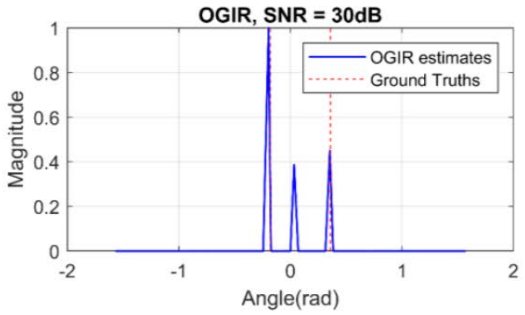

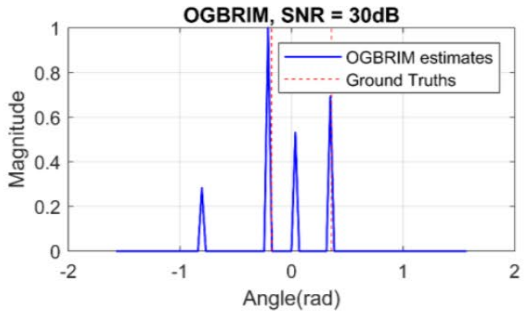

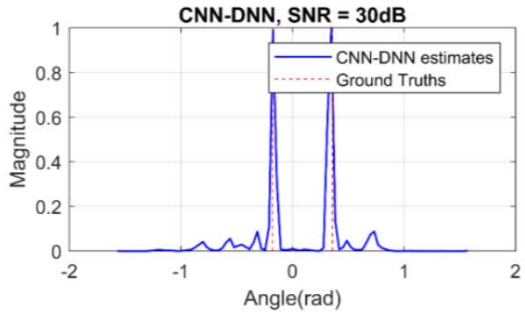

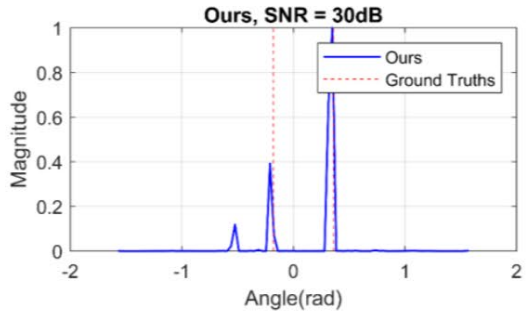

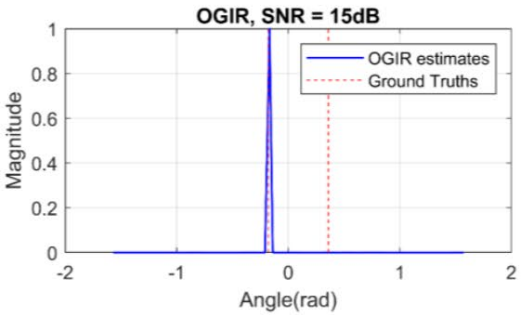

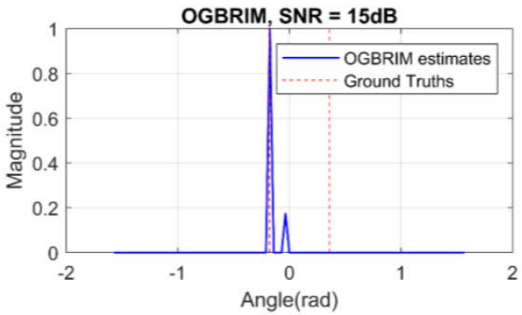

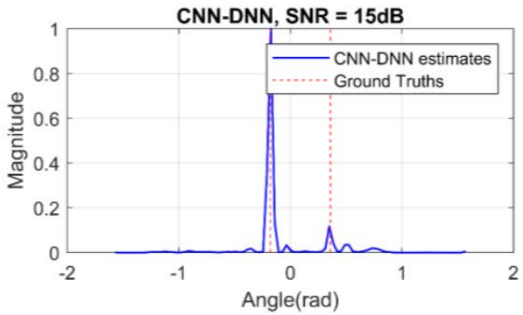

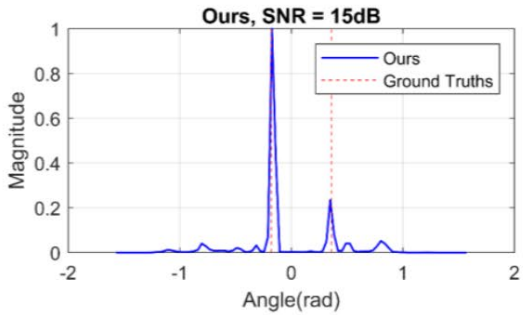

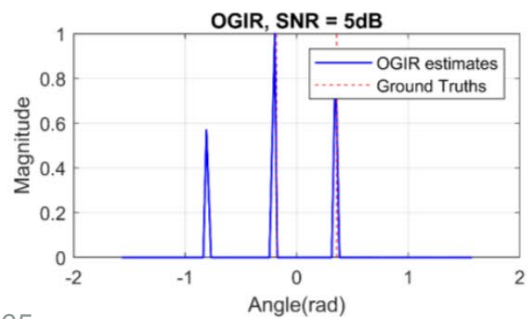

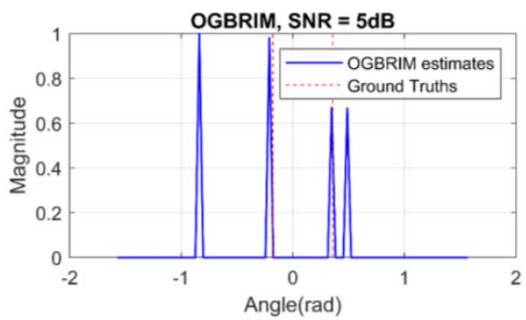

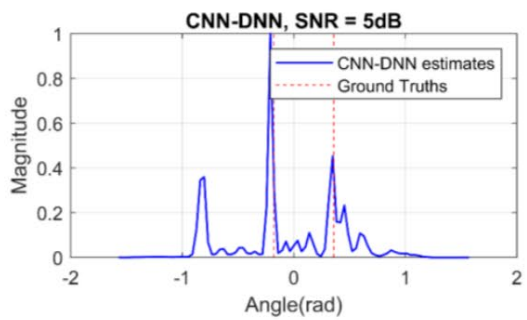

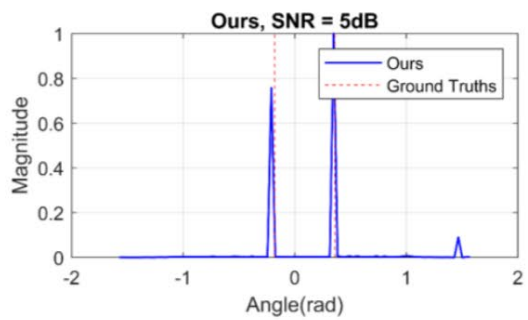

Agenda

- **Background and Motivation of DL for DOA Estimation**
  - ✓ Overview of deep learning (DL) for DOA estimation
  - ✓ Comparison: data-driven vs. model-based approaches
  - ✓ Why hybrid model-based deep learning matters
- **DL for High-Resolution Radar Imaging**
  - ✓ Unrolling IAA
  - ✓ Physics-guided 1D neural networks for radar imaging
  - ✓ DOA estimation considering antenna failure
  - ✓ Off-grid DOA estimation with 1-bit single-snapshot sparse array
  - ✓ Siamese neural networks for DOA estimation
- **DL for Integrated Sensing and Communications (ISAC)**
- **DL Enabled Sparse Array Interpolation**
  - ✓ Unrolling IHT for matrix completion
  - ✓ Transformer based array interpolation

Siamese Neural Networks for DOA Estimation

Emergence of Deep Learning Approaches

Advantages:

- Rapid inference for real-time use.
- Enhanced super-resolution.
- Effective in low SNR conditions.

Challenges:

- Large datasets required for fine angular resolution.
- Class imbalance issues in multi-label classification.
- Sensitivity to noise and sparse input signals.

Our Contribution

- Proposed a Siamese Neural Network (SNN) for single-snapshot DOA estimation.
- Introduced a Sparse Augmentation (SA) Layer for enhanced training with sparse data.
- Designed a Frequency Embedding (FE) Layer for frequency-domain signal processing.
- Applied contrastive loss to refine feature representation with minimal labeled data.

R. Zheng, S. Sun, H. Liu and Y. D. Zhang, "Advancing single-snapshot DOA estimation with Siamese neural networks for sparse linear arrays," in Proc. IEEE 50th International Conference on Acoustics, Speech, and Signal Processing (ICASSP), Hyderabad, India, April 6-11, 2025.

Sparse Linear Arrays (SLAs)

- **Sparsity Definition**:

$$\text{Sparsity} = 1 - \frac{N_{\text{SLA}}}{N_{\text{ULA}}} \qquad (4)$$

- **Example**:
  - Figure 3(a): SLA sparsity is 0.3, reducing elements by 30% compared to the ULA.
  - Scenario: SNR 20 dB, three targets (DOAs: -40°, -20°, 30°; Reflectivity: 0.2, 0.5, 1).
  - Spectral differences exist, but all share the same label in supervised learning.
  - SNNs are used to exploit signal similarities in SLAs.

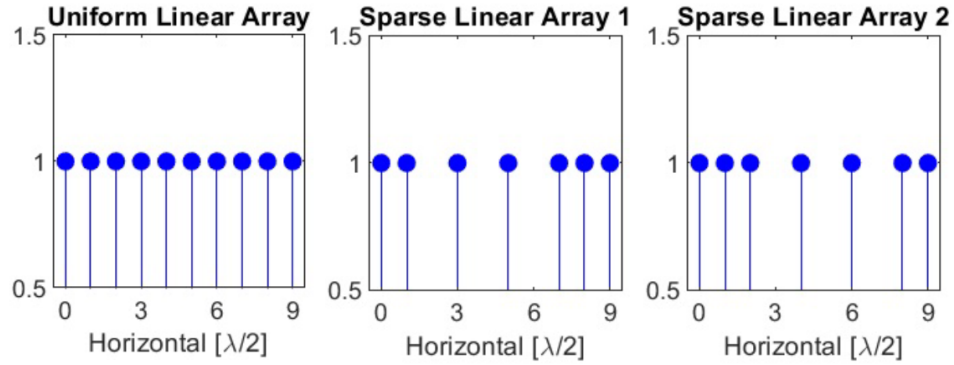

(a)

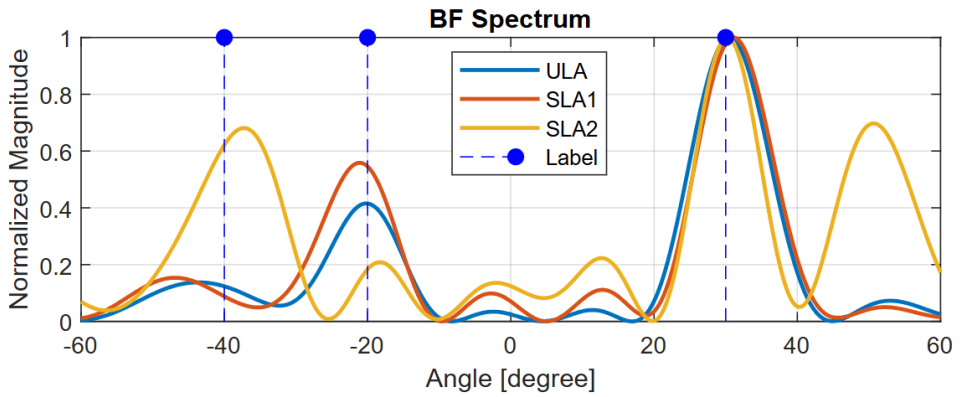

(b)

(a) Example of ULA and SLAs. The SLAs have a 0.3 sparsity. (b) The beamforming spectrum of a single-snapshot signal at 20 dB SNR, depicting three targets with different amplitudes and DOAs, consistently labeled across various array configurations.

Siamese Neural Network

- A Siamese neural network (SNN) is a class of neural network architectures that contain two or more identical subnetworks.
- SNNs use only a few images to get better predictions. SNNs have wide applications in facial recognition and signature verification.

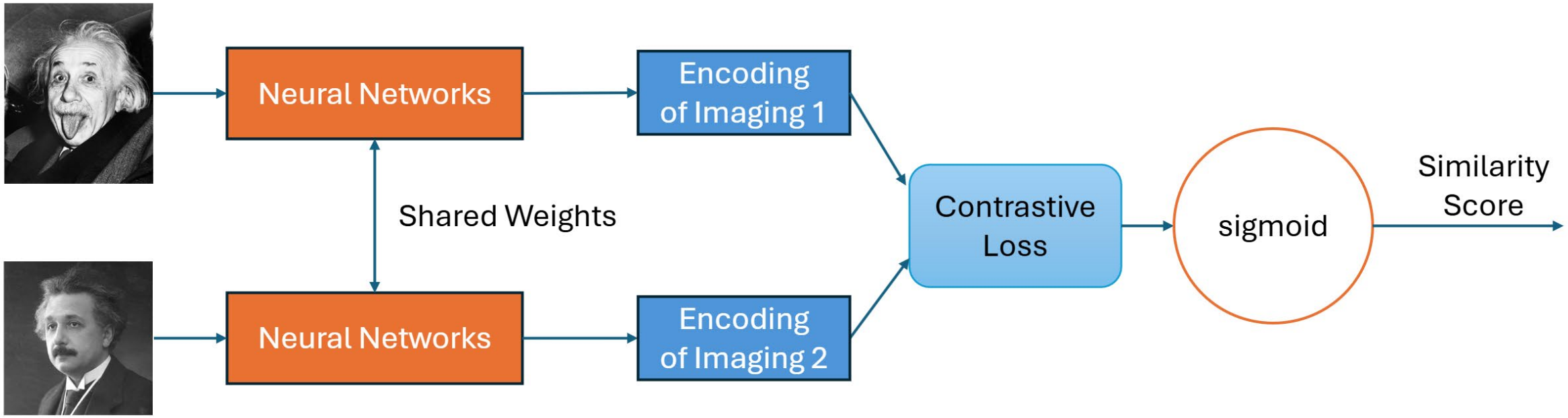

G. Kosh, R. Zemel, and R. Salakhutdinov, “Siamese neural networks for one-shot image recognition,” in Proc. 32nd Int. Conf. Machine Learning, 2015.

Neural Network for DOA Estimation

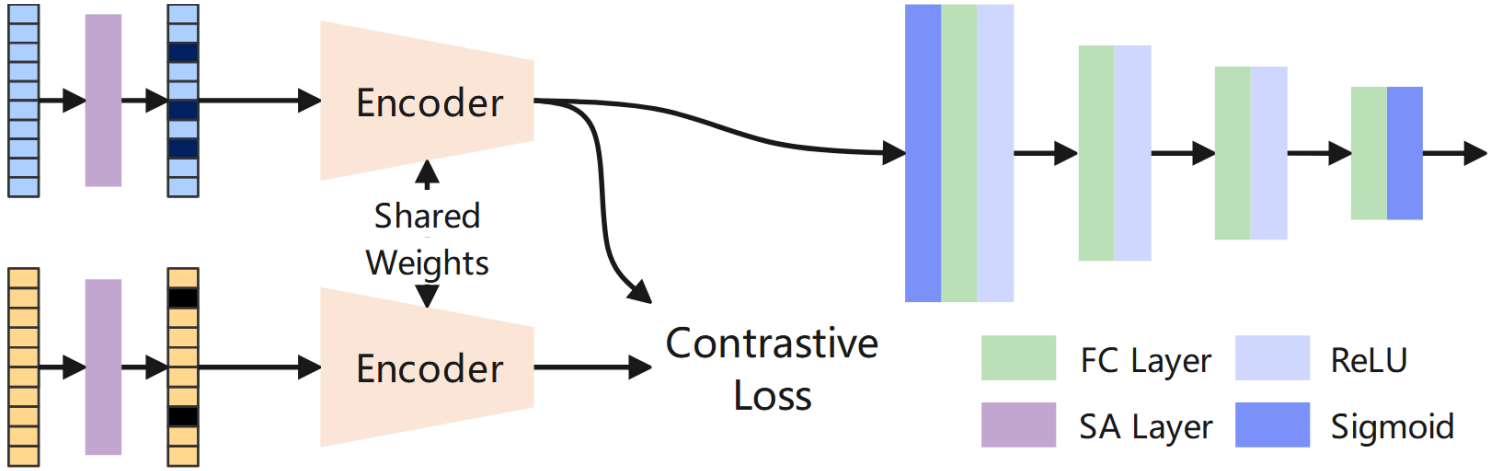

Figure 5: Network architecture of the proposed SNN with sparse augmentation layer.

- **Challenges**:
  - $$N_{\text{labels}} = \sum_{k=1}^{N_{\text{targets}}} \binom{N_{\text{out}}}{k}. \quad (5)$$
  - Exponential growth in training data
  - Severe class imbalance.
  - Vast but underrepresented label space.
- **Components**:
  - Sparse Augmentation (SA) Layer
  - Frequency Embedding (FE) Layer
  - Siamese Neural Network
- **Benefits**:
  - Enhance training with sparse input data.
  - Process sparse signals in the frequency domain.
  - Improve feature representation and reduce the need for extensive labeled data.

Sparse Augmentation Layer

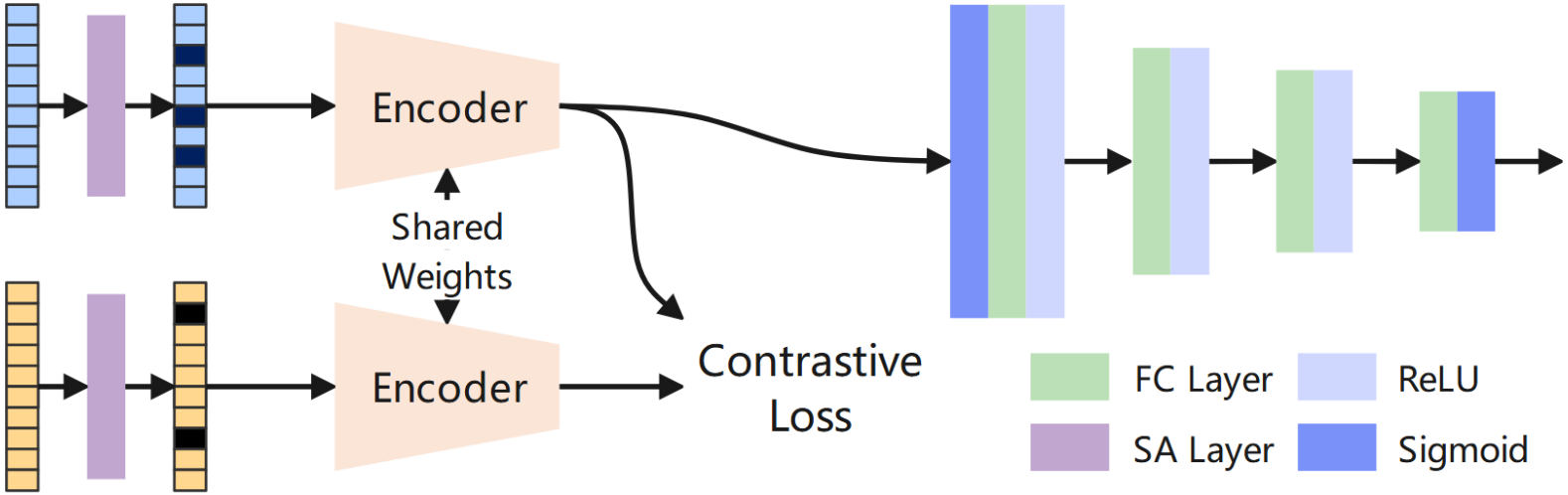

Figure 6: Network architecture of the proposed SNN with sparse augmentation layer.

- **Purpose**:
  - Introduce controlled sparsity into the dataset.
  - Enhance model robustness and prevent overfitting.
- **Mechanism**:
  - Generates a random binary mask.
  - Applies mask to input signal to create sparsity.
  - Configurable maximum sparsity level.

- **Normalization**:

$$\text{output} = \frac{\text{input}}{N_{\text{SLA}}} \tag{6}$$

  - N_{SLA}: Number of active antennas.
  - Ensures output features are adjusted relative to active inputs.

Encoder

- **Importance**:
  - Enhances deep learning by integrating domain knowledge.
- **Signal Encoder**:
  - Consists of four FC layers, each followed by a ReLU layer, to extract signal features
- **Frequency Encoder**:
  - Transforms sparse signals into the continuous frequency domain, enabling convolutional feature extraction.
  - $$g(\mathbf{y}) = \frac{\mathbf{A}^H(\theta)\mathbf{y}}{N_{\text{SLA}}}, \quad (7)$$
  - $\mathbf{A}^H$: Hermitian transpose of array manifold matrix.

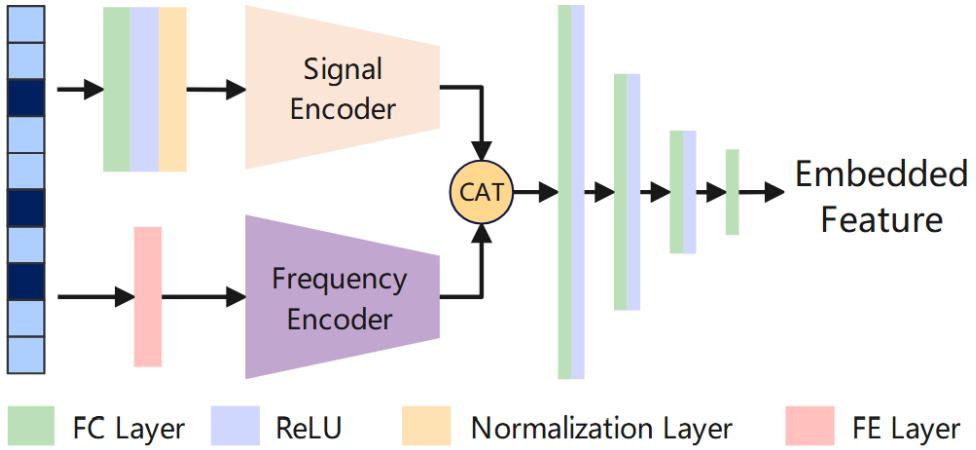

Figure 7: Encoder architecture for feature extraction, where 'CAT' indicates vector concatenation.

Siamese Neural Networks for DOA Estimation

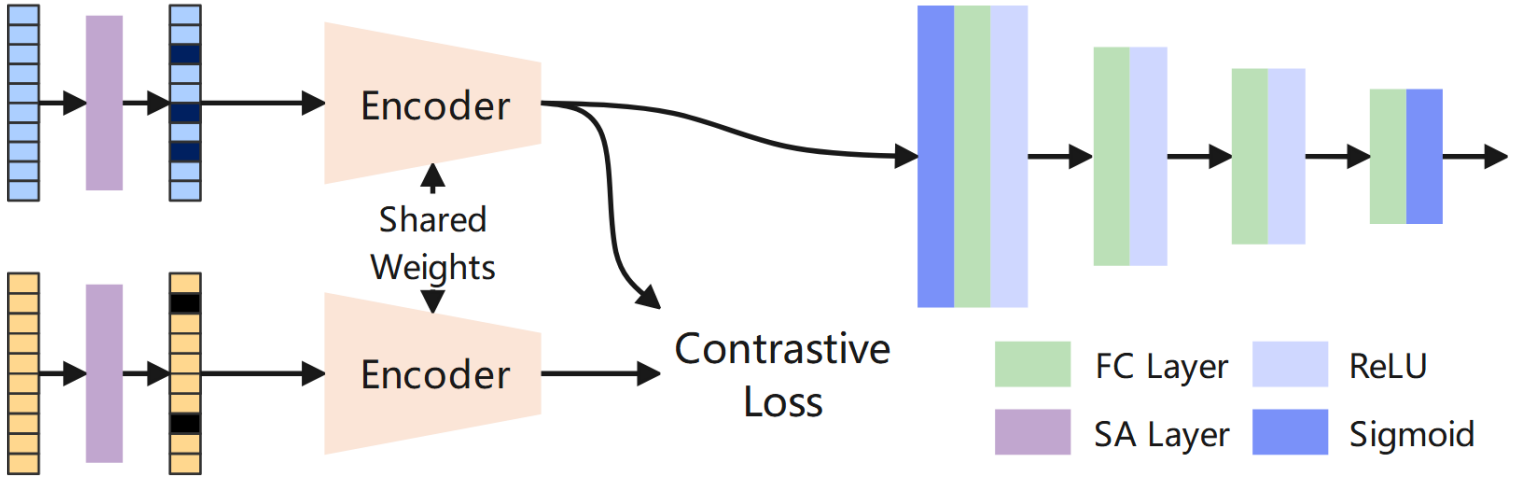

Figure 8: Network architecture of the proposed SNN with sparse augmentation layer.

- **Input Pairs**:
  - **Similar pairs**: Same DOAs, different reflection coefficients and SNRs.
  - **Dissimilar pairs**: Different DOAs.
  - Similar pairs also **differ in sparse array configurations**.
- **Feature Extraction and Learning**:
  - Signals pass through an **encoder**.
  - **Contrastive loss** minimizes distance between similar pairs and enforces separation for dissimilar pairs.

Siamese Neural Networks for DOA Estimation

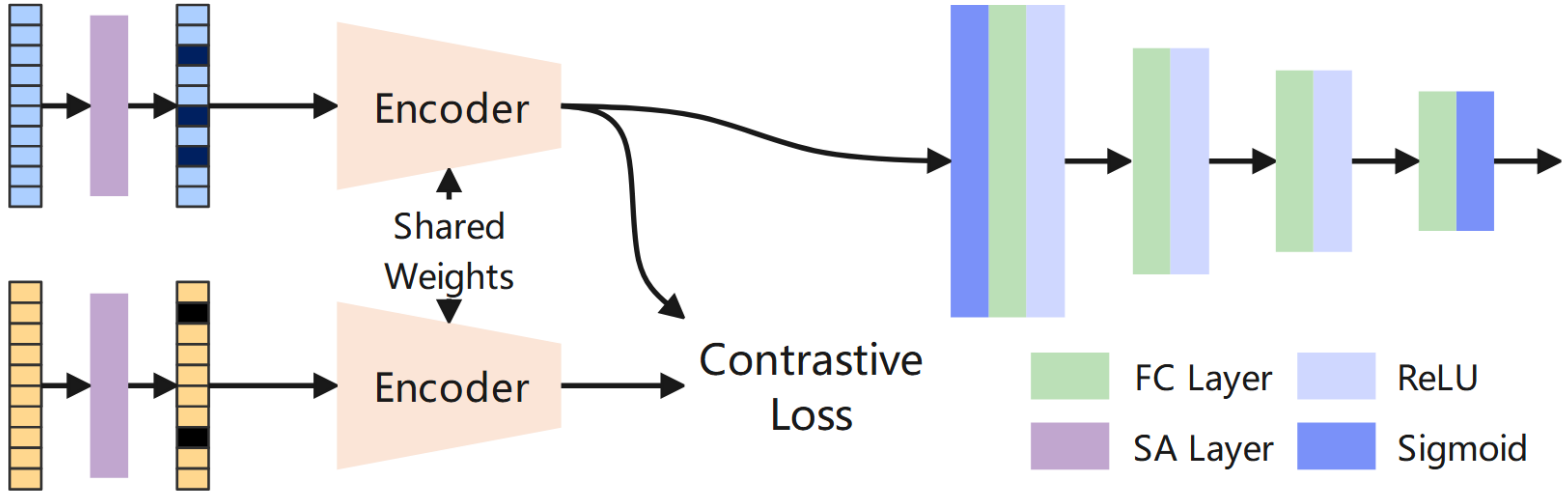

Figure 9: Network architecture of the proposed SNN with sparse augmentation layer.

- **Contrastive Loss Function**:

$$S = \frac{1}{P}\sum_{j=1}^{P}\left(z_j g_j^2 + (1-z_j)\max(0, m-g_j)^2\right), \quad (8)$$

  - $g_j = \|v_{j1} - v_{j2}\|$ is the Euclidean distance between embeddings.
  - z_j is the binary label (1 = similar, 0 = dissimilar).
  - m is the margin controlling separation of dissimilar pairs.

- **Total Loss Function:**
  - Contrastive Loss + Binary Cross-Entropy Loss (for multilabel classification).

Feature Analysis

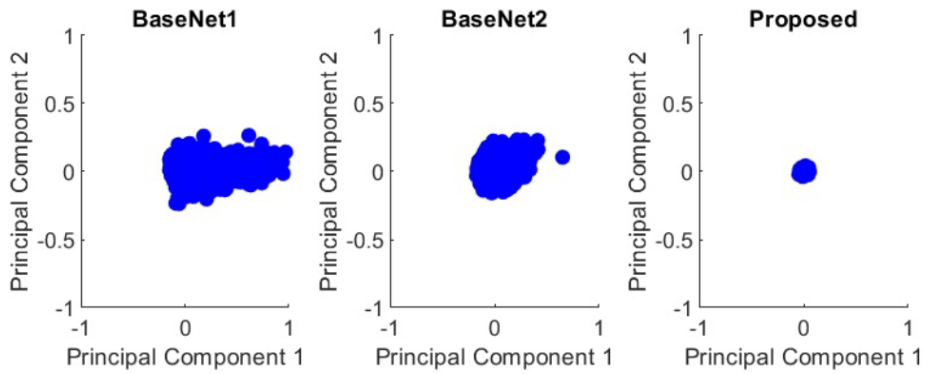

(a)

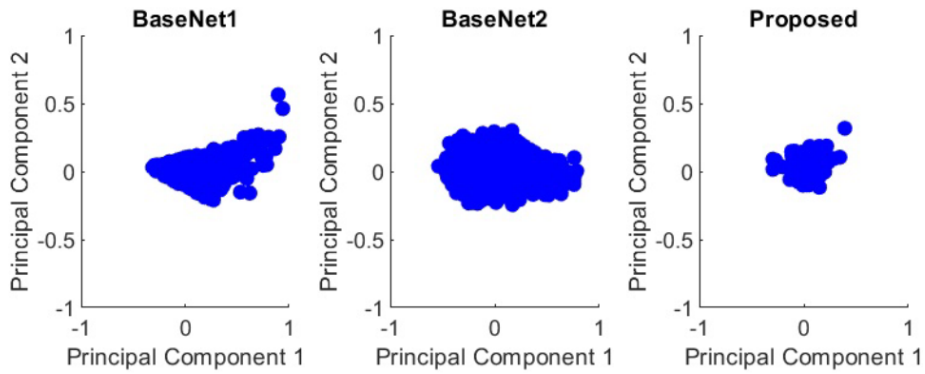

(b)

Figure 10: PCA-reduced embedding features for (a) ULA and (b) Random SLAs with a sparsity of 0.3.

- **Benchmark Models**:
  - **BaseNet1**: Without SA layer and contrastive loss.
  - **BaseNet2**: Without contrastive loss.
- **Feature Representation & Clustering**:
  - Ideal feature representations should be **identical or closely clustered** within the same class.
  - **Tighter clustering** improves classification performance.

- **Setup**:
  - **5,000 test signals with random SLAs** (sparsity 0.3, six random positions set to zero).
  - Signal sparsity affects all models, but **the proposed SNN is least impacted**, benefiting from the **Siamese architecture and contrastive loss**.

DOA Estimation: Accuracy vs SNR

- **Setup**:
  - **5,000 test signals** across **random SLAs** (sparsity = 0.3).
  - Input **SNR levels: 0 dB to 30 dB**.
  - Decision **threshold:** 0.5.
- **Evaluation Metrics:**
  - **DOA estimation** is treated as a **multilabel classification** problem.
  - Performance is evaluated using:
    - ★ **Accuracy**

$$\text{Accuracy} = \frac{1}{M}\sum_{m=1}^{M}\frac{TP_m + TN_m}{TP_m + TN_m + FP_m + FN_m}. \qquad (10)$$

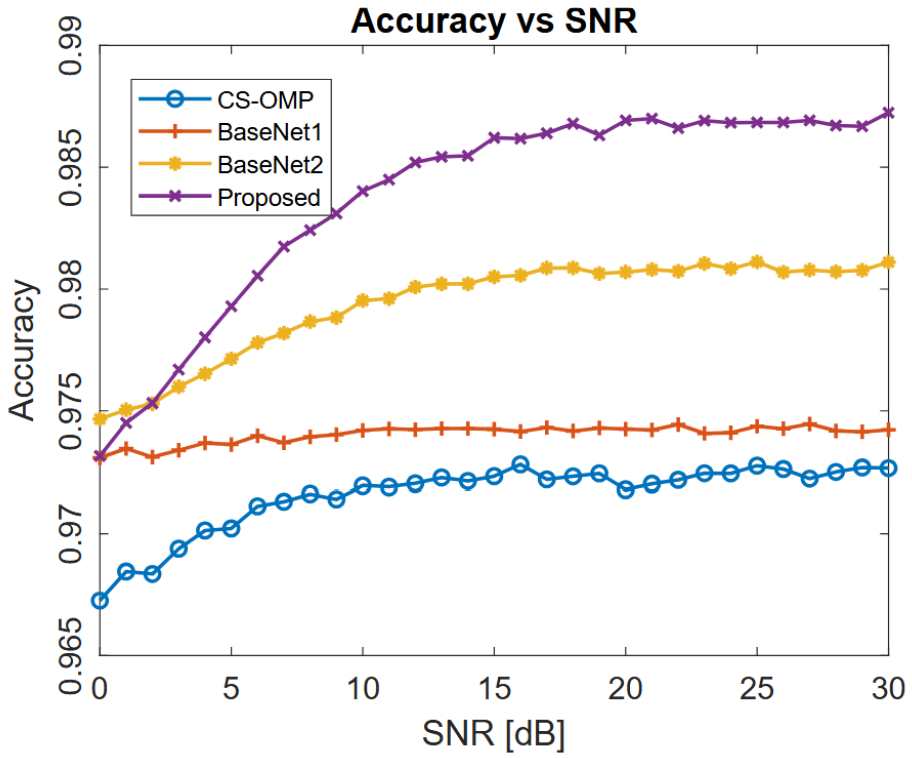

DOA Estimation: Precision vs SNR

- **Setup**:
  - **5,000 test signals** across **random SLAs** (sparsity = 0.3).
  - Input **SNR levels: 0 dB to 30 dB**.
  - Decision **threshold:** 0.5.
- **Evaluation Metrics:**
  - **DOA estimation** is treated as a **multilabel classification** problem.
  - Performance is evaluated using:
    - ★ **Accuracy**
    - ★ **Precision**

$$\text{Precision} = \frac{1}{M}\sum_{m=1}^{M}\frac{TP_m}{TP_m + FP_m}. \qquad (11)$$

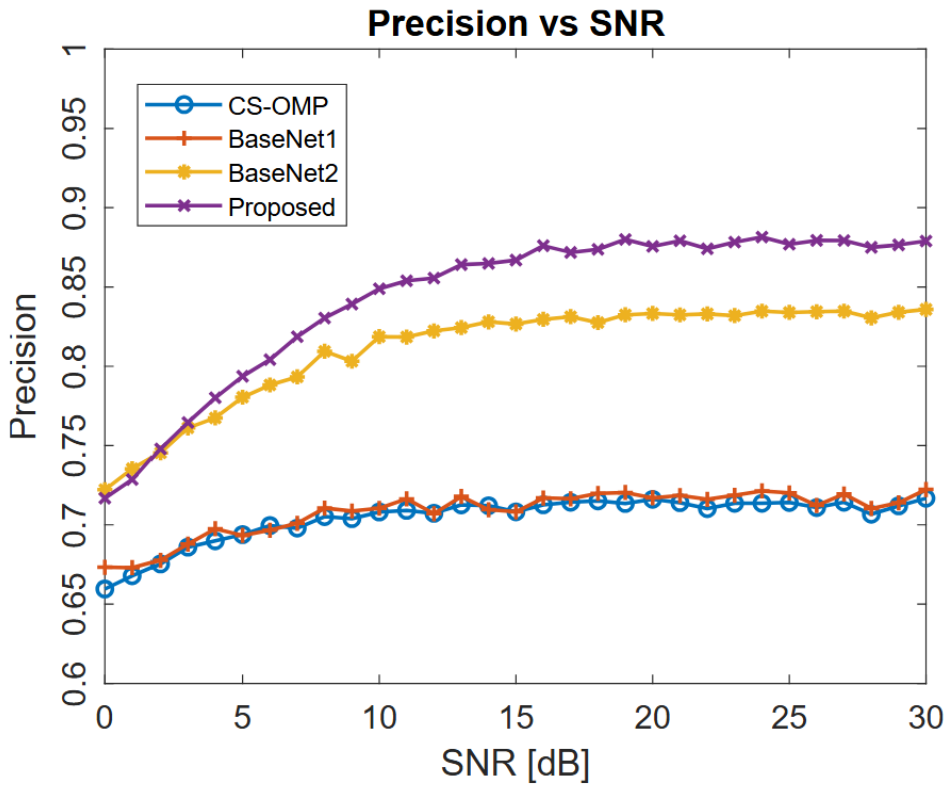

DOA Estimation: Recall vs SNR

- **Setup**:
  - **5,000 test signals** across **random SLAs** (sparsity = 0.3).
  - Input **SNR levels: 0 dB to 30 dB**.
  - Decision **threshold:** 0.5.
- **Evaluation Metrics:**
  - **DOA estimation** is treated as a **multilabel classification** problem.
  - Performance is evaluated using:
    - ★ **Accuracy**
    - ★ **Precision**
    - ★ **Recall**

$$\text{Recall} = \frac{1}{M} \sum_{m=1}^{M} \frac{TP_m}{TP_m + FN_m}. \qquad (12)$$

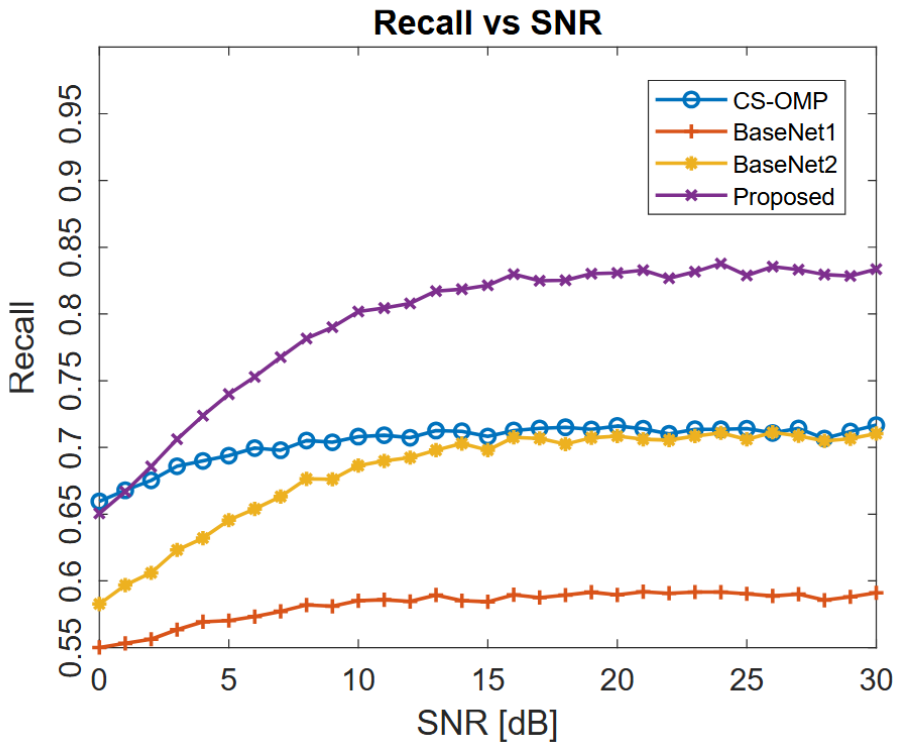

DOA Estimation: F1 vs SNR

- **Setup**:
  - **5,000 test signals** across **random SLAs** (sparsity $= 0.3$).
  - Input **SNR levels: 0 dB to 30 dB**.
  - Decision **threshold:** 0.5.
- **Evaluation Metrics:**
  - **DOA estimation** is treated as a **multilabel classification** problem.
  - Performance is evaluated using:
    - ★ **Accuracy**
    - ★ **Precision**
    - ★ **Recall**
    - ★ **F1 Score**

$$\text{F1-Score} = 2 \cdot \frac{\text{Precision} \times \text{Recall}}{\text{Precision} + \text{Recall}}. \qquad (13)$$

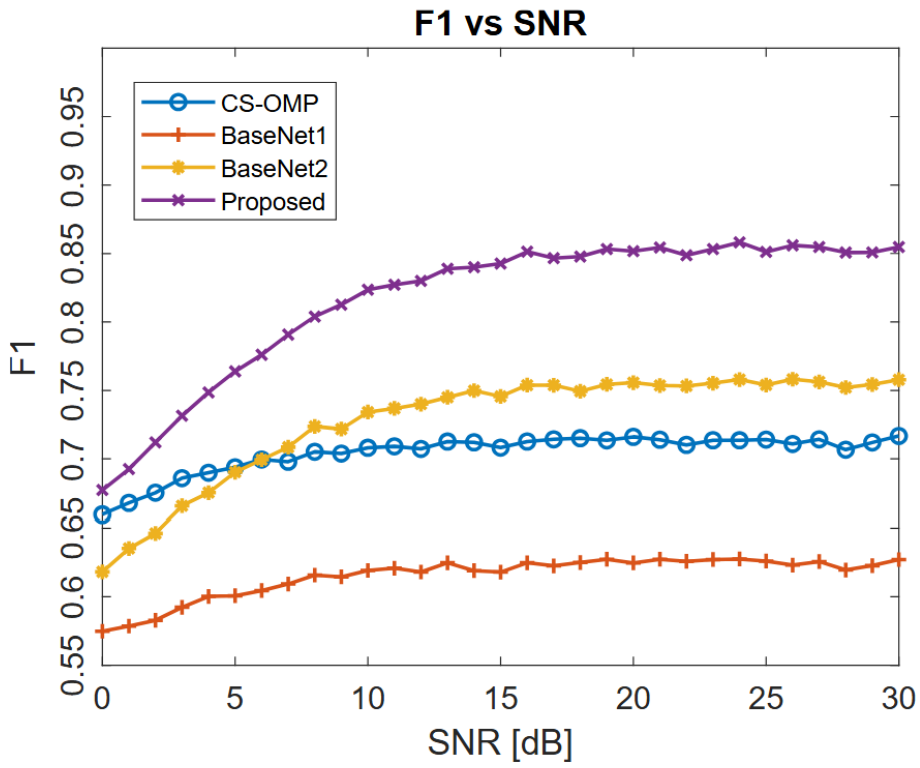

DOA Estimation: F1 vs SNR

- **Setup**:
  - **5,000 test signals** across **random SLAs** (sparsity $= 0.3$).
  - Input **SNR levels: 0 dB to 30 dB**.
  - Decision **threshold:** 0.5.
- **Evaluation Metrics:**
  - **DOA estimation** is treated as a **multilabel classification** problem.
  - Performance is evaluated using:
    - ★ **Accuracy**
    - ★ **Precision**
    - ★ **Recall**
    - ★ **F1 Score**

$$\text{F1-Score} = 2 \cdot \frac{\text{Precision} \times \text{Recall}}{\text{Precision} + \text{Recall}}. \qquad (13)$$

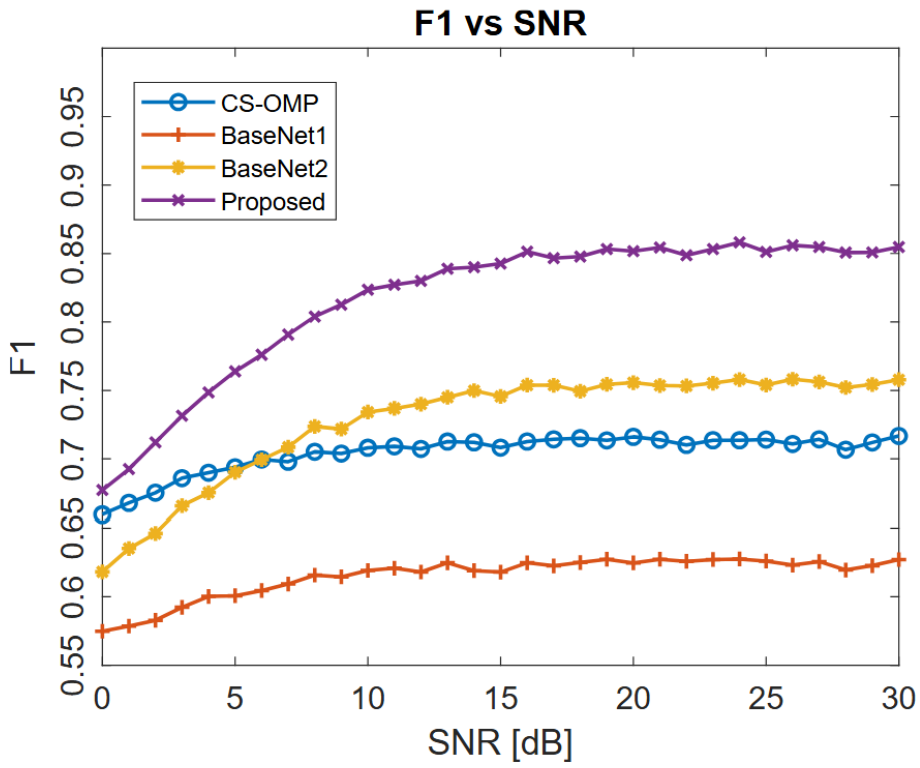

Code is available at: https://github.com/ruxinzh/SNNS_SLA

Agenda

- **Background and Motivation of DL for DOA Estimation**
  - ✓ Overview of deep learning (DL) for DOA estimation
  - ✓ Comparison: data-driven vs. model-based approaches
  - ✓ Why hybrid model-based deep learning matters
- **DL for High-Resolution Radar Imaging**
  - ✓ Unrolling IAA
  - ✓ Physics-guided 1D neural networks for radar imaging
  - ✓ DOA estimation considering antenna failure
  - ✓ Off-grid DOA estimation with 1-bit single-snapshot sparse array
  - ✓ Siamese neural networks for DOA estimation
- **DL for Integrated Sensing and Communications (ISAC)**
- **DL Enabled Sparse Array Interpolation**
  - ✓ Unrolling IHT for matrix completion
  - ✓ Transformer based array interpolation

Reinforcement Learning

- Reinforcement learning is a framework where an agent interacts with an environment via actions, receives rewards or penalties, and learns a policy to maximize long-term return.

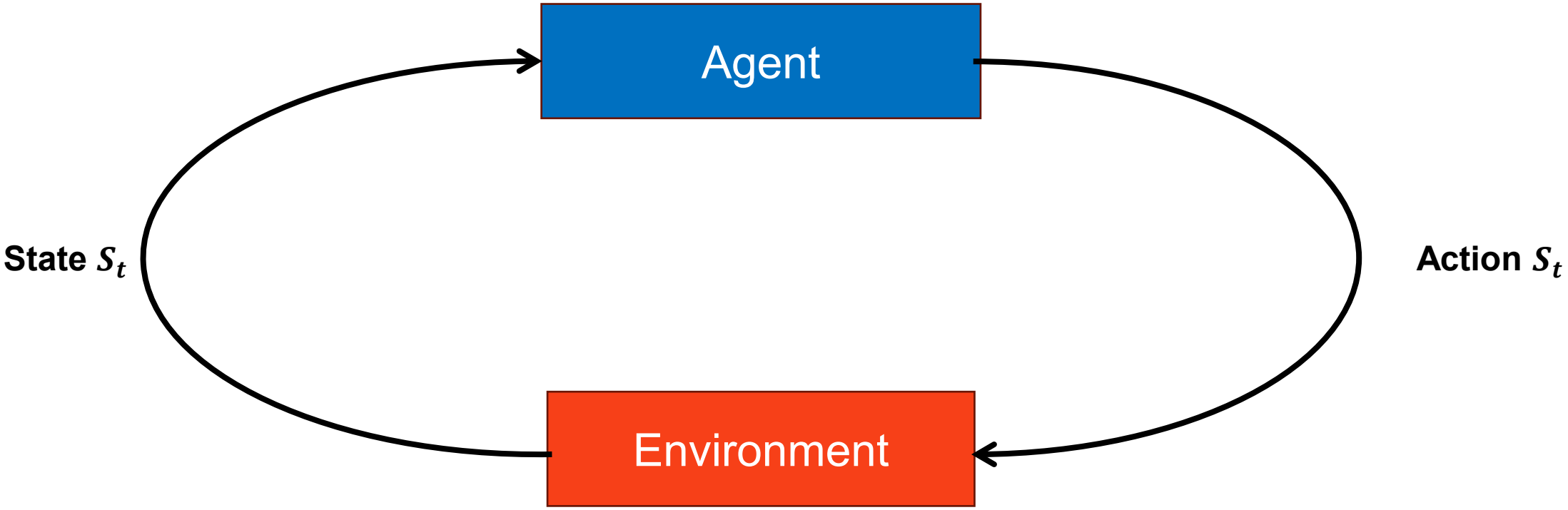

Reinforcement Learning

- Reinforcement learning is a framework where an agent interacts with an environment via actions, receives rewards or penalties, and learns a policy to maximize long-term return

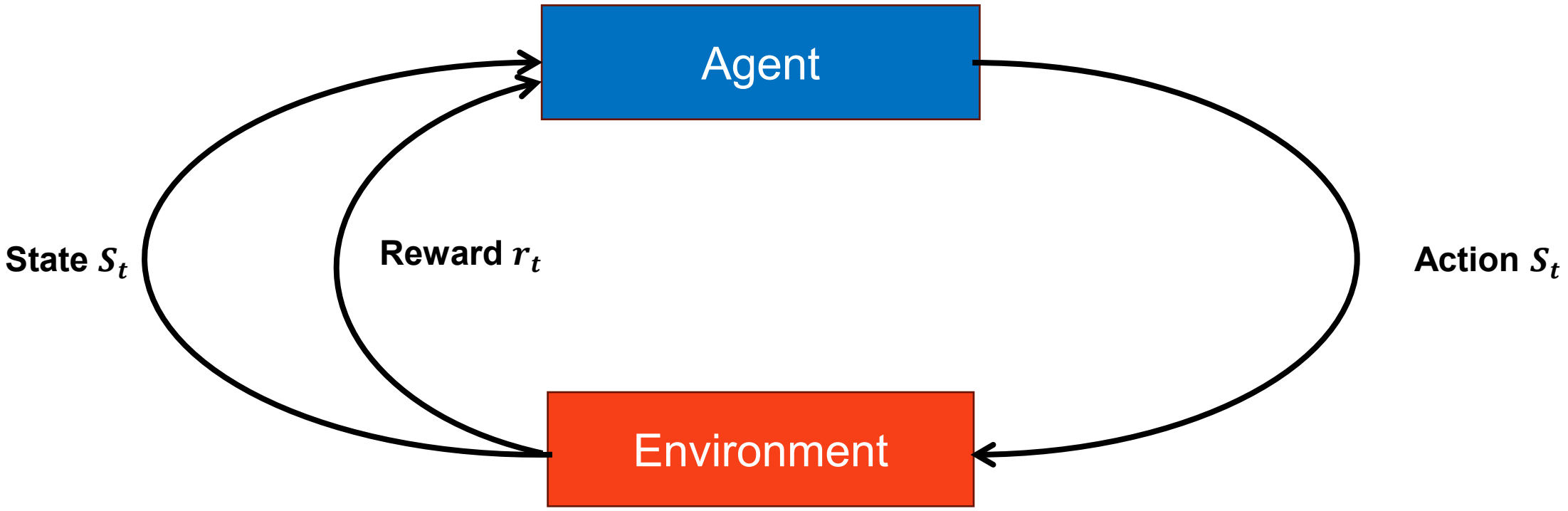

DRL in Wireless Communication and Radar

Deep reinforcement learning in radar enables adaptive waveform design, beamforming, and target tracking by learning optimal sensing policies directly from environmental feedback and rewards.

Deep reinforcement learning for integrated sensing and communication (ISAC) optimizes joint resource allocation, waveform design, and beam management to simultaneously enhance communication quality and radar sensing performance through interaction with the dynamic environment.

Feriani and E. Hossain, "Single and Multi-Agent Deep Reinforcement Learning for AI-Enabled Wireless Networks: A Tutorial," in *IEEE Communications Surveys & Tutorials*, vol. 23, no. 2, pp. 1226-1252, 2021.

C. E. Thornton, M. A. Kozy, R. M. Buehrer, A. F. Martone and K. D. Sherbondy, "Deep Reinforcement Learning Control for Radar Detection and Tracking in Congested Spectral Environments," in *IEEE Transactions on Cognitive Communications and Networking*, vol. 6, no. 4, pp. 1335-1349, Dec. 2020.

N. C. Luong *et al*., "Applications of Deep Reinforcement Learning in Communications and Networking: A Survey," in *IEEE Communications Surveys & Tutorials*, vol. 21, no. 4, pp. 3133-3174, 2019.

ISAC with Sparse Arrays and Quantized Phase Shifters

Adaptively select a small subset of transmit antennas and adjust quantized double-phase shifters, such that the transmitted energy is concentrated on the communication user and target of interest, while reducing interference to other radars by creating nulls towards their respective directions.

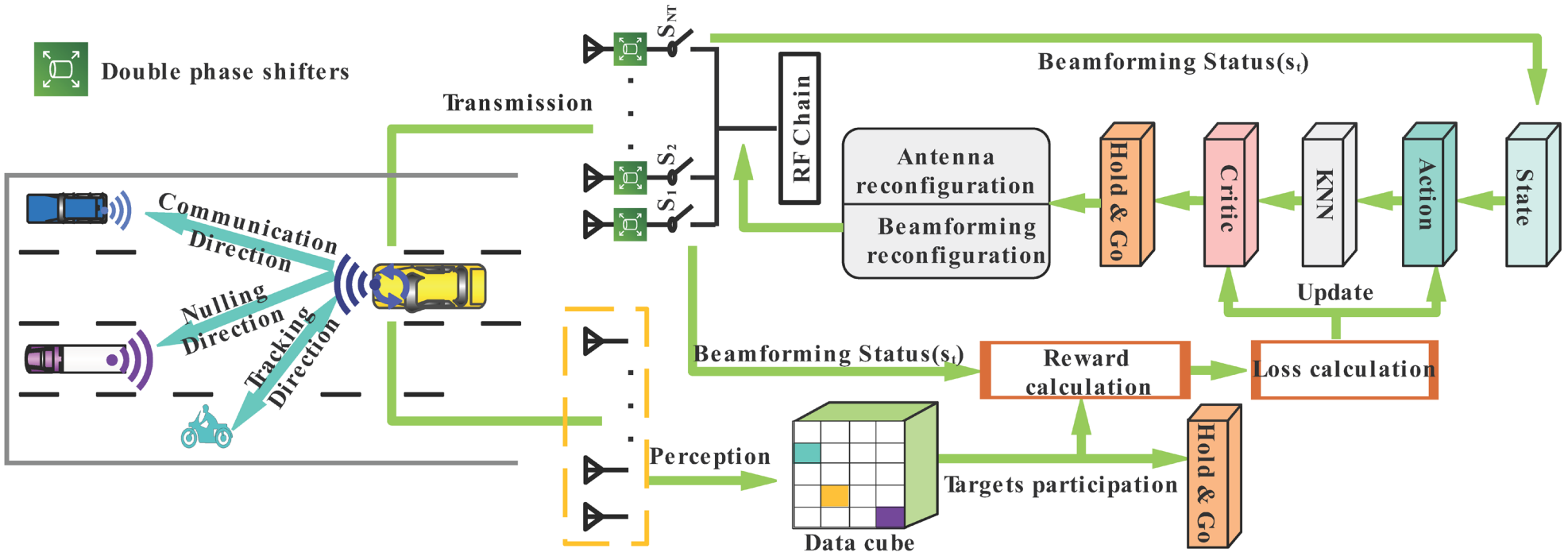

L. Xu, S. Sun, Y. D. Zhang and A. P. Petropulu, "Reconfigurable beamforming for automotive radar sensing and communication: A deep reinforcement learning approach," IEEE Journal of Selected Areas in Sensors, vol. 1, pp. 124-138, 2024.

L. Xu, S. Sun, Y. D. Zhang and A. P. Petropulu, "Joint antenna selection and beamforming in integrated automotive radar sensing-communications with quantized double phase shifters," in Proc. IEEE 48th International Conference on Acoustics, Speech, and Signal Processing (ICASSP), Rhodes Island, Greece, June 4-9, 2023.

Transmit Beamforming

- Transmit beamforming $B(\theta) = \boldsymbol{a}_t^H(\theta)\boldsymbol{W}\boldsymbol{a}_t(\theta)$, where $\boldsymbol{W}$ is the beamforming weighting matrix composed by quantized phase terms.
- Analog precoder is controlled by the phase shifter.
- The radar sensing beamformer is $w_r = \left[e^{jw_1}, \ldots, e^{jw_{N_t}}\right]^T$.
- The communication receiver is assumed to have N_c antennas. Assuming there are L independent propagation paths, the downlink channel matrix is $H_d = \sum_{l=1}^{L} \beta_l \boldsymbol{b}_c(\theta_{cl})\boldsymbol{a}_t^H(\theta_{tl})$. The analog precoder is replaced with $w_c = \left[e^{j\Omega_1}, \ldots, e^{j\Omega_{N_t}}\right]^T$

Transmit Beamforming Design for ISAC

Beam Synthesis vis Double Phase Shifters: $\boldsymbol{w} = c_1\boldsymbol{w_r} + c_2\boldsymbol{w_c}$
Here, c_1 and c_2 are coefficients to balance the radar sensing and communication capabilities.

Transmit Beamforming Optimization:
Beamforming needs to
1) maintain a certain power toward both sensing targets and communication direction
2) generate minimal interference
3) maintain a low peak sidelobe level (PSL).

$$\min_{\{\boldsymbol{w},\boldsymbol{S},\alpha_1,\alpha_2,\alpha_3\}} \gamma_1\,\alpha_1 + \gamma_2\alpha_2 + \gamma_3\alpha_3$$
$$s.t.\ \left|\boldsymbol{w^H S a}(\theta_r)\right| = p_1$$
$$\left|\boldsymbol{w^H S a}(\theta_c)\right| = p_2$$
$$\left|\boldsymbol{w^H S a}(\theta_l)\right| < \rho_1 + \alpha_1$$
$$\left|\boldsymbol{w^H S a}(\theta_i)\right| < \rho_2 + \alpha_2$$
$$\left|\theta_r - \widehat{\theta_r}\right| < \alpha_3$$
$$tr(\boldsymbol{S}) = M + 2$$
$$\boldsymbol{w} = c_1\boldsymbol{w_r} + c_2\boldsymbol{w_c}$$

Transmit Beamforming Design with DRL

Action Space: Select of subset (M+2) of a ULA (with N_t elements) with both end elements fixed. The number of solutions is $Q = C_{N_t-2}^{M}$. Each element has q-bit quantized phase shifters. The number of actions is $Q2^{q(M+2)}$. An antenna selection matrix $\boldsymbol{S} = [\boldsymbol{u}_1, \boldsymbol{u}_2, \dots, \boldsymbol{u}_{N_t}]$, with $tr(\boldsymbol{S}) = M + 2$.

State: At each iteration, the status is represented by the vector $\boldsymbol{s} = [w_1, \dots, w_{M+2}]^T$, where each element represents the phase of the selected antenna.

Reward for Sensing: $r_{ri} = \begin{cases} 1, & if\ \xi_i > \xi_{i-1}\ and\ d_{ri} \le d_{ri-1} \\ -1, & if\ \xi_i \le \xi_{i-1}\ and\ d_{ri} > d_{ri-1} \\ 0, & otherwise \end{cases}$

Here, ξ_i quantifies the difference between main lobe and peak sidelobe, while $d_r = \left|\theta_r - \widehat{\theta_r}\right|$ quantifies the main beam deviation.

Reward for Communication: $r_{ci} = \begin{cases} 1, & if\ \ g_{ci} > g_{ci-1} \\ 0, & if\ \ g_{ci} = g_{ci-1} \\ -1, & if\ \ g_{ci} < g_{ci-1} \end{cases}$, where $g_c = |\boldsymbol{Hw}|^2$ is the received signal gain.

Transmit Beamforming Design with DRL

Reward for Interference: $r_{pi} = \begin{cases} 1, & if \quad p_i < p_{i-1} \\ 0, & if \quad p_i = p_{i-1} \\ -1, & if \quad p_i > p_{i-1} \end{cases}$, where $\mathrm{p} = \left|\boldsymbol{w}^{\boldsymbol{H}}\boldsymbol{a}(\theta_i)\right|^2$ is the beamforming attenuation in the direction of θ_i.

Total reward: $r_i = \lambda_1 r_{ri} + \lambda_2 r_{ci} + \lambda_3 r_{pi}$, where λ_1, λ_2 and λ_3 are weighting trade off between sensing, communication and interference suppression.

When the action dimension is high, it becomes difficult to use DQN RL to find the desired mapping policy.

Wolpertinger policy comprises three basic elements: an action network, a K-nearest neighbor (KNN) map, and a critic network. The deep deterministic policy gradient (DDPG) is used to train the networks. The Wolpertinger policy scales linearly with the number of selected actions.

In DDPG, the KNN network is used to select the best action from the set of actions generated by the actor network.

The goal of critic network is to choose the corresponding action to the maximum Q value.

Transmit Beamforming Design with DRL

We choose 12 antennas from 15 antennas to form the final transmission array.. There are 455 possible selection schemes. Each antenna is connected to a 3-bit quantization double-phase shifter.

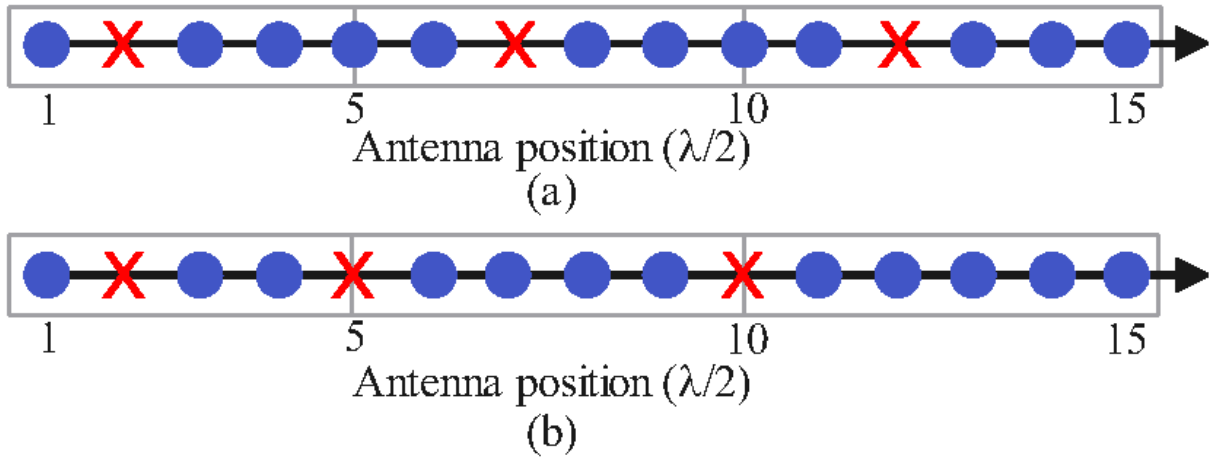

(a) The transmit array configuration in the initial phase; (b) The transmit array configuration after optimization.

Numerical Results: Beampattern

The energy of communication and tracking direction optimized by DRL is more balanced and the sidelobes are reduced.

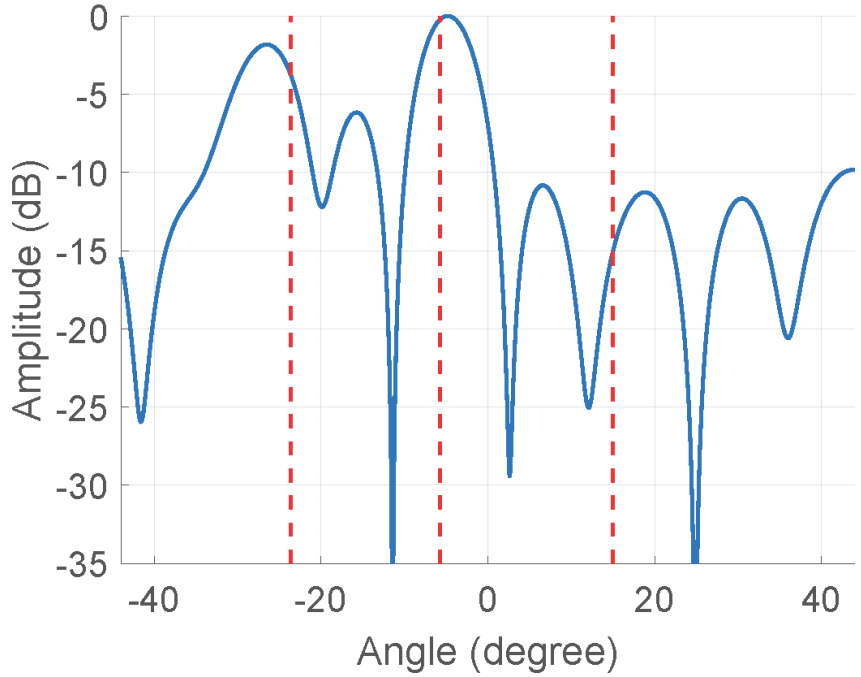

(a)

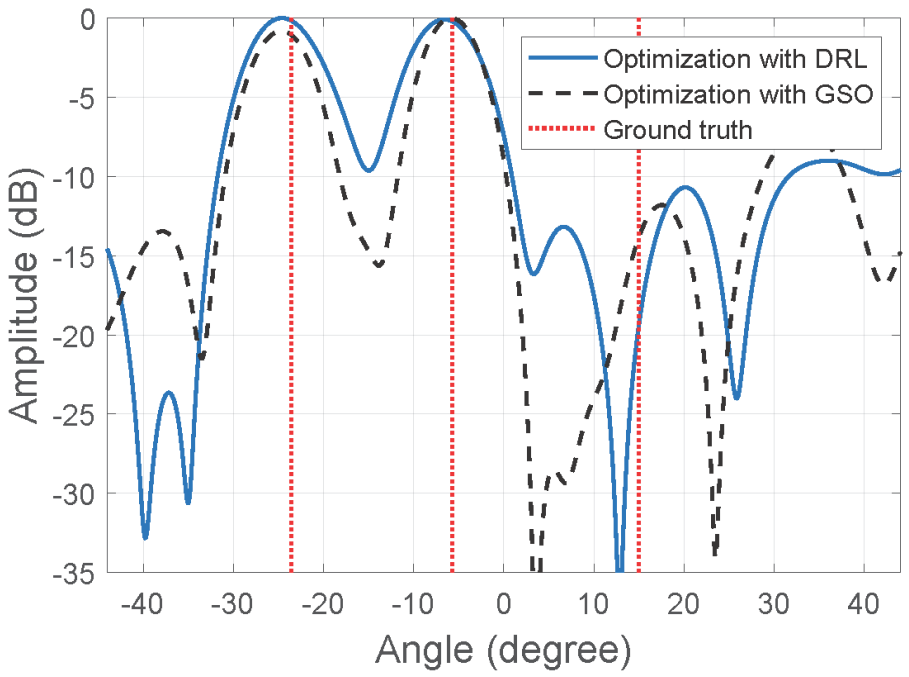

(b)

(a) The transmit beamforming in the initial phase; (b) The transmit beamforming after optimization with DRL and GSO, Ground truth directions are indicated in red dash lines..

Agenda

- **Background and Motivation of DL for DOA Estimation**
  - ✓ Overview of deep learning (DL) for DOA estimation
  - ✓ Comparison: data-driven vs. model-based approaches
  - ✓ Why hybrid model-based deep learning matters
- **DL for High-Resolution Radar Imaging**
  - ✓ Unrolling IAA
  - ✓ Physics-guided 1D neural networks for radar imaging
  - ✓ DOA estimation considering antenna failure
  - ✓ Off-grid DOA estimation with 1-bit single-snapshot sparse array
  - ✓ Siamese neural networks for DOA estimation
- **DL for Integrated Sensing and Communications (ISAC)**
- **DL Enabled Sparse Array Interpolation**
  - ✓ Unrolling IHT for matrix completion
  - ✓ Transformer based array interpolation

Sparse Array Interpolation: Matrix Completion

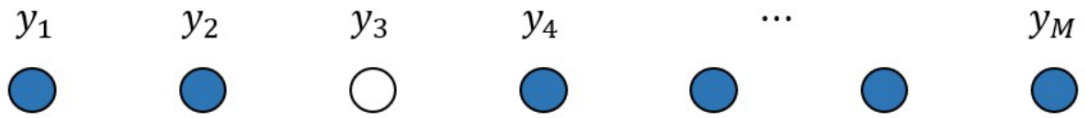

- Missing sum coarray elements render a Hankel matrix with missing elements:

$$\mathcal{H}(\mathbf{y}) = \begin{bmatrix} y_1 & y_2 & \cdots & y_L \\ y_2 & y_3 & \cdots & y_{L+1} \\ y_3 & y_4 & \cdots & y_{L+2} \\ \vdots & \vdots & \ddots & \vdots \\ y_{M_1} & y_{M_1+1} & \cdots & y_M \end{bmatrix}$$

- The forward-only Hankel matrix completion problem[3] is to find a Hankel matrix $\mathbf{x}$ that has a minimum rank and its distance to the original data matrix at the observed positions meets the required error bound δ:

$$\begin{aligned} \min_{\mathbf{x}} \quad & \operatorname{rank}(\mathcal{H}(\mathbf{x})) \\ \text{s.t.} \quad & \|\mathcal{H}(\mathbf{x}) \odot \mathbf{M}_{FO} - \mathcal{H}(\mathbf{y})\|_F \leq \delta, \end{aligned}$$

where $\mathbf{M}_{FO}$ is a mask matrix.

S. Sun and Y. D. Zhang, "4D automotive radar sensing for autonomous vehicles: A sparsity-oriented approach," IEEE Journal of Selected Topics in Signal Processing, vol. 15, no. 4, pp. 879-891, 2021.

Sparse Array Interpolation: Hankel Matrix

- The sum coarray may be designed to be sparse so as to achieve an extended aperture.
- Directly performing DOA estimation based on sparse sum arrays may yield high sidelobes and obscure target detection.
- The missing elements in the "holes" can be recovered through structured interpolation so as to reduce the sidelobe levels.
- For an M-element ULA, the noiseless array response $\mathbf{y} = [y_1, y_2, \cdots, y_M]^T$ can be used to construct a Hankel matrix with dimensional of $M_1 \times L$ as

$$\mathcal{H}(\mathbf{y}) = \begin{bmatrix} y_1 & y_2 & \cdots & y_L \\ y_2 & y_3 & \cdots & y_{L+1} \\ y_3 & y_4 & \cdots & y_{L+2} \\ \vdots & \vdots & \ddots & \vdots \\ y_{M_1} & y_{M_1+1} & \cdots & y_M \end{bmatrix} = \mathbf{A}\mathbf{\Sigma}\mathbf{B}^T,$$

where $M_1 = M - L + 1$, and L is the pencil parameter,

$$\mathbf{A} = [\mathbf{a}(\theta_1), \cdots, \mathbf{a}(\theta_K)] \text{ with } \mathbf{a}(\theta_k) = \left[1, e^{j2\pi \frac{d\sin(\theta_k)}{\lambda}}, \cdots, e^{j2\pi \frac{(M_1-1)d\sin(\theta_k)}{\lambda}}\right]^T$$

$$\mathbf{B} = [\mathbf{b}(\theta_1), \cdots, \mathbf{b}(\theta_K)] \text{ with } \mathbf{b}(\theta_k) = \left[1, e^{j2\pi \frac{d\sin(\theta_k)}{\lambda}}, \cdots, e^{j2\pi \frac{(L-1)d\sin(\theta_k)}{\lambda}}\right]^T$$

$$\mathbf{\Sigma} = \mathrm{diag}([\beta_1, \cdots, \beta_K])$$

- When K ($K < M_1$ and $K < L$) sources imping to the array, the Hankel matrix $\mathcal{H}(\mathbf{y})$ has a Vandermonde decomposition structure with rank K.

S. Sun, Y. Wen, R. Wu, D. Ren, and J. Li, "Fast forward-backward Hankel matrix completion for automotive radar DOA estimation using sparse linear arrays," in Proc. IEEE Radar Conference, San Antonio, TX, May 1-5, 2023.

Iterative Hard Thresholding (IHT) Algorithm

- In the n-th iteration, the new forward-backward array beamvectors $\mathbf{X}_n = \begin{bmatrix} \mathbf{x}_n & \bar{\mathbf{x}}_n \end{bmatrix} \in \mathbb{C}^{M\times 2}$ is updated as

$$\mathbf{X}_n = \mathbf{X}_{n-1} - \alpha_n \mathbf{D}_{n-1}, \tag{2}$$

where $\alpha_n = \frac{1}{\sqrt{n}}$ is the step size, and $\mathbf{D}_{n-1} \in \mathbb{C}^{M\times 2}$ is the sub-gradient, defined as

$$\mathbf{D}_{n-1} = \begin{bmatrix} \mathbf{z}_S & \bar{\mathbf{z}}_S \end{bmatrix} - \mathbf{X}_{n-1} \odot \begin{bmatrix} \mathbf{m} & \bar{\mathbf{m}} \end{bmatrix}. \tag{3}$$

- In the n-th iteration, the obtained FB Hankel matrix $\mathbf{H}_n = \begin{bmatrix} \mathcal{H}(\mathbf{x}_n) & \mathcal{H}(\bar{\mathbf{x}}_n) \end{bmatrix} = \mathbf{U}_n \mathbf{\Sigma}_k \mathbf{V}_n^H$, with $\mathbf{U}_n \in \mathbb{C}^{M_1\times K}$ and $\mathbf{V}_n \in \mathbb{C}^{2L\times K}$, is first projected onto a tangent subspace $\mathbf{T}_n \in \mathbb{C}^{M_1\times 2L}$, which is defined as

$$\mathbf{T}_n = \{\mathbf{U}_n \mathbf{A}^H + \mathbf{B}\mathbf{V}_n^H | \mathbf{A} \in \mathbb{C}^{2L\times K}, \mathbf{B} \in \mathbb{C}^{M_1\times K}\}. \tag{4}$$

- The projection can be rewritten as

$$\mathcal{P}_{\mathbf{T}_n}\mathbf{H}_n = \begin{bmatrix} \mathbf{U}_n & \mathbf{Q}_2 \end{bmatrix} \mathbf{M}_n \begin{bmatrix} \mathbf{V}_n & \mathbf{Q}_1 \end{bmatrix}^H, \tag{5}$$

where

$$\mathbf{M}_n = \begin{bmatrix} \mathbf{U}_n^H \mathbf{H}_n \mathbf{V}_n & \mathbf{R}_1^H \\ \mathbf{R}_2 & \mathbf{0} \end{bmatrix} \in \mathbb{C}^{2K\times 2K}. \tag{6}$$

Here, $\mathbf{Q}_1 \in \mathbb{C}^{2L\times K}$ and $\mathbf{R}_1 \in \mathbb{C}^{K\times K}$ are from QR decompositions of the following matrix of dimensional $2L \times K$, with computational cost of $\mathcal{O}\left(2LK^2\right)$.

$$\left(\mathbf{I} - \mathbf{V}_n \mathbf{V}_n^H\right) \mathbf{H}_n^H \mathbf{U}_n = \mathbf{Q}_1 \mathbf{R}_1, \tag{7}$$

$$\left(\mathbf{I} - \mathbf{U}_n \mathbf{U}_n^H\right) \mathbf{H}_n \mathbf{V}_n = \mathbf{Q}_2 \mathbf{R}_2. \tag{8}$$

IHT-Net for Matrix Completion

- Low-rank Hankel matrix completion algorithms such as singular value thresholding (SVT) have high computational cost due to the compact singular value decomposition (SVD) in each iteration.
- The main steps in the i-th iteration of the IHT algorithm are as follows

$$\mathbf{X}_i = \mathcal{H}\left(\mathbf{x}_i + \beta\left(\mathbf{x}_s - \mathbf{x}_i\right)\right), \tag{9}$$

$$\mathbf{x}_{i+1} = \mathcal{H}^{\dagger}\left(\mathcal{T}_r\left(\mathbf{X}_i\right)\right), \tag{10}$$

where (9) is gradient descent update for current estimate $\mathbf{x}_i$ with fixed step size β on a Riemannian manifold. In step (10), $\mathcal{T}_r$ represents t-SVD for $\mathbf{X}_i$, which projects $\mathbf{X}_i$ onto the fixed-rank manifold to derive a low-rank approximation of $\mathbf{X}_i$.

$$\mathcal{T}_r\left(\mathbf{X}_i\right) = \sum_{k=1}^{r} \sigma_k \mathbf{u}_k \mathbf{v}_k^*, \quad \sigma_1 \geq \sigma_2 \geq \cdots \geq \sigma_r. \tag{11}$$

- We utilize a recurrent neural network structure to parameterize the IHT algorithm[6].

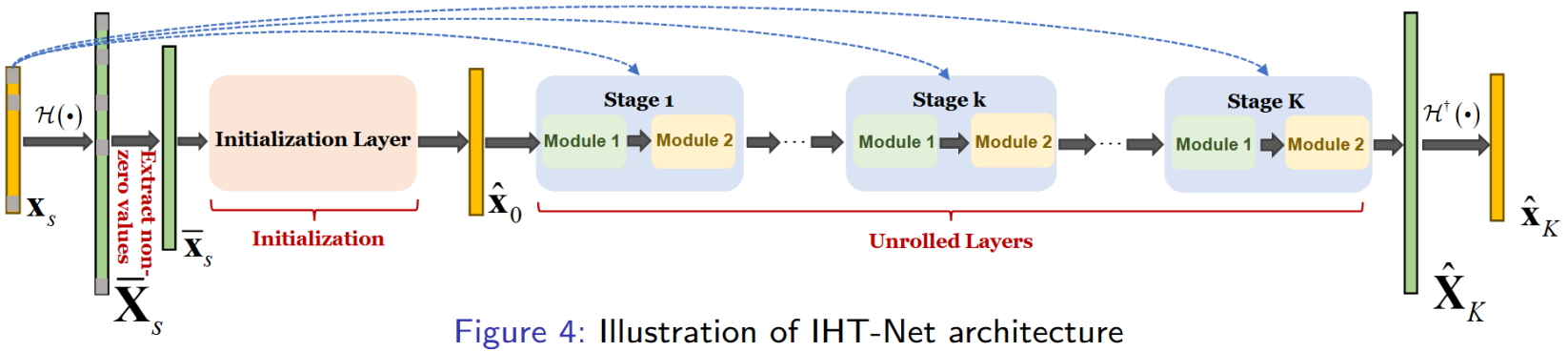

Figure 4: Illustration of IHT-Net architecture

Y. Hu and S. Sun, "IHT-inspired neural network for single-snapshot DOA estimation with sparse linear arrays," in Proc. IEEE 49th International Conference on Acoustics, Speech, and Signal Processing (ICASSP), Seoul, Korea, April 14-19, 2024.

Initialization Layer of IHT-Net

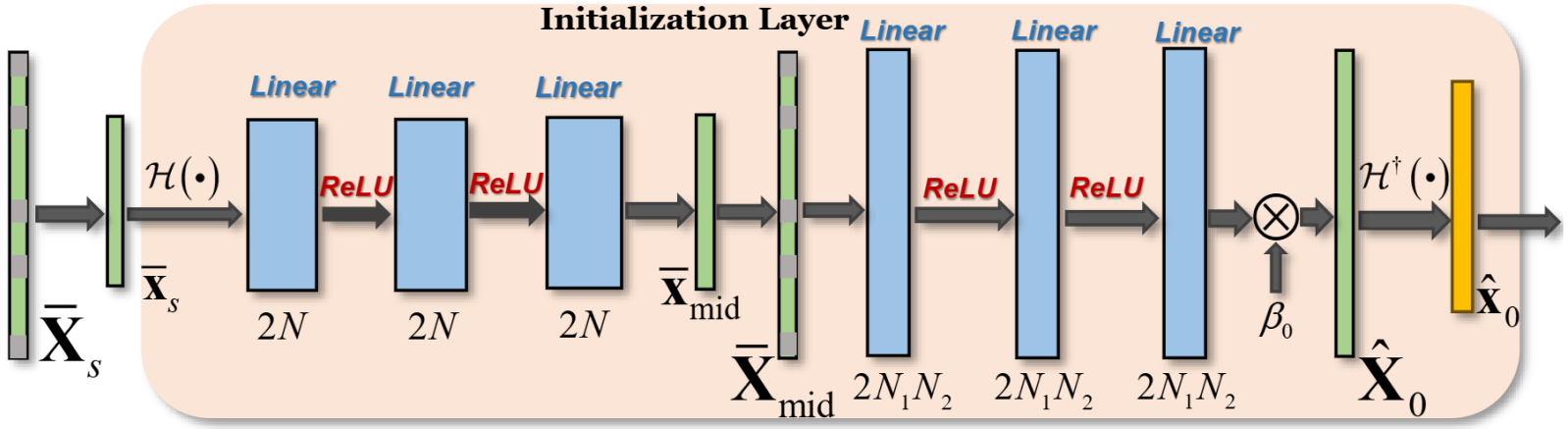

Figure 5: Illustration of initialization layer of IHT-Net

- We replace t-SVD with shallow layers autoencoder structures, avoiding the need for rank knowledge and SVD computation.
- We adopt mask encoder[7]. We implement an asymmetric structure that allows an encoder to operate only on observed values (without mask tokens) in the input Hankel vector and a decoder that reconstructs the full signal from the latent representation with mask token.
- We denote the encoder in this layer as $\mathcal{F}_1^{(0)}(\cdot)$, so the output of the encoder is defined as

$$\bar{\mathbf{x}}_{mid} = \mathcal{F}_1^{(0)}(\bar{\mathbf{x}}_s). \tag{12}$$

- Denoting the decoder in this layer as $\mathcal{F}_2^{(0)}(\cdot)$, then the final output of the initialization layer is

$$\hat{\mathbf{X}}_0 = \beta_0 \mathcal{F}_2^{(0)}\left(\mathcal{F}_1^{(0)}(\bar{\mathbf{x}}_s)\right) \tag{13}$$

where β_0 is a learnable scalar.

Implicit Rank-Minimization

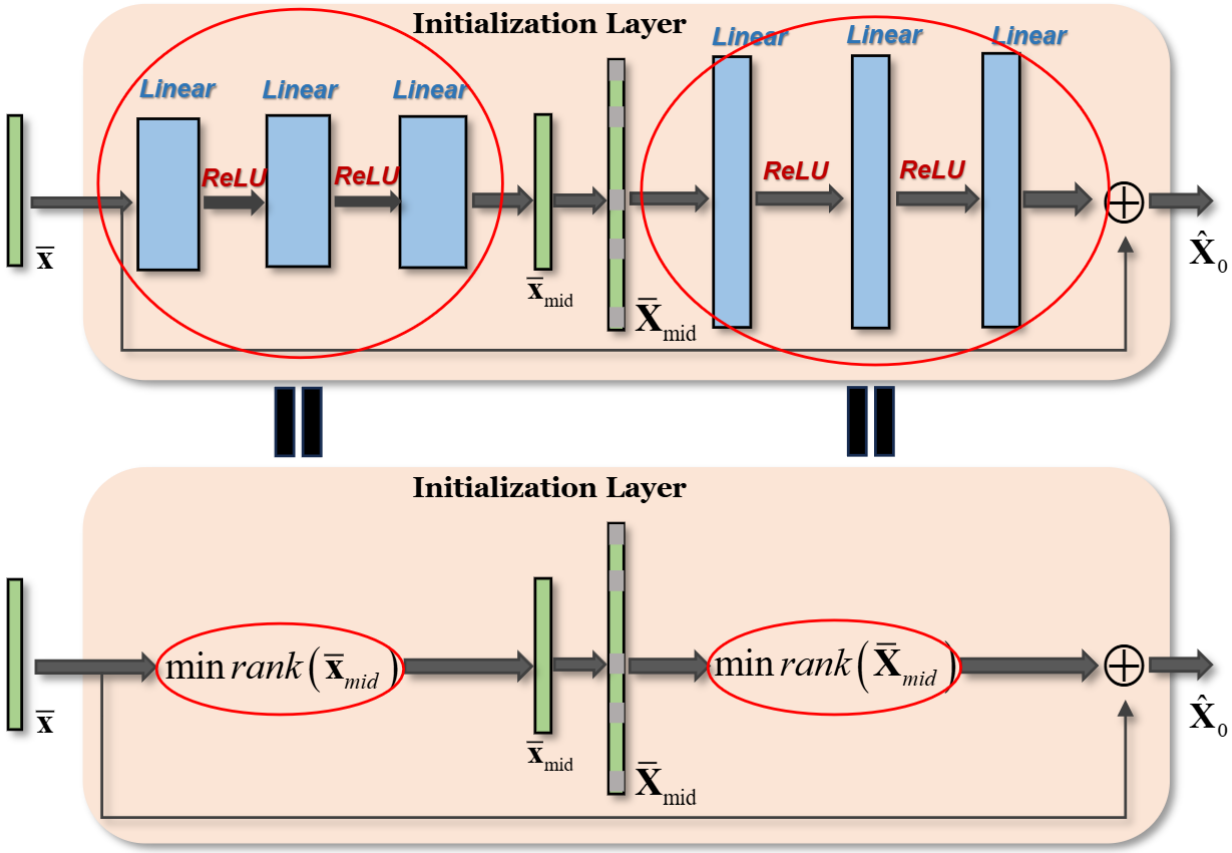

- Implicit rank-minimizing autoencoder consists in adding extra linear matrices between the encoder and decoder. ReLU activations are added between the linear layers aiming at speeding up the training process.

L Jing, J. Zbontar, and Y. Lecun, “Implicit rank-minimizing autoencoder,” NeurIPS, 2020.

Unrolling Layer of IHT-Net

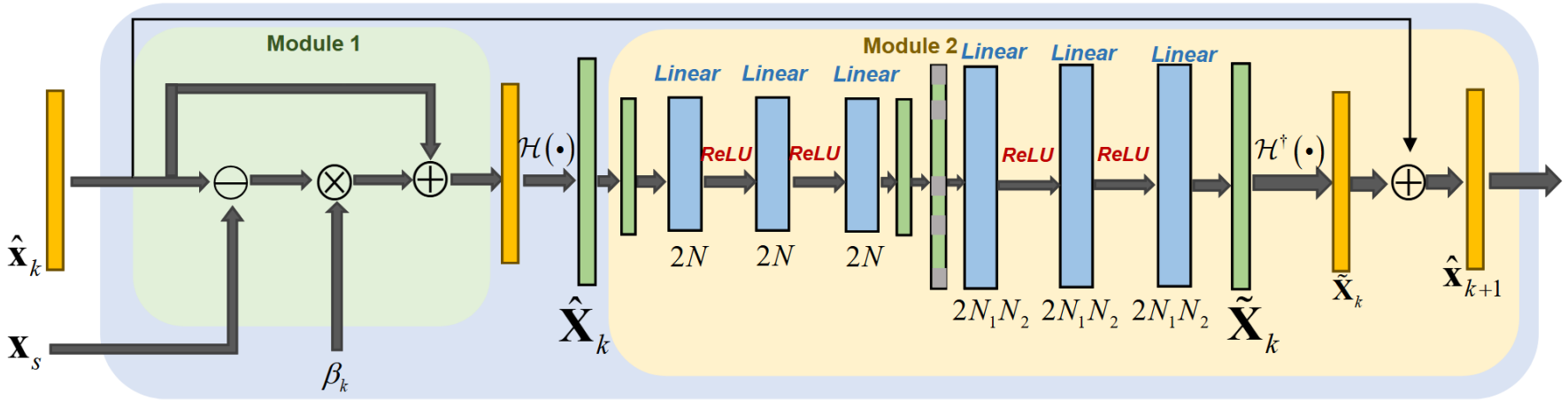

Figure 7: Illustration of the kth unrolled layer of IHT-Net.

- The Gradient Descent Module corresponds to Eq.(9) in the IHT algorithm. With the input $\hat{\mathbf{x}}_k$ from the $(k-1)$-th stage, and $\mathbf{x}_s$ which is broadcasted to every unrolled stage, the intermediate recovery result in k-th stage can be defined as

$$\hat{\mathbf{X}}_k = \mathcal{H}\left(\hat{\mathbf{x}}_k + \beta_k\left(\mathbf{x}_s - \hat{\mathbf{x}}_k\right)\right), \tag{14}$$

  where the step size β_k is a learnable parameter.

- The Low-Rank Approximation Module keeps the same architecture as the initialization layer while introducing a skip connection within the layers. We firstly extract $\hat{\mathbf{x}}_k$ from the output $\hat{\mathbf{X}}_k$ according to the non-zero values position list ϕ. Then the output of this module is derived by passing it through the encoders-decoders, resulting in

$$\tilde{\mathbf{x}}_k = \mathcal{F}_2^{(k)}\left(\mathcal{F}_1^{(k)}\left(\hat{\mathbf{x}}_k\right)\right). \tag{15}$$

- With the skip connection between the input $\hat{\mathbf{x}}_k$ and the output $\tilde{\mathbf{x}}_k$, the final output of the k-th unrolled stage is

$$\hat{\mathbf{x}}_{k+1} = \tilde{\mathbf{x}}_k + \gamma_k\left(\tilde{\mathbf{x}}_k - \hat{\mathbf{x}}_k\right) \tag{16}$$

  where γ_k is a learnable parameter weighting the residual term $(\tilde{\mathbf{x}}_k - \hat{\mathbf{x}}_k)$.

Numerical Results of IHT-Net

We generate P point-target sources in the same range-Doppler bin. The angles of the sources follow a uniform distribution within the field of view (FoV) spanning $[-60^\circ, 60^\circ]$. Their amplitudes have a uniform distribution ranging from $[0.5, 1]$, while their phases are uniformly distributed between $[0, 2\pi]$. In our experiment $P = 2$ for both training and testing, $N_b = 700,000$ with SNR randomly chosen from $[10\text{dB}, 30\text{dB}]$.

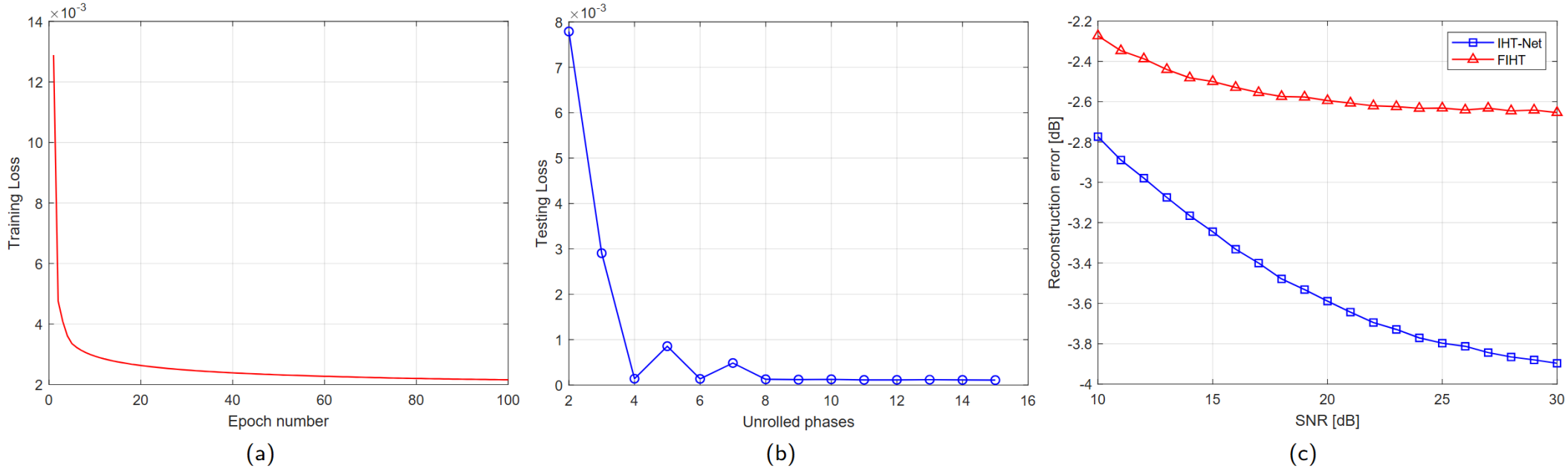

(a) IHT-Net training loss v.s. epoch for IHT-Net with 8 unrolled phases; (b) IHT-Net testing loss with various numbers of unrolled phases of IHT-Net; (c) Signal reconstruction error comparison between IHT-Net and FIHT in different SNRs.

Numerical Results of IHT-Net

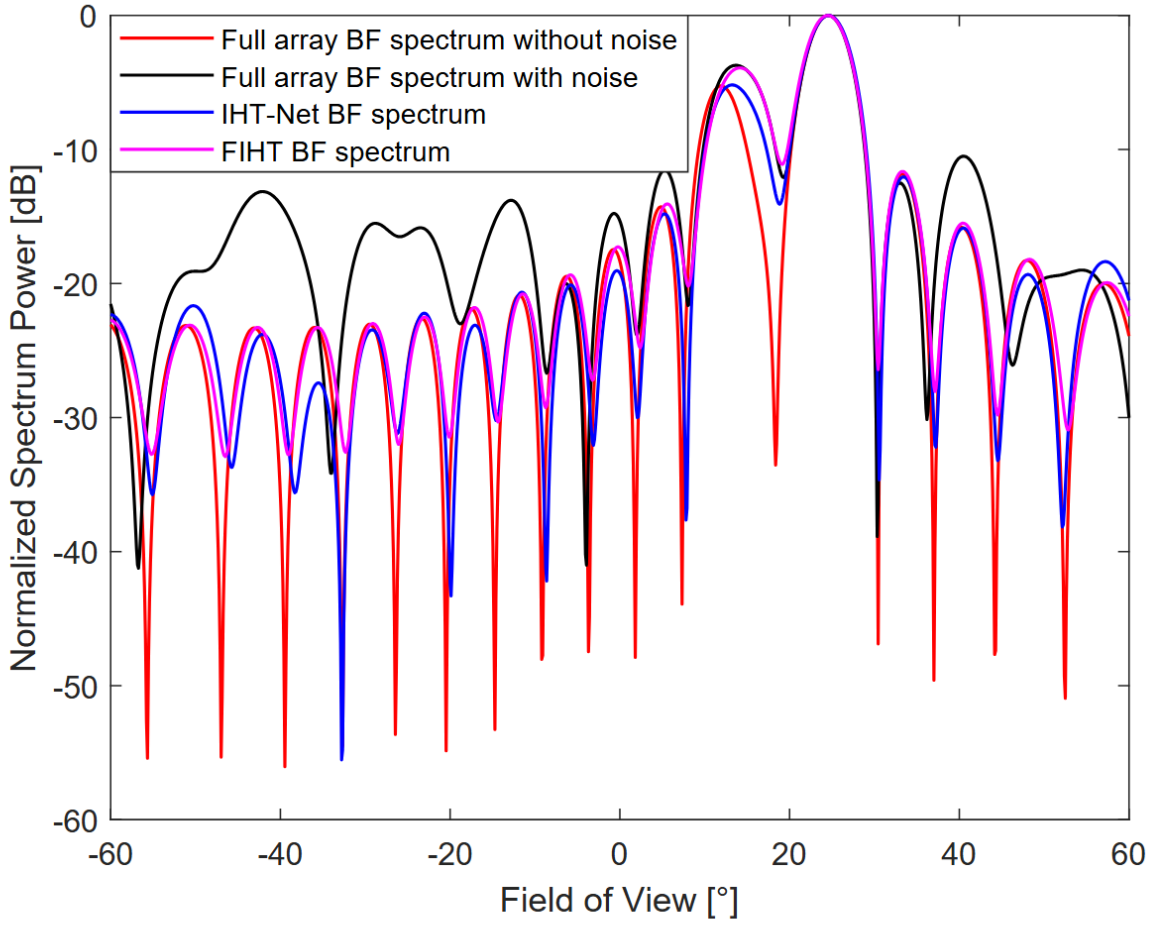

(a)

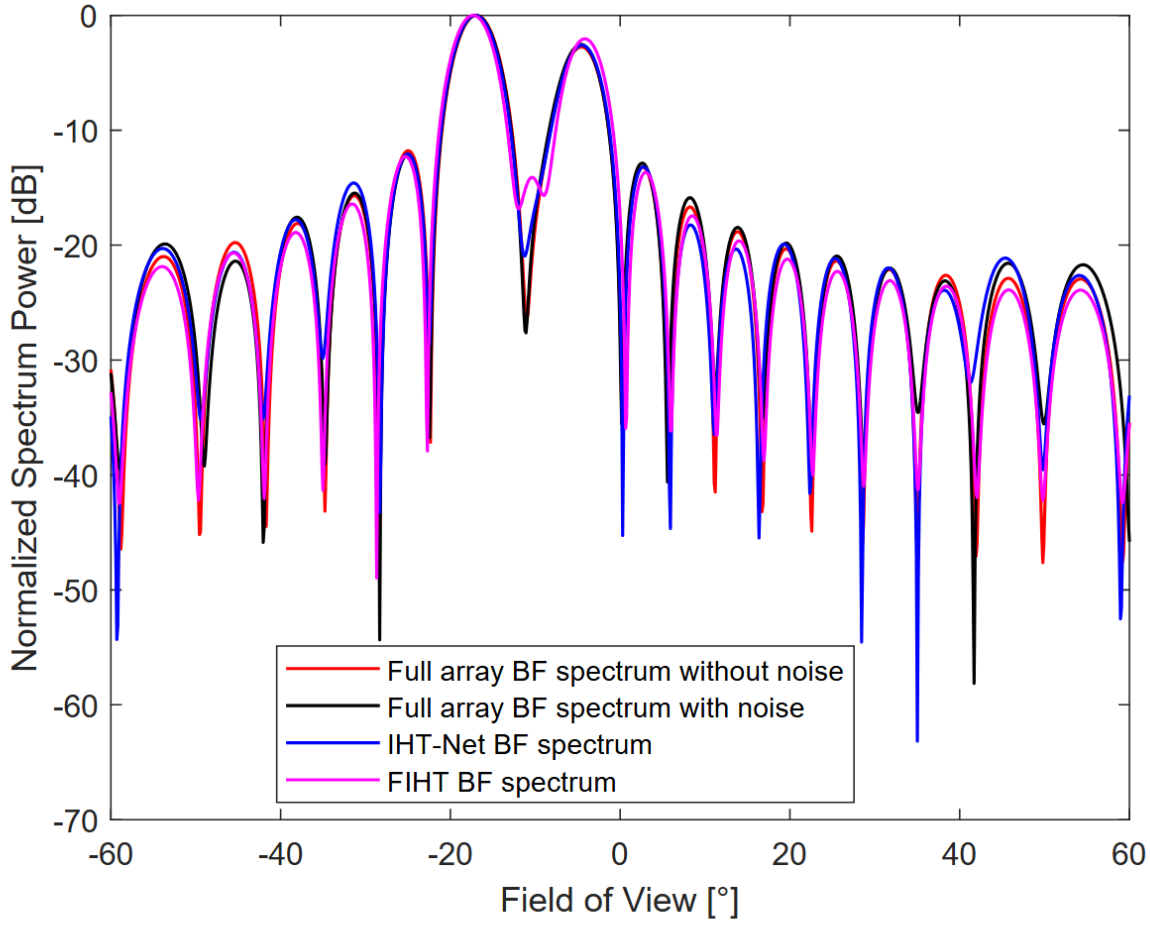

(b)

Beamforming spectrum examples in different SNRs with different SLAs; (a) SNR=10dB, 18-element SLA; (b) SNR=30dB,18-element SLA.

Numerical Results of IHT-Net

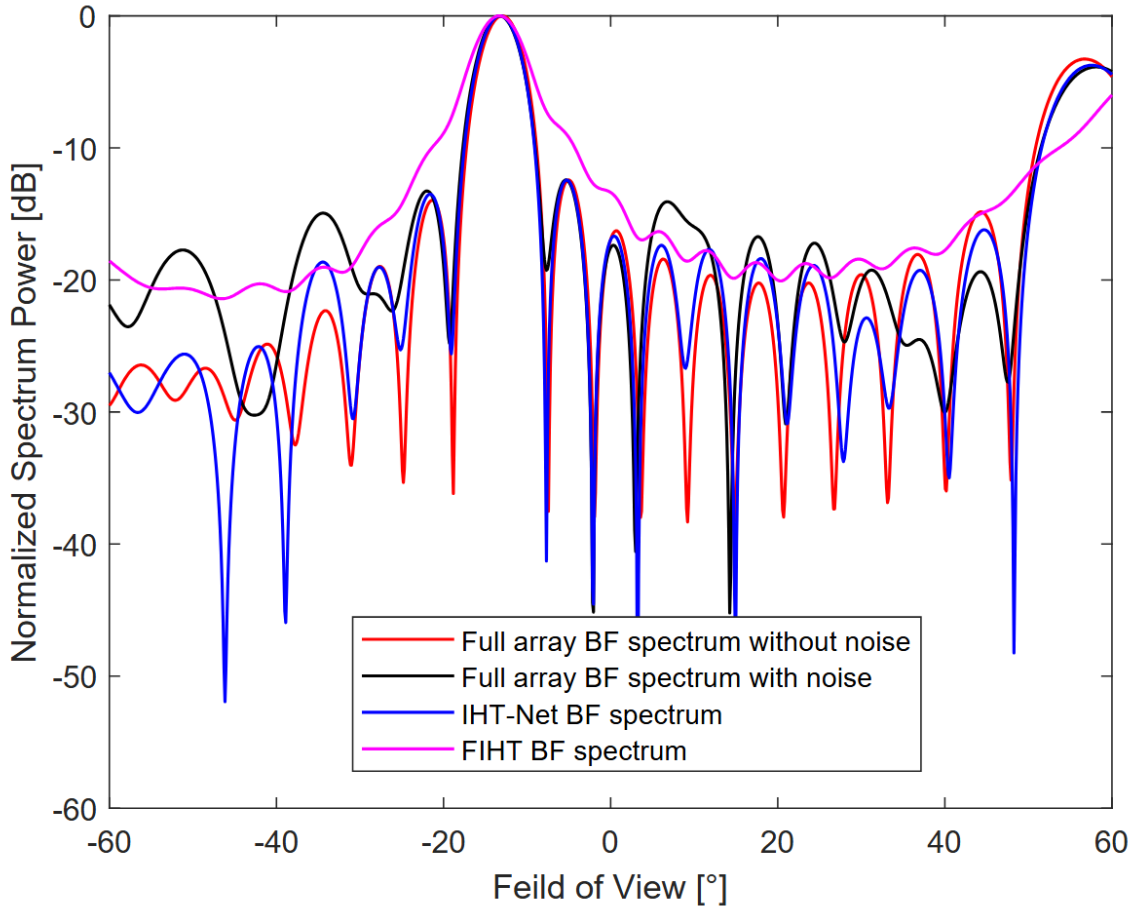

(a)

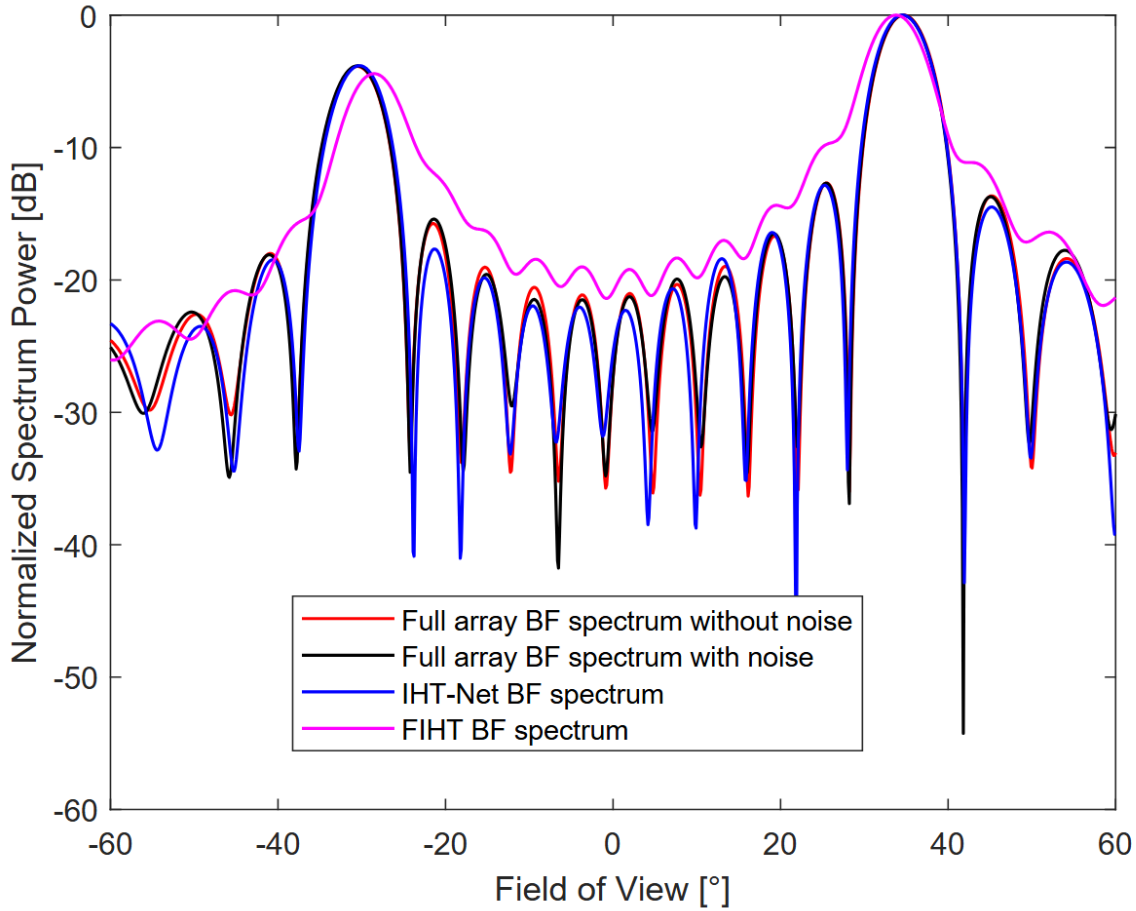

(b)

Beamforming spectrum examples in different SNRs with different SLAs; (a) SNR=10dB, 10-element SLA; (b) SNR=30dB,10-element SLA. Full array has 21 elements.

Agenda

- **Background and Motivation of DL for DOA Estimation**
  - ✓ Overview of deep learning (DL) for DOA estimation
  - ✓ Comparison: data-driven vs. model-based approaches
  - ✓ Why hybrid model-based deep learning matters
- **DL for High-Resolution Radar Imaging**
  - ✓ Unrolling IAA
  - ✓ Physics-guided 1D neural networks for radar imaging
  - ✓ DOA estimation considering antenna failure
  - ✓ Off-grid DOA estimation with 1-bit single-snapshot sparse array
  - ✓ Siamese neural networks for DOA estimation
- **DL for Integrated Sensing and Communications (ISAC)**
- **DL Enabled Sparse Array Interpolation**
  - ✓ Unrolling IHT for matrix completion
  - ✓ Transformer based array interpolation

Deep Frequency Attention Networks for Single Snapshot Sparse Array Interpolation

- Automotive radar → critical for autonomous driving
- Need **high angular resolution** with **low hardware cost**
- Sparse arrays:
  - ✓ Large aperture,
  - ✓ Fewer elements,
  - ✓ Reduced coupling.

  BUT: high sidelobes, missing elements
- Single snapshot challenge:
  - ✓ Covariance-based methods need many snapshots
  - ✓ Snapshot-limited in automotive radar
- Traditional approaches:
  - ✓ Model-based (e.g., Hankel completion, IHT)
  - ✓ Require expert tuning, high compute cost
- Gap:
  - ✓ Need efficient, adaptive, generalizable solution

R. Zheng, S. Sun, and H. Liu, "Deep frequency attention networks for single snapshot sparse array interpolation," in Proc. European Radar Conference (EuRAD), Utrecht, The Netherlands, Sept. 24-26, 2025.

Deep Frequency Attention Networks for Single Snapshot Sparse Array Interpolation

- Propose **FA-Net (Frequency Attention Network)**
- Key ideas:
  - ✓ Sparse & noise augmentation layer
  - ✓ Frequency-domain tokenization
  - ✓ Frequency attention mechanism
- Advantages**:**
  - ✓ Robust across sparse arrays
  - ✓ Handles random failures
  - ✓ Efficient for edge deployment

Ashish Vaswani, Noam Shazeer, Niki Parmar, Jakob Uszkoreit, Llion Jones, Aidan N Gomez, Łukasz Kaiser, Illia Polosukhin, “Attention is all you need”, NIPS, 2017.

Signal Model

- **Full Array Model**:

$$y = A(\theta)s + n$$

  - $A(\theta)$:Array manifold matrix
  - s: source vector, n: noise
- **Sparse Array Selection**:

$$y_s = My$$

  - M :binary selection matrix
  - Only $M < N$ sensors are active
- **Sparsity Definition**:

$$\text{Sparsity} = 1 - \frac{M}{N}$$

  - Proportion of missing elements relative to full array
- **Goal:** Reconstruct the full signal $A(\theta)s$ from y_s(single snapshot, noisy).

FA-Net Architecture

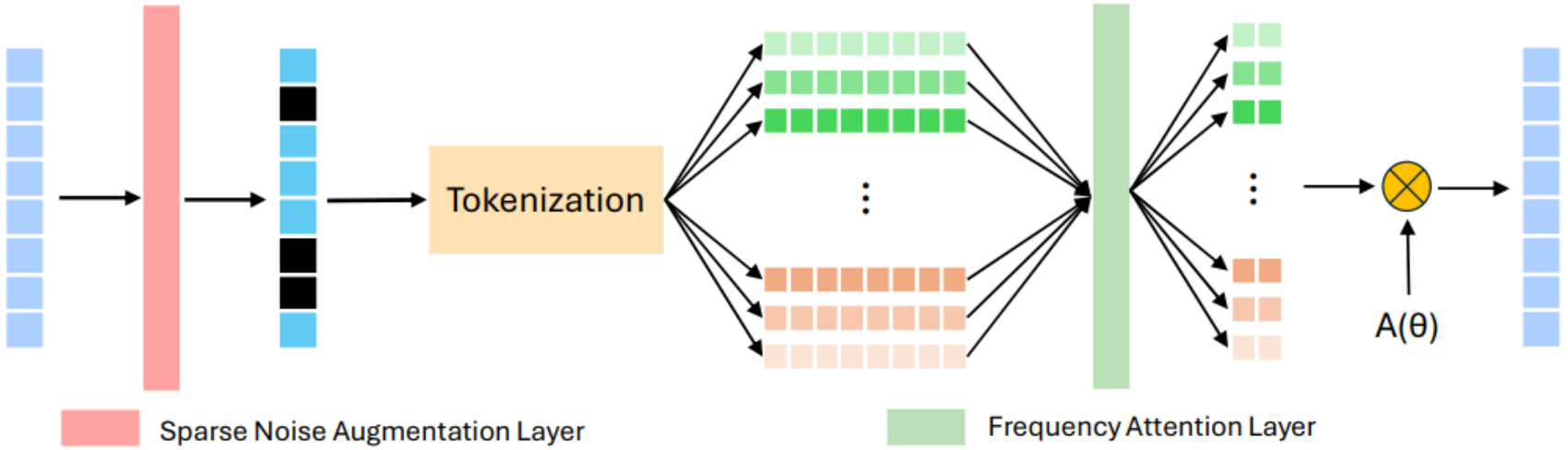

Fig. 1. Network architecture incorporating a sparse noise augmentation layer and a frequency attention mechanism within a signal reconstruction framework.

- Three components:
  - ✓ Sparse & noise augmentation
  - ✓ Frequency tokenization
  - ✓ Attention mechanism

FA-Net Sparse & Noise Augmentation Layer

- Purpose: simulate sensor failures + noisy conditions during training
- Random binary masking → variable sparsity
- Add Gaussian noise → simulate SNR variations
- Only applied during training for robustness

Frequency-Domain Tokenization

- Transform sparse signal → frequency domain
- Define frequency grid of size P
- Each frequency bin = token
- Token contains: Steering vector $a(\theta_p)$ Sparse measurement y_s

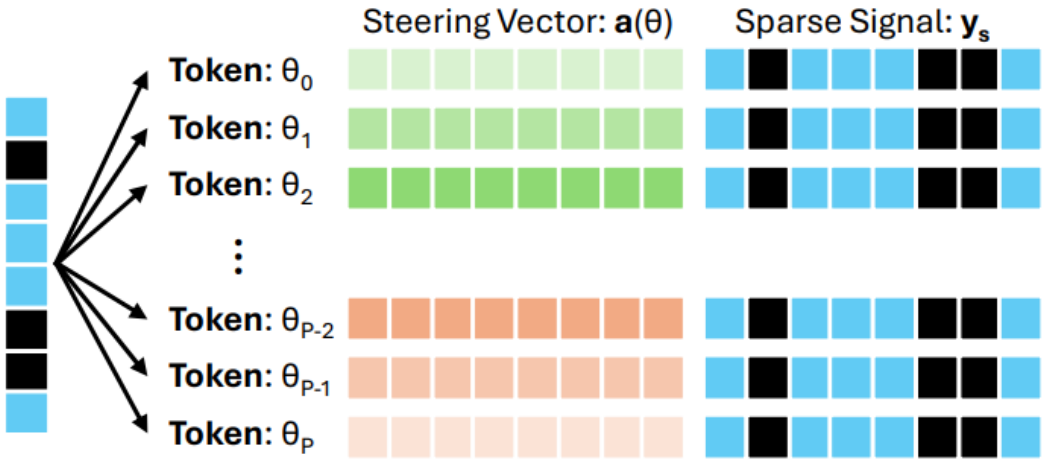

Fig. 2. Frequency domain tokenization.

Frequency Attention Mechanism

- Not all frequencies equally informative
- Attention assigns weights:
  High weight → true target frequencies
  Low weight → noisy or sidelobe regions
- Scaled Dot-Product Attention:

$$\text{Attention}(Q, K, V) = Softmax\left(\frac{QK^T}{\sqrt{d}}\right)V$$

- Output:
  refined frequency representation → reconstruct signal

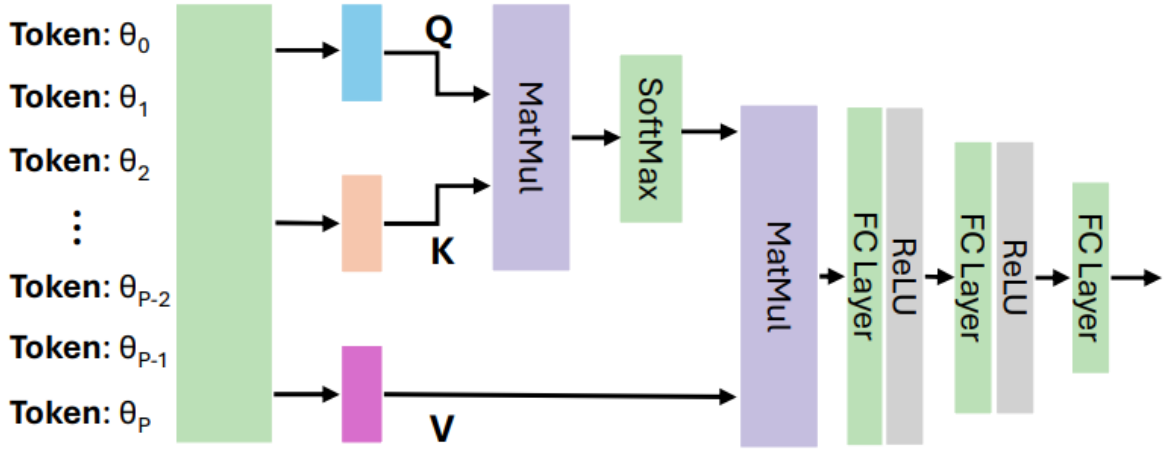

Fig. 3. Attention layer.

Training Setup

- **Simulation Environment**
- 20-element ULA, spacing = $\lambda/2$
- Up to 2 targets per snapshot
- Field of view (FOV): $[-, 30°30°]$
- 64 frequency bins (uniform grid)
- **Data Generation**
- **Reflection coefficients:**
- $|s_k| \sim \mathcal{U}[0.5, 1]$,
- $\angle s_k \sim \mathcal{U}[0, 2\pi]$
- Total: **131,072** training signals

- Augmentation
  - Random masking (max sparsity = 40%)
  - Gaussian noise injection: SNR ∈ [10, 30] dB
- Training Configuration:
  - Loss: Mean Squared Error (MSE)
  - Optimizer: Adam, LR = 0.001
  - Batch size = 512,
  - Epochs = 500
- Hardware:
  - 4 × NVIDIA RTX A6000 GPUs

Qualitative Results

- **Baselines**
- **IHT-Thresholding**
- Iterative Hard Thresholding with signal subspace estimated by simple thresholding
- Practical method, no oracle knowledge
- **IHT-GT (Ground Truth)**
- IHT with oracle knowledge of true model order (unrealistic but gives an upper bound)
- **Quantitative Results**
- FA-Net consistently outperforms IHT-Thresholding across all SNRs
- FA-Net even surpasses IHT-GT above 20 dB
- **Demonstrates robustness under low SNR and high sparsity conditions**

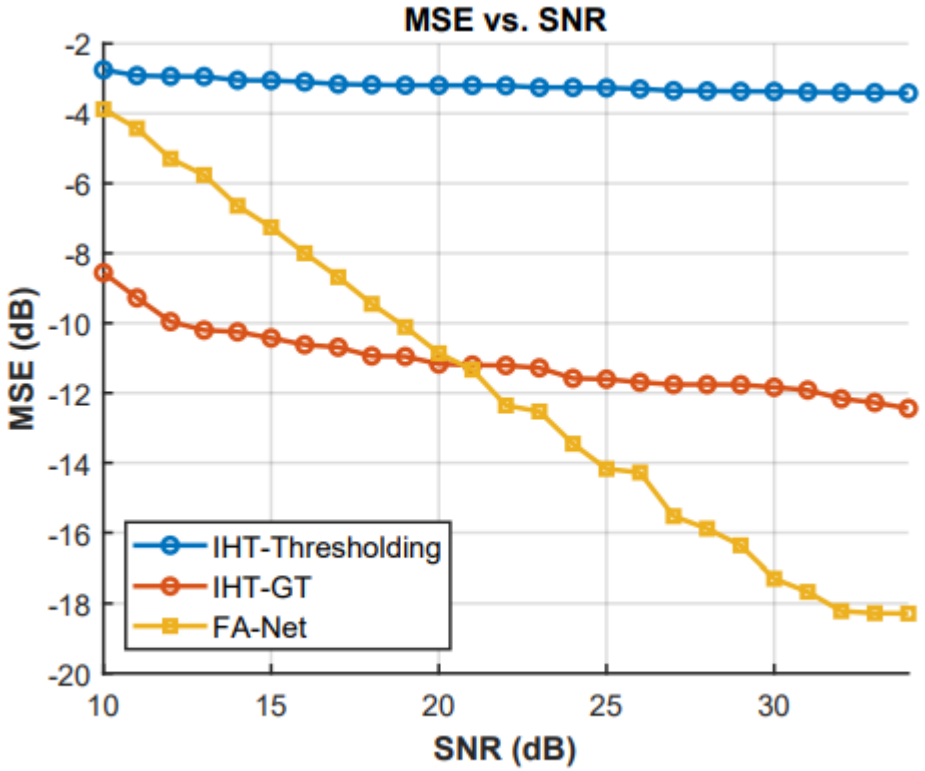

Fig. 4. Signal Reconstruction Error vs SNR.

Qualitative Results

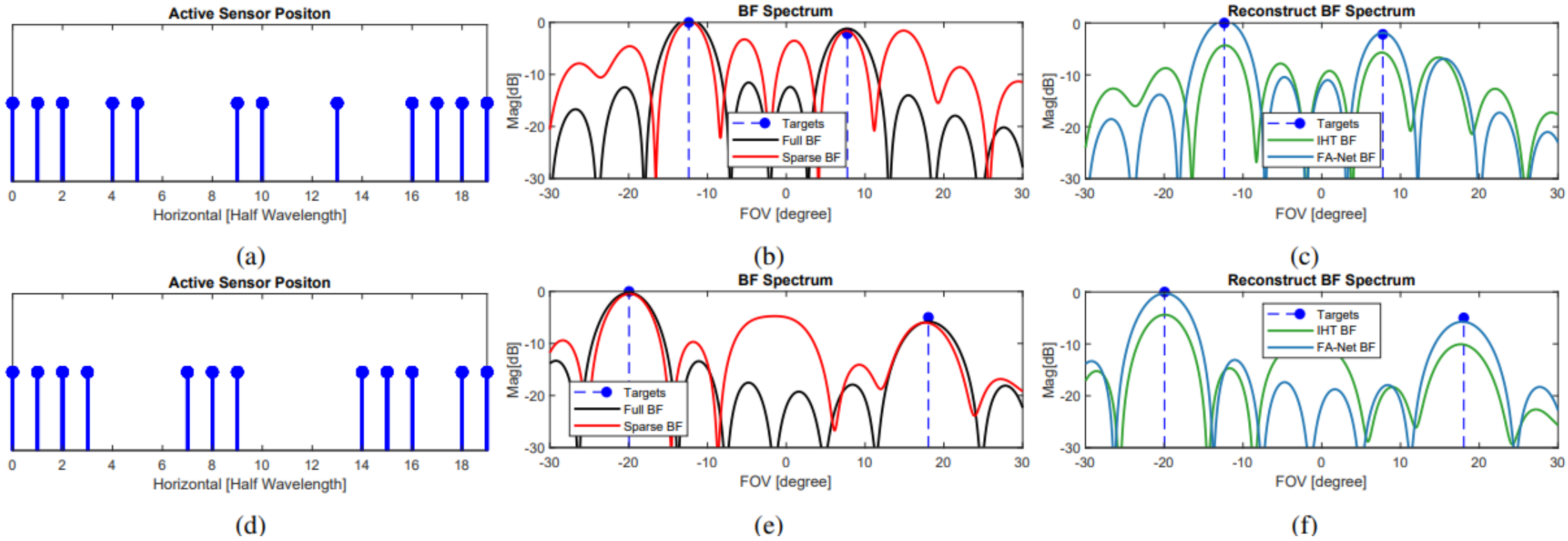

Beamforming spectrum comparisons: Sparse vs reconstructed (IHT vs FA-Net)

Qualitative Results

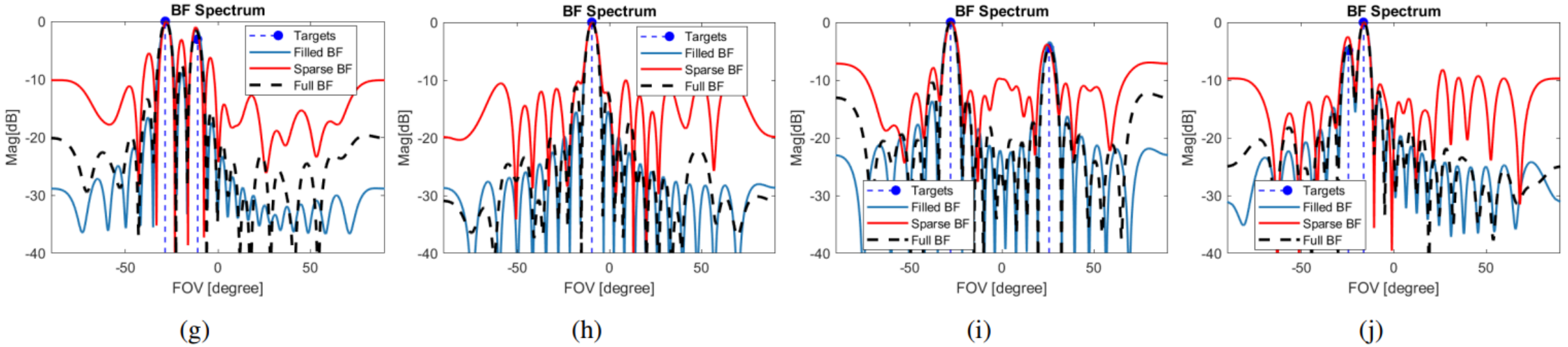

Beamforming spectrum comparisons: Real radar data examples

Summary

- Deep learning for DOA estimation offers high-resolution, real-time capability but faces challenges in generalization, interpretability, and data requirements.
- Hybrid model-based deep learning (e.g., unrolling algorithms, physics-guided networks) bridges theory and data, improving robustness and efficiency.
- Robust radar imaging can be achieved through DL methods on sparse arrays that handle antenna failures, 1-bit quantization, and off-grid estimation.
- Advanced architectures (e.g., Siamese networks, Transformers) extend DL's role to sparse array interpolation and ISAC applications.
- Future directions: scalable, interpretable, and generalizable frameworks that unify sensing and communication for next-generation intelligent systems.

References

- L. Xu, S. Sun, R. Wu, B. Shi and J. Li, ‘‘Broad neural networks for sparse signal retrieval and array interpolation in automotive radar,’’ IEEE Transactions on Radar Systems, vol. 3, pp. 1103-1118, 2025.
- R. Zheng, S. Sun, H. Liu, H. Chen and J. Li, ‘‘Model-based knowledge-driven learning approach for enhanced high-resolution automotive radar imaging,’’ IEEE Transactions on Radar Systems, vol. 3, pp. 709-723, 2025.
- L. Xu, S. Sun, Y. D. Zhang and A. P. Petropulu, “Reconfigurable beamforming for automotive radar sensing and communication: A deep reinforcement learning approach,” IEEE Journal of Selected Areas in Sensors, vol. 1, pp. 124-138, 2024.
- R. Zheng, S. Sun, H. Liu, H. Chen and J. Li, “Interpretable and efficient beamforming-based deep learning for single snapshot DOA estimation,” IEEE Sensors Journal, vol. 24, no. 14, pp. 22096-22105, 2024.
- R. Zheng, S. Sun, H. Liu and T. Wu, ‘‘Deep neural networks-enabled vehicle detection using high-resolution automotive radar imaging,’’ IEEE Transactions on Aerospace and Electronic Systems, vol. 59, no. 5, pp. 4815-4830, 2023.
- S. Sun and Y. D. Zhang, ‘‘4D automotive radar sensing for autonomous vehicles: A sparsity-oriented approach,” IEEE Journal of Selected Topics in Signal Processing, vol. 15, no. 4, pp. 879-891, 2021.
- S. Sun, A. P. Petropulu and H. V. Poor, “MIMO radar for advanced driver-assistance systems and autonomous driving: Advantages and challenges,” IEEE Signal Processing Magazine, vol. 37, no. 4, pp. 98-117, 2020.

References

- R. Zheng, S. Sun, and H. Liu, “Deep frequency attention networks for single snapshot sparse array interpolation,” in Proc. European Radar Conference (EuRAD), Utrecht, The Netherlands, Sept. 24-26, 2025.
- R. Zheng, S. Sun, H. Liu, H. Caesar, H. Chen and J. Li, ‘‘Advancing high-resolution and efficient automotive radar imaging through domain-informed 1D deep learning,’’ in Proc. IEEE 50th International Conference on Acoustics, Speech, and Signal Processing (ICASSP), Hyderabad, India, April 6-11, 2025.
- R. Zheng, S. Sun, H. Liu and Y. D. Zhang, ‘‘Advancing single-snapshot DOA estimation with Siamese neural networks for sparse linear arrays,’’ in Proc. IEEE 50th International Conference on Acoustics, Speech, and Signal Processing (ICASSP), Hyderabad, India, April 6-11, 2025.
- S. Rao, R. Narasimha and S. Sun, ‘‘Signal processing challenges in automotive radar,’’ in Proc. IEEE 50th International Conference on Acoustics, Speech, and Signal Processing (ICASSP), Hyderabad, India, April 6-11, 2025.
- R. Zheng, S. Sun, H. Liu, H. Chen, M. Soltanalian and J. Li, “Antenna failure resilience: Deep learning-enabled robust DOA estimation with single snapshot sparse arrays,” in Proc. 58th Annual Asilomar Conference on Signals, Systems, and Computers (Asilomar), Pacific Grove, CA, Oct. 27 – Oct. 30, 2024.
- Y. Hu, S. Sun and Y. D. Zhang, “Enhancing off-grid one-bit DOA estimation with learning-based sparse Bayesian approach for non-uniform sparse array,” in Proc. 58th Annual Asilomar Conference on Signals, Systems, and Computers (Asilomar), Pacific Grove, CA, Oct. 27 – Oct. 30, 2024. (Invited)
- R. Zheng, H. Liu, S. Sun, and J. Li, “Deep learning based computationally efficient unrolling IAA for direction-of-arrival estimation,” in Proc. European Signal Processing Conference (EUSIPCO), Helsinki, Finland, Sept. 4-8, 2023.

References

- L. Xu, S. Sun, Y. D. Zhang and A. P. Petropulu, “Joint antenna selection and beamforming in integrated automotive radar sensing-communications with quantized double phase shifters,” in Proc. IEEE 48th International Conference on Acoustics, Speech, and Signal Processing (ICASSP), Rhodes Island, Greece, June 4-9, 2023.
- S. Sun, Y. Wen, R. Wu, D. Ren, and J. Li, “Fast forward-backward Hankel matrix completion for automotive radar DOA estimation using sparse linear arrays,” in Proc. IEEE Radar Conference, San Antonio, TX, May 1-5, 2023.
- R. Zheng, S. Sun, H. Liu, and T. Wu, “Time-sensitive and distance-tolerant deep learning-based vehicle detection using high-resolution radar birds-eye-view images,” in Proc. IEEE Radar Conference, San Antonio, TX, May 1-5, 2023.
- R. Zheng, H. Liu, and S. Sun, ‘‘A deep learning approach for Doppler unfolding in automotive TDM MIMO radar,’’ in Proc. 56th Annual Asilomar Conference on Signals, Systems, and Computers (Asilomar), Pacific Grove, CA, Oct. 30 – Nov. 2, 2022.
- R. Zheng, S. Sun, D. Scharff and T. Wu, ‘‘SpectraNet: A High resolution imaging radar deep neural network for autonomous vehicles,’’ in Proc. IEEE Sensor Array and Multichannel Signal Processing Workshop (SAM), Trondheim, Norway, June 20-23, 2022.
- L. Xu, R. Zheng and S. Sun, ‘‘A deep reinforcement learning approach for integrated automotive radar sensing and communication,’’ in Proc. IEEE Sensor Array and Multichannel Signal Processing Workshop (SAM), Trondheim, Norway, June 20-23, 2022.